

**MARITIME TRANSPORTATION RESEARCH AND EDUCATION CENTER
TIER 1 UNIVERSITY TRANSPORTATION CENTER
U.S. DEPARTMENT OF TRANSPORTATION**



**Bio-Inspired Stabilization of Levee Slope on Expansive Yazoo Clay at the Maritime and
Multimodal Transportation Infrastructure in Mississippi**

March 15, 2020, to August 31, 2023

Prepared by:

Sadik Khan, Ph.D., P.E.
Robert Whalin, Ph. D., PE
Amber Spears, P.E.
Avipriyo Chakraborty

Department of Civil and Environmental Engineering,
Jackson State University,
1400 J. R. Lynch St, Box 17068
Jackson, MS, 39217
Phone: 601-979-6373
Email: J00797693@jsums.edu

August 2023

FINAL RESEARCH REPORT

Prepared for:
Maritime Transportation Research and Education Center

University of Arkansas
4190 Bell Engineering Center
Fayetteville, AR 72701
479-575-6021

ACKNOWLEDGEMENT

This material is based upon work supported by the U.S. Department of Transportation under Grant Award Number 69A3551747130. The work was conducted through the Maritime Transportation Research and Education Center at the University of Arkansas.

DISCLAIMER

The contents of this report reflect the views of the authors, who are responsible for the facts and the accuracy of the information presented herein. This document is disseminated in the interest of information exchange. The report is funded, partially or entirely, by a grant from the U.S. Department of Transportation's University Transportation Centers Program. However, the U.S. Government assumes no liability for the contents or use thereof.

ABSTRACT

Mississippi's expansive Yazoo clay experiences slope failures and shallow landslides that result in distressed foundations, roadways, and levees that are integral components of the maritime and multimodal transportation infrastructure. The wet-dry cycles inherent in the Mississippi climate cause shrinking and swelling that result in desiccation cracks, and the increased annual precipitation caused by climate change is allowing more moisture to infiltrate the weathered Yazoo clay, which means that the frequency of shallow landslides is expected to increase. The significant cost of remediation is borne by the maintenance budget of the Mississippi Department of Transportation, the US Army Corps of Engineers, and private and public property owners, and finding sustainable solutions that reduce costs and improve mitigation is vital.

Vetiver grass is a sustainably sourced perennial bunchgrass that originated in Southeast Asia, primarily India, and has been in the United States for 100 years. It is classified as a sterile noninvasive plant by the United States Department of Agriculture and is an excellent, cost-effective bio-engineered solution for repairing shallow landslides on expansive soil, as its roots penetrate the soil more than 3 m under ideal conditions. Unfortunately, it is minimally used in the United States due to a lack of understanding of its performance. This report aims, therefore, to provide a more comprehensive view of the ability of vetiver grass roots to stabilize levee slopes and embankments in Mississippi's maritime and multimodal transportation infrastructures.

Testing was conducted at two locations: a test levee located at the Rapid Levee Repair Test Facility in Vicksburg, Mississippi, which is a part of the United States Army Engineer Research and Development Center, and an embankment on Highway 120 in Jackson, Mississippi. The test levee section was 12.2 m long and 9.1 m wide and was located on a 3H:1V slope with a crest height of 3.7 m above the downstream toe. The highway embankment had previously been repaired with H-piles and consisted of a 6 m² area north of the repaired section on a 3.5 H:1V to 4H:1V slope with a height of 4.6 m. Both slopes were instrumented with industrial grade moisture and matric suction sensors at depths of 15.2 cm and 45.7 cm below the ground surface, vapor pressure and relative humidity (RH) measurement apparatus, thermometers, barometric pressure sensor stations, rain gauges, and data loggers. The embankment section was also equipped with inclinometers, and both slopes were monitored for more than two years. After it was determined that vetiver can grow in expansive Yazoo clay, changes in the in situ physical properties of the Yazoo clay were compared with soil properties elucidated in the literature and revealed trends related to the changes in weather.

While no landslides, seepage, or desiccation cracks were observed in the slopes, extreme changes in the moisture content and matric suction indicated potential sources of excess moisture that could threaten their stability. Numerical analysis was performed to allow variations in the soil properties and determine whether the vetiver grass could improve the slope by increasing the shear strength of the new composite root-soil matrix and considering whether the roots could reinforce the soil through the transfer of shear stress in the soil matrix to the roots as tensile inclusions. Similar numerical analyses were conducted to study the performance of the grass under different rainfall conditions, and the findings showed that vetiver grass improves a slope in a marginal condition and prevents it from reaching failure (landslide). The results of this study suggest that future studies that further assess the benefit of vetiver grass on shallow slopes in Yazoo clay would tremendously and positively impact the maritime and multimodal transportation infrastructure in Mississippi and other states with expansive soil.

Table of Contents

| | |
|--|-----------|
| Chapter 1 : Introduction | 1 |
| Chapter 2 : Literature Review | 5 |
| 2.1 Indirect Measurement of Potential Swell..... | 6 |
| 2.1.1 Classification of potential swell based on Casagrande’s plasticity chart..... | 6 |
| 2.1.2 Classification of potential swell based on plasticity table..... | 7 |
| 2.1.3 Classification of potential swell based on advanced physical properties of soils..... | 7 |
| 2.1.4 Determination of Potential Swelling Based on Suction Values..... | 10 |
| 2.2 Atterberg Limits and Swelling of Yazoo Clay..... | 10 |
| 2.3 Relationship between Yazoo Clay and Landslides | 10 |
| 2.4 Utilization of Vegetation as a Soil Bioengineering Technique for Landslide Mitigation..... | 11 |
| 2.5 Vetiver Grass | 12 |
| 2.6 Different Applications of Vetiver | 13 |
| 2.7 Mechanical Properties of Vetiver | 14 |
| 2.7.1 Tensile strength and shear strength of vetiver roots..... | 15 |
| 2.7.2 Pullout force on vetiver-rooted soil..... | 16 |
| 2.7.3 Impact of vetiver on soil shear strength..... | 16 |
| Chapter 3 : Laboratory Testing..... | 21 |
| 3.1 Laboratory Testing Preparation | 21 |
| 3.2 Vetiver Root Strength Testing | 23 |
| 3.3 Data collection | 23 |
| 3.4 Data analysis..... | 24 |
| 3.5 Results..... | 24 |
| 3.5.1 Stress vs. strain..... | 24 |
| 3.5.2 Load vs. deformation | 27 |
| 3.5.3 Ultimate tensile strength vs. root diameter | 28 |
| Chapter 4 : Field Investigation of Slopes Improved with Vetiver Grass | 31 |
| 4.1 Site Selection | 31 |
| 4.2 Slope 1: ERDC Test Levee Section | 31 |
| 4.2.1 Phase 1: Summer growth monitoring..... | 32 |
| 4.2.2 Field instrumentation | 35 |
| 4.2.3 Field monitoring results | 36 |
| 4.3 Slope 2: Terry Rd Highway Embankment Section..... | 39 |
| 4.3.1 Vetiver planting and growth monitoring..... | 41 |
| 4.3.2 Field instrumentation | 42 |
| 4.3.3 Field monitoring results | 44 |
| Chapter 5 : Numerical Analyses of Slopes Improved with Vetiver..... | 51 |
| 5.1 Numerical Modeling Background..... | 51 |
| 5.2 Scenario 1: Slope 1 Levee Improved with Vetiver Modeled as a Root-Soil Composite in Slide..... | 51 |
| 5.3 Scenario 2: Levee Improved with Vetiver Modeled as a Root-Soil Composite in Slide..... | 54 |
| 5.4 Scenario 3: Slope 2 Highway Embankment Improved with Vetiver as a Bio-Anchor..... | 57 |
| 5.5 Comparison of Scenarios 1 through 3, Results, and Discussion..... | 61 |
| Chapter 6 : Conclusion..... | 63 |

References..... 64

Table of Figures

| | |
|--|----|
| Figure 1.1 Comparisons of peak, residual, and fully softened shear strength (Skempton, 1970)..... | 2 |
| Figure 1.2 Boundary boxes of the Jackson formation, including Yazoo clay and its geological equivalents, in Mississippi, Alabama, and Louisiana | 3 |
| Figure 2.1 Atterberg limits description, volume change, and generalized stress-strain response of expansive soils (adapted from Holtz and Kovacs, 1981)..... | 6 |
| Figure 2.2 Plot of clay minerals on Casagrande’s Chart (Chleborad et al., 2005)..... | 7 |
| Figure 2.3 Graph for evaluation of potential expansiveness (Seed et al., 1960)..... | 8 |
| Figure 2.4 Classification chart for swelling potential proposed by Carter and Bentley (1991)..... | 9 |
| Figure 2.5 Impact of vegetation on soil (Coppin and Richards, 1990)..... | 12 |
| Figure 2.6 (a) Long busy network of vetiver roots (Kim et al., 2022), and (b) vetiver roots grown in sandy soil in 110 days (Badhon et al., 2021) | 13 |
| Figure 2.7 Vetiver stabilizing a previously failed highway slope in Mississippi, United States | 14 |
| Figure 2.8 Variations of root tensile strength of vetiver roots with increased diameter | 15 |
| Figure 2.9 Variation of pullout force of Vetiver roots (a) with displacement (Newton vs. mm) (b) lateral root spread (Newton vs. mm) (figure courtesy of Mickovski et al., 2005) | 16 |
| Figure 2.10 Comparison of the shear strength of soil in different normal loading in undrained conditions between non-rooted and vetiver rooted soil (a) In clay soil (values issued from Mickovski and Van Beek, 2009) (b) in silty sand (values issued from Islam et al., 2013) (b) in low plasticity clay (values issued from Islam et al., 2013)..... | 17 |
| Figure 2.11 Variation of peak shear stress values with depth in vetiver-rooted soil based on a direct shear test (values issued from D’Souza et al. 2019)..... | 17 |
| Figure 2.12 Variation of peak shear stress with root area ratio in vetiver rooted soil based on a direct shear test (Values issued from D’Souza et al. 2019)..... | 18 |
| Figure 2.13 Variation of shear Stress on different strain conditions and depth (a) laboratory setup, and (b) un-rooted soil c) vetiver- rooted soil (figure courtesy of D’Souza et al., 2019) | 19 |
| Figure 2.14 Comparison of Mohr-Coulomb failure envelopes at zero matric suction with the original soil, soil with local tree Orange Jasmine, and vetiver grass roots (figure courtesy of Rahardjo et al., 2014).... | 20 |
| Figure 3.1 (a) Vetiver grown at Jackson State University, (b) vetiver collected for root testing | 21 |
| Figure 3.2 GEOJAC testing device (figure courtesy of Liu, 2015) | 22 |
| Figure 3.3 (a) Circular plate for vetiver root strength testing (b) GeoJac with plate before testing | 23 |
| Figure 3.4 (a) Two-inch vetiver root before testing, (b) rupture of vetiver root..... | 24 |
| Figure 3.5 Root stress vs. root strain curve for vetiver roots (based on six-month samples) | 25 |
| Figure 3.6 Best fit root stress vs. root strain curve (MPa vs mm/mm) | 26 |
| Figure 3.7 Actual stress vs predicted stress on the derived stress-strain curve equation (MPa Vs. MPa).. | 27 |
| Figure 3.8 Vetiver root strength at different root strain (MPa Vs. mm/mm %)..... | 28 |
| Figure 3.9 Load vs. deformation curve for vetiver roots at: (a) six months and (b) one year (N vs. mm) | 29 |
| Figure 3.10 Variation of root ultimate tensile strength with root diameter (MPa vs. mm)..... | 30 |
| Figure 3.11 Comparison of different studies on root ultimate tensile strength with present study (MPa vs mm)..... | 29 |
| Figure 3.12 Comparison of ultimate tensile strength in different studies with present study (in MPa)..... | 30 |
| Figure 4.1 Location of slope 1: (a) aerial location, and (b) looking east | 32 |
| Figure 4.2 Planting vetiver on test levee at ERDC: (a) looking east, (b) vetiver tiller before planting, (c) vetiver tillers planted, and (d) looking north after planting vetiver | 33 |
| Figure 4.3 2020 summer growth monitoring of vetiver at 1 week, 1 month, and 2 months | 33 |
| Figure 4.4 2020 winter through 2021 summer growth: monitoring at 2 weeks, 1 month, 2 months, 5 months, 6 months, and 11 months..... | 34 |
| Figure 4.5 Tallest vetiver grass height observed and measured as 1.4 m in August 2022..... | 35 |
| Figure 4.6 (a) Instrumentation profile at ERDC, and (b) individual sensors at ERDC..... | 35 |
| Figure 4.7 Instrumentation setup at ERDC..... | 36 |

| | |
|---|-----|
| Figure 4.8 Field measurements of Slope 1: (a) moisture(mm-day), (b) suction (kPa-day), and (c) temperature (degree celsius- day)..... | 41 |
| Figure 4.9 Location of Slope 2..... | 39 |
| Figure 4.10 CPT and borehole locations at Slope 2..... | 40 |
| Figure 4.11 (a) Initial state of Terry Rd section, and (b) repaired, control, and vetiver grass (reinforced) sections..... | 41 |
| Figure 4.12 Planting vetiver on highway embankment at Terry Rd: (a) looking southwest at reinforced section, (b) looking southwest at reinforced section after vetiver has had a few weeks' growth, (c) looking southwest at reinforced section in October 2020 | 42 |
| Figure 4.13 (a) Instrumentation profile at Terry Rd: vetiver section (left) and across all sections (right), and (b) original individual sensors..... | 44 |
| Figure 4.14 Field Measurements of slope 2: (a) moisture(cm-day), (b) suction(kPa-day), and (c) temperature (degree Celsius -day)..... | 49 |
| Figure 4.15 Instrumentation layout at Slope 2 in 2018, excluding vetiver section instrumentation installed in 2020. | 47 |
| Figure 4.16 Horizontal displacements of (a) Inclinator 1 (as built section) and (b) Inclinator 2 (repair section) (meter vs mm)..... | 49 |
| Figure 5.1 Four-day storm transient condition for Slope 1 without vetiver (Stage 2): (a) profile (b) results . | |
| Figure 5.2 Four-day Storm for Slope 1 with vetiver (Stage 2): (a) Profile (b) Results..... | 56 |
| Figure 5.3 Back analysis of failure condition of the levee: (a) initial levee profile, and (b) results | 568 |
| Figure 5.4 Slope failure following maturation of vetiver section: (a) levee with vetiver, and (b) results . | 59 |
| Figure 5.5 Geometry and soil stratigraphy of Slope 2 | 580 |
| Figure 5.6 Perched water condition to 1.5 m depth | 580 |
| Figure 5.7 Slope failure of Slope 2 at 1.5 m depth in back calculated model..... | 591 |
| Figure 5.8 Vetiver roots modeled as embedded beams..... | 602 |
| Figure 5.9 Impact of vetiver on slope failure mitigation compared to unrooted slope (in meters) | 613 |

Table of Tables

Table 2.1 Potential Swell based on Plasticity (Holtz and Gibbs, 1956)..... 7
Table 2.2 Identification of Possible Expansion based on Plasticity (Carter and Bentley, 1991)..... 10
Table 2.3 Heavy Metal Absorption Capacity of Vetiver Compared to Vascular Plants (Danh et al. 2010)
..... 14
Table 4.1 Selected Site Locations 31
Table 4.2 Forensic Investigation at Slope 2..... 40
Table 4.3 Field Instrumentation for Data Collection 43
Table 5.1 Soil Parameters for Scenario 1 52
Table 5.2 Soil Parameters for Scenario 2..... 557
Table 5.3 Soil Parameters for Scenario 3..... 591

Chapter 1: Introduction

A landslide is a sudden downward movement of a mass of soil, debris, or rock from slopes, mountains, or hills that can result in significant harm, financial loss, and even fatalities. The areas affected by landslides are typically smaller than those of other natural disasters such as earthquakes, storms, or flooding, so their impact, though significant, is sometimes underestimated (Kalia, 2018). From January 2004 to December 2016, however, 55,997 people were killed in 4,862 landslide events globally (Nix et al., 2006), and from 2008 to 2017, the lives of more than 3 million people throughout the world were impacted and the economic losses exceeded \$2.7 billion (Seguin et al., 2018).

Landslides are classified as either deep-seated or shallow-seated failures: those within 1 - 1.5 m below the ground surface are considered shallow; those beyond those depths are considered deep-seated (Hengchaovanich, 2003). The standard approach to slope protection employs civil engineering structures, such as piles, that are expensive, resource-intensive, and necessitate comprehensive site-specific research (Punetha et al., 2019); additionally, by nature, their effectiveness declines with age (Mohamed et al., 2022). Many factors contribute to landslides, but the three most prevalent causes are geological (i.e., earthquakes, volcanic eruptions, etc.), hydrological (i.e., intense rainfalls, storm waves, and rapid snow melting), and human interventions resulting from development activities (i.e., improper slope excavation and loading, rapid reservoir depletion, and vibrations from blasting) (Acharya et al., 2016; Dai et al., 2002; Cruden, 218). Climate change is exacerbating the adverse effects on all three and negatively affecting the stability of slopes.

The effects of climate change are far-reaching and are impacting the world's ecological systems and environment. The global temperature is rising worldwide (Battisti and Naylor, 2009), thereby increasing the air's water-holding capacity, as each degree of temperature increase leads to a 7% increase in water-holding capacity and leading to excessive rainfall. Several recent landslides were attributed to excessive precipitation, and in the U.S., rain-induced landslides are the most frequent and widespread (USGS, 2018). In tropical regions, where heavy rainfall is common, it is one of the primary causes of shallow slope collapses (Rahardjo et al., 1995).

Intense rainfall for a short period can trigger failure in high-permeability soil; rainfall for an extended period can cause failure in low-permeability soil (Cardinali et al., 2006; Johnson and Sitar, 1990;). Highly permeable soils can be granular-to-fine in consistency and include gravel, sand, and silt; low permeability soils can be granular with fines, such as silty or clayey sand, or composed solely of fines with minimal granular content. The shear strength of clay diminishes more rapidly with increased infiltration than that of sand and silt, (Stark and Duncan, 1991), and the shear strength of high-plasticity clay is impacted by long-term wetting and drying, which causes shrinking and swelling, as the moisture content is naturally higher than in low plasticity clay. The shrinking and swelling that occurs during alternating wet and dry periods result in the development of residual shear, which is one of the primary reasons for slope failure. After repeated periods of wetting and drying, high-plasticity clay can develop desiccation cracks that create preferential flow paths for infiltration and reduce strength (Skempton, 1970). This decreases the effective peak shear strength of compacted clays towards the fully softened shear strength and ultimately decreases from the fully softened to the residual strength, as depicted in Figure 1.1.

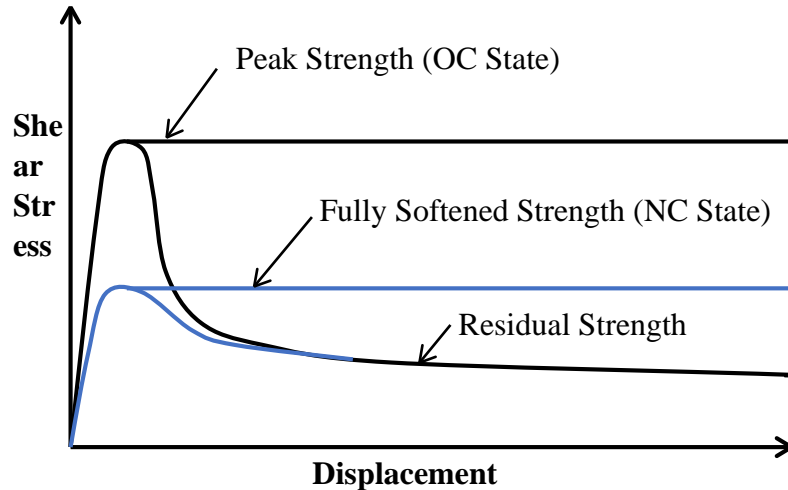


Figure 1.1 Comparisons of peak, residual, and fully softened shear strength (Skempton, 1970)

Other natural soil properties, such as saturated hydraulic conductivity and soil water retention capacity, are also influenced by rainfall and lead to slope instability (Cai and Ugai, 2004; Cho, 2014). High-plasticity, or expansive, clay, which is prevalent in the US region's upper stratigraphy (Alabama, Louisiana, Mississippi, and Texas), is subject to high volume change (Douglas and Dunlap, 2000; Lee, 2012). Yazoo clay is an expansive clay that spans the metropolitan area of Jackson, MS, with its horizontal bounds of approximately 56 km on the west to less than 16 km on the east, as depicted in Figure 1.2. Surface exposures of Yazoo clay that are weathered to a maximum depth of approximately 13.7 m below the ground surface have a distinctive yellow-brown color, while un-weathered Yazoo clay is blue-gray. Its mineralogy consists of 28% smectite (likely montmorillonite), 24% kaolinite, 22% quartz, 15% calcite, 8% illite, 2% feldspar, and 1% gypsum (Taylor, 2005). Soil textures usually result from factors like soil composition, sedimentation, climatic and hydrologic conditions, precipitation, and pH level. A surface examination is required to identify expansive soil (Lucian, 2008).

According to a recent study, the United States has experienced a 10% rise in precipitation over the past 50 years (Groisman and Easterling, 1994; Karl and Knight, 1998; Kunkel et al., 1999), and eight of the ten most severe one-day rainfall events have occurred since 1990. Mississippi has a hot and humid subtropical climate with mild, brief winters, and is the second-wettest state in the continental United States (after Louisiana). The high temperatures and heavy precipitation throughout the summer significantly threaten the slopes built of expansive Yazoo clay, as the summer's gradual wet-dry cycles cause desiccation fractures to develop that increase the water's vertical permeability at the top of the slope (Khan et al., 2020).

Surface examination of soil is both visual and a careful inspection that includes testing to determine the most effective slope stability techniques for a particular soil. Morphological properties like the groundwater table; the color, consistency, texture, and structure of the soil; and texture groups are also defining factors of the soil properties (Charles, 2008). Atterberg limits, unit weight, and grain size analysis tests are used to identify geotechnical index properties; the swell potential is determined by volume change tests; and X-Ray diffraction and total suction tests reveal the coefficient of linear extensibility (COLE) and mineralogical compositions.

Many different solutions are used to mitigate slope failures and control erosion. Among them, nature-based solutions such as hydroseeding, turfing, trees, bushes, and geosynthetics are frequently used, with the plants or plant-based materials used for slope protection, either individually or in conjunction with other slope protection methodologies (Gray and Sotir, 1996; Schacht and Stern, 1996). Vegetation is one

of the most effective soil bioengineering techniques for reducing slope failure, and the techniques are cost-effective and more environmentally friendly than traditional landslide mitigation methods.

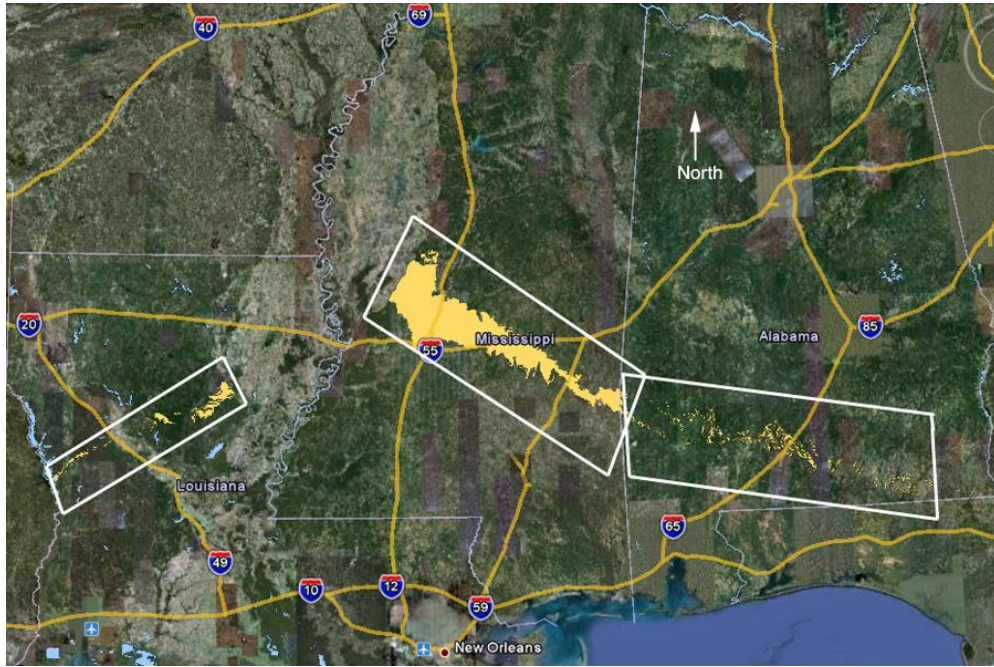


Figure 1.2 Boundary boxes of the Jackson formation, including Yazoo clay and its geological equivalents in Mississippi, Alabama, and Louisiana

The use of plants for recovering water and replenishing soil is a widely accepted biological method. Root fibers from vegetation mechanically strengthen soil by reinforcing it and enhancing various mechanical soil qualities (Nguyen et al., 2019). They can impact the soil's permeability and water retention behavior by removing excess water from the soil through evapotranspiration, a process by which plant roots and the atmosphere absorb soil moisture, resulting in a decrease in pore water pressure and an increase in the shear strength of the soil (Leknoi and Likitlersuang, 2020).

Vetiver grass is one of the plants employed in vegetation-based soil bioengineering for landslide prevention and mitigation. It is a perennial, herbaceous, and graminaceous plant, which means that it is an herbal grass that does not have to be replanted annually. It is most closely related to sorghum, but shares several morphological traits with other aromatic grasses, including lemongrass, citronella, and palmarosa (D'Souza et al., 2019). Vetiver is adaptable to a variety of climatic and soil conditions, and despite being a tropical plant, it can thrive in a variety of temperatures and climates, including semi-tropical and Mediterranean climates. Its root system consists of a large, thick, and rapidly expanding network of fibrous filaments that can reach a height of 3 m (Mickovski et al., 2005) and can drain surplus soil water through evapotranspiration and boost the soil's shear strength. Vetiver grass is used for other bioengineering applications but has been demonstrated to be a highly effective instrument globally for preventing landslides.

Vetiver has been successfully utilized for roadside stabilization in Africa, Asia, Australia, Central America, and southern Europe, as well as for stabilizing railroad ballasts (Mickovski et al., 2005). Since the beginning of the twentieth century, the West Indies, South Africa, Brazil, and Fiji have used it to protect slopes, enhance embankments, and support soil excavations from agricultural regions (Hengchaovanich, 2003); China has used it to prevent erosion on more than 150,000 kilometers of embankments; and Nigeria, Venezuela, Indonesia, Australia, and China tout it as discharging more effectively and reducing soil erosion

better than any other plant species (Truong and Loch, 2004). The World Bank promotes vetiver as a vegetation that conserves water and soil on farmlands by reducing soil erosion, and according to Maffei (2002), it is one of the most versatile products of the 21st century.

This report aims to investigate the ability of vetiver grass to stabilize earthen slopes that are the basis of Mississippi's maritime and multimodal transportation infrastructure. The grass was grown for six months in Mississippi soil consisting mainly of Yazoo clay at Jackson State University, then the plant and its roots were extracted from the soil. The strength of individual vetiver 2-inch (50 mm) long roots with different diameters was determined, and they were planted on a test levee in Vicksburg, MS and an embankment in Jackson, MS. Numerical analyses were performed on slopes comparable to the field sites to see whether it prevents shallow slope failures.

Chapter 2: Literature Review

Climate, hydrology, environment, topography, and geology govern the formation and behavior of soils. Climate is one of the essential factors in developing the soil's profile, as precipitation, wind, sunlight, and temperature, accelerate soil formation as it changes the parent rock material into soil. Soils vary, as they are a mixture of rock fragments, minerals, air, water, and organic materials that are subject to varying climatic events. For example, the climatic and topographical conditions under which smectite clay is formed are entirely different from those that form kaolinite clay. The formation of smectite requires low relief, low permeability, low rainfall, and low temperature, and the environment offers extreme disintegration, intense hydration, and restrained leaching appropriate for forming smectite-rich, expansive soils (Tourtelot, 1973). In contrast, high temperatures, strong hydrolysis by high permeability, and high rainfall intensities favor the formation of kaolinite (Tourtelot, 1973; Weaver, 1989). Additionally, expansive clays like smectite are more prevalent in drier environments, while non-expansive clays like kaolinite are more common in warm, humid environments. Climate, hydrology, environment, and geology also play significant roles in the plasticity of expansive clays.

The plasticity of expansive soil such as Yazoo clay can be determined from an Atterberg limits test, which identifies the liquid limit (LL), plastic limit (PL), shrinkage limit (SL), and plasticity index (PI) of the soil. These indices contain essential information on soil properties, e.g., they provide the water-holding capacity at different consistencies. The liquid limit is the water content at which soil changes from a plastic state to a liquid state; in contrast, the plastic limit is the water content at which soil changes from plastic to semisolid, as illustrated in Figure 2.1. The plasticity index is identified by subtracting the plastic limit from the liquid limit and is indicated by "PI" in Figure 2.1. Soils such as sand that do not contain clay minerals do not exhibit plasticity; they are non-plastic. Plastic soils lose plasticity and flexibility at lower moisture content and swell after rainfall, which results in significant instability. Expansive soils with high levels of montmorillonite absorb more water and exhibit more swelling than chlorite, illite, and kaolinite. The determination of swelling is often indirect, using correlations with other readily accessible soil index properties.

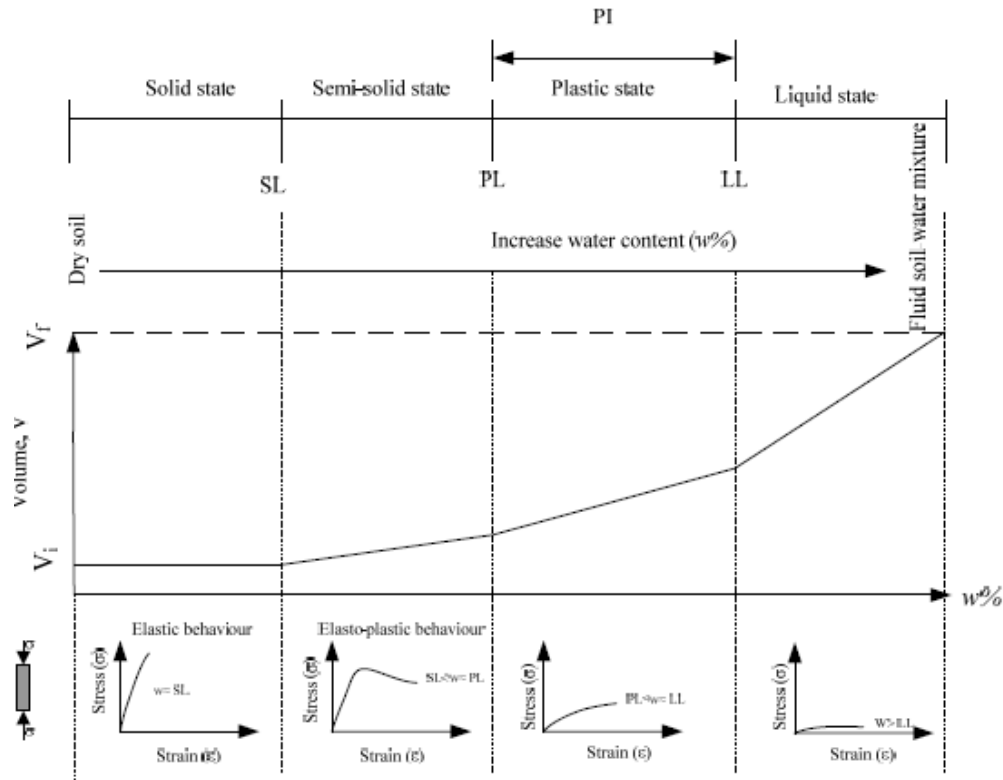


Figure 2.1 Atterberg limits description, volume change, and generalized stress-strain response of expansive soils (adapted from Holtz and Kovacs, 1981)

2.1 Indirect Measurement of Potential Swell

2.1.1 Classification of potential swell based on Casagrande's plasticity chart.

The plot of PL vs. LL in Figure 2.2 provides the potential mineralogy of soil according to Casagrande's plasticity chart. The clay soil type can be identified based on the liquid limit and plasticity index. The U-line at the top is the upper boundary above which natural soils do not exist. Above the A-line, the soil is heavy or plastic clay, and below it is organic soils, silts, and clayey soils that contain a sizeable portion of rock flour (BS 5930, 1981).

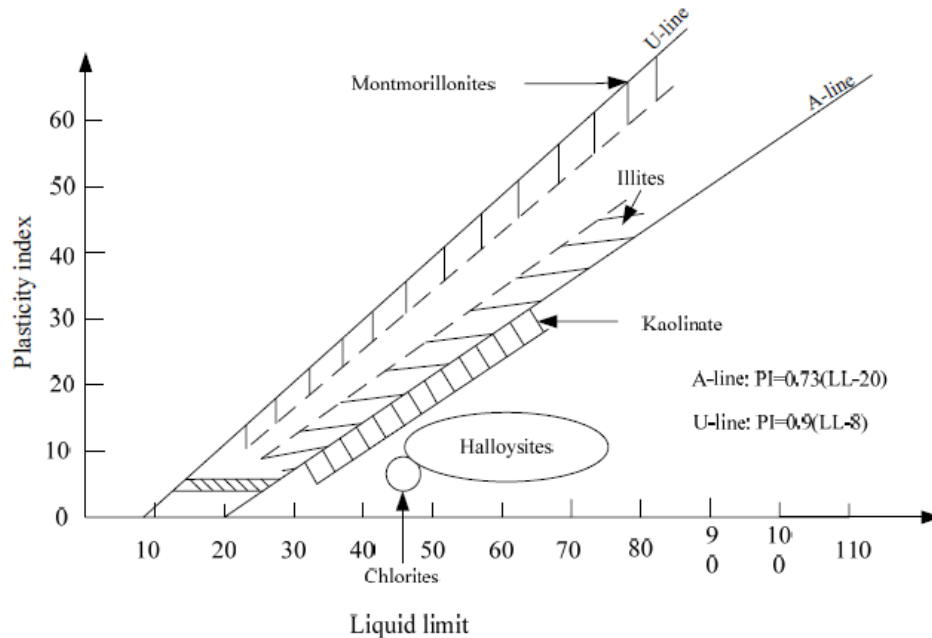


Figure 2.2 Plot of clay minerals on Casagrande's Chart (Chleborad et al., 2005)

2.1.2 Classification of potential swell based on plasticity table.

Atterberg Limit tests can be used to identify the swelling potential of soil. In Table 2.1, the liquid limit, plasticity index, and shrinkage limit values have been divided to correspond to swelling potential classifications from low to very high. For instance, soil with a liquid limit of 65 and a PI of 35 has a significant swelling potential. Overlapping intervals in the plasticity index and shrinkage limit presumably account for variations in the chemical properties and environment of soils.

Table 2.1 Potential Swell based on Plasticity (Holtz and Gibbs, 1956)

| Classification of potential swell | Liquid limit (LL), % | Plasticity index (PI), % | Shrinkage limit (SL), % |
|-----------------------------------|----------------------|--------------------------|-------------------------|
| Low | 20-35 | <18 | >15 |
| Medium | 35-50 | 15-28 | 10-15 |
| High | 50-70 | 25-41 | 7-12 |
| Very high | >70 | >30 | <11 |

2.1.3 Classification of potential swell based on advanced physical properties of soils.

The graph shown in Figure 2.3 depicts the differences in soil, based on the clay content, soil activity, and plasticity index. A preliminary classification based on the PI and percent clay fraction (soil particles < 0.002 mm or 2 μm, in percent), usually determined by a hydrometer test, was used to categorize the potential expansiveness.

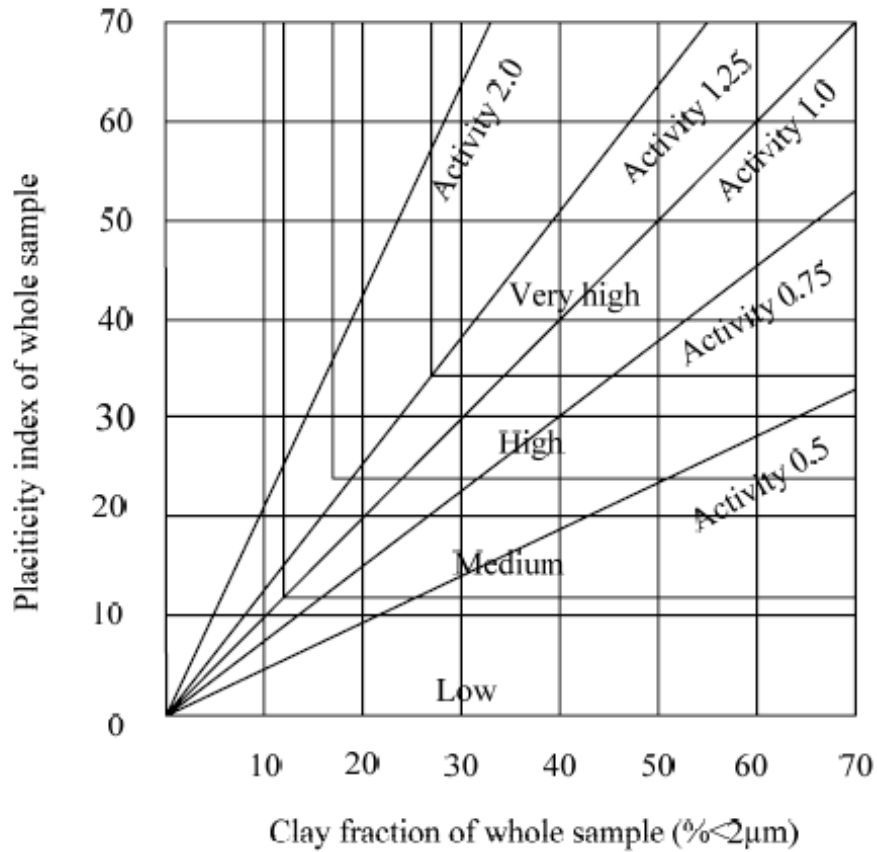


Figure 2.3 Graph for evaluation of potential expansiveness (Seed et al., 1960)

The soil was divided into categories, based on the empirical formula, with activity levels from 0.5 to 2.0 and potential expansiveness from low to very high. For example, a soil sample with 40 to 50 percent clay fraction and a plasticity index value of 35 has a very high potential for shrinkage and swelling in response to environmental changes (Lucian, 2008). The empirical formula developed to identify the activity of the soil is provided in Equation 2.1.

$$\text{Activity (A}_c\text{)} = \text{Plasticity index (PI) in \%} / \text{clay fraction finer than } 2\mu\text{m in \%} \quad \text{(Equation 2.1)}$$

Activity can indicate the volume change, i.e., low activity indicates low volume change, while higher activity indicates high swelling and shrinkage potential. The empirical formula developed in 1991 by Carter and Bentley (1991) to classify soil based on activity is provided in Equation 2.2 and illustrated graphically in Figure 2.4.

$$A_c = \text{Plasticity index (PI)} / (\text{Clay Content (C)} - 5) \quad \text{(Equation 2.2)}$$

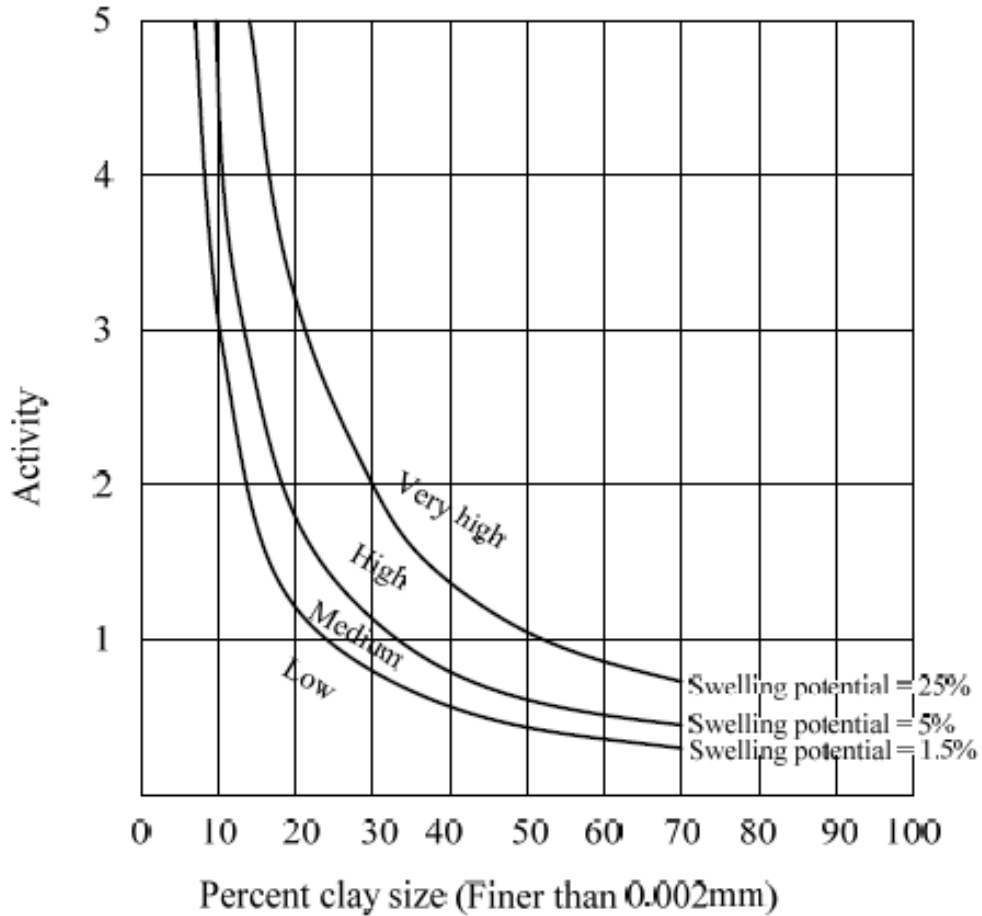


Figure 2.4 Classification chart for swelling potential proposed by Carter and Bentley (1991)

There are several theories for predicting the swelling pressure of soil using empirical relationships. Potential swell can be calculated from the plasticity index, as provided in Equation 2.3 and Table 2.2.

$$\text{Swell (\%)} = 60 \times \text{Constant } (\kappa) \times (\text{Plasticity Index (PI)})^{2.44} \quad \text{(Equation 2.3)}$$

where κ is equal to 3.6×10^{-5} (Carter and Bentley, 1991)

Another relation of the swell with the clay content can be calculated from the activity, as shown in **Error! Reference source not found.** (Seed et al., 1962).

$$\text{Swell (\%)} = \text{Constant } (\kappa) \times \text{Activity } (A_c^{2.44}) \times \text{Clay Content } (C^{3.44}) \quad \text{(Equation 2.4)}$$

Table 2.2 Identification of Possible Expansion based on Plasticity (Carter and Bentley, 1991)

| Classification of Potential Swell | Plasticity Index (%) | Volume Change (%) |
|--|-----------------------------|--------------------------|
| Low (0-1.5%) | 0-15 | 0-15 |
| Medium (1.5-5%) | 10-30 | 15-24 |
| High (5-25%) | 20-55 | 25-46 |
| Very high (>25%) | >40 | >46 |

2.1.4 Determination of Potential Swelling Based on Suction Values

Soil suction is the energy state of soil required to extract a unit volume of water from a given soil mass and is formed by the interaction of soil, air, and water. It is a microscopic property representing the negative pressure required to remove water from the soil and is comprised of two components: osmotic and matric (capillary). The osmotic suction appears due to salt inside the soil pore, and the matric suction, which varies with the soil type, creates capillarity inside the soil. The total suction is a combination of the two suctions, as shown in Equation 2.5 (Zhan et al., 2007).

Error! Reference source not found.

The swell can be calculated once the suction has been obtained. The swelling pressure based on suction values and effective overburden stress at the depth in question was proposed by Brackley (1980), as shown in Equation 2.6.

Error! Reference source not found.).

Determining the swelling potential and other properties of Yazoo clay has led to further characterization of this soil.

2.2 Atterberg Limits and Swelling of Yazoo Clay

Yazoo clay is an expansive soil with high plasticity, shrinkage and swelling potential, a liquid limit between 70 and 100%, and a plastic limit that fluctuates between 20 and 30 percent (Douglas and Dunlap, 2000). It can have damaging effects on structures, and increasing ponded water can cause a landslide. The volume changes from wet-dry cycles in Yazoo clay range from 100 to 235 percent (Johnson, 1973).

2.3 Relationship between Yazoo Clay and Landslides

There is a direct relationship between fully softened shear strength and landslides. Henkel and Skempton (1954) discovered that a failed, over-consolidated clay slope can develop fully softened shear strength. Residual shear strength forms after the soil achieves peak shear stress, and fully softened shear strength lies between peak and residual strength (Skempton, 1970). The peak strength of consolidated clay is usually equal to the fully softened strength of over-consolidated clay. Fully softened strength can occur in Yazoo clay, as well as other high plasticity clays, due to frequent wetting and drying of the soil, which, in Mississippi, is caused by the large amounts of rainfall and warm climate. This causes volume changes in

the soil that may result in structural damage to infrastructures built on it. Continuous swelling and shrinking can also cause cracks in the soil, which may lead to the presence of perched water and a reduction in the shear strength. Lee (2012) identified several correlations between different soil parameters for Yazoo clay (from **Equation 2.7** to **Equation 2.12**). These relationships illustrate the interactions between free swell, liquid limit, volume change, and water content and represent the non-strength properties that contribute to landslides. One nature-based solution to mitigating the expansive properties of Yazoo clay is the use of vetiver.

$$\text{Free Swell (FS) (\%)} = 1636.4e^{(-0.034 \times \text{dry density } (\gamma))} \quad (R^2=0.88). \quad \text{(Equation 2.5)}$$

$$\text{Liquid Limit (LL) (\%)} = 6.6168 \times \text{FS}^{0.5741} \quad (R^2=0.90) \text{ for } (70\% < \text{FS} < 140\%). \quad \text{(Equation 2.6)}$$

$$\text{Volume Change (VC) (\%)} = 0.5665 \times \text{LL}^{1.2368} \quad (R^2=0.88) \text{ for } (80\% < \text{LL} < 120\%). \quad \text{(Equation 2.7)}$$

$$\text{Free Swell (FS) (\%)} = 0.08 \times \text{LL}^{1.5754} \quad (R^2=0.90). \quad \text{(Equation 2.8)}$$

$$\text{Water Content after 24 hours } (\omega_{24\text{hr}}) (\%) = 2.5559 \times \text{LL}^{0.8571} \quad (R^2=0.92). \quad \text{(Equation 2.9)}$$

$$\text{Liquid Limit (LL) (\%)} = 0.5344 \omega_{24\text{hr}}^{1.0708} \quad (R^2=0.92) \text{ for } (100\% < \omega_{24\text{hr}} < 150\%) \quad \text{(Equation 2.10)}$$

2.4 Utilization of Vegetation as a Soil Bioengineering Technique for Landslide Mitigation

The roots of vegetation can strengthen soil and reduce porewater pressure by absorbing water for evaporation and transpiration (Krzeminska et al., 2019; Stokes et al., 2014). This method of slope protection is particularly efficient for shallow landslides, where the slip surface is within 1 - 1.5 m. (Hengchaovanich, 2003). Vegetation also minimizes surface water runoff, protects soil from wind-induced erosion, lessens the effects of rain, and promotes infiltration, as illustrated in Figure 2.5 (Coppin and Richards, 1990).

Vetiver has been utilized extensively for slope protection in several world regions (Mickovski and Van Beek, 2009), and numerous researchers have studied the effects of it and other forms of vegetation on landslides. Ziemer and Swanston, 1977; Wu et al., 1979; Riestenberg and Sovonick-Dunford, 1983; Reneau and Dietrich, 1987; and Riestenberg, 1994 conducted field research; Endo and Tsuruta, 1969; Waldron, 1977; Waldron and Dakessian, 1981; and Waldron et al., 1983 conducted laboratory-based research, and Sidle, 1992 and Krogstad, 1995 performed numerical modelling to substantiate that vegetation lowers surface runoff and prevents slope erosion. Slopes without vegetation experience more landslides (Kurupparachchi and Wyrwoll, 1992; Bishop and Stevens, 1964; Gray, 1981), and even a decrease in the amount of vegetation has been reported to increase slope displacement. (DeGraff, 1979; Swanston, 1988).

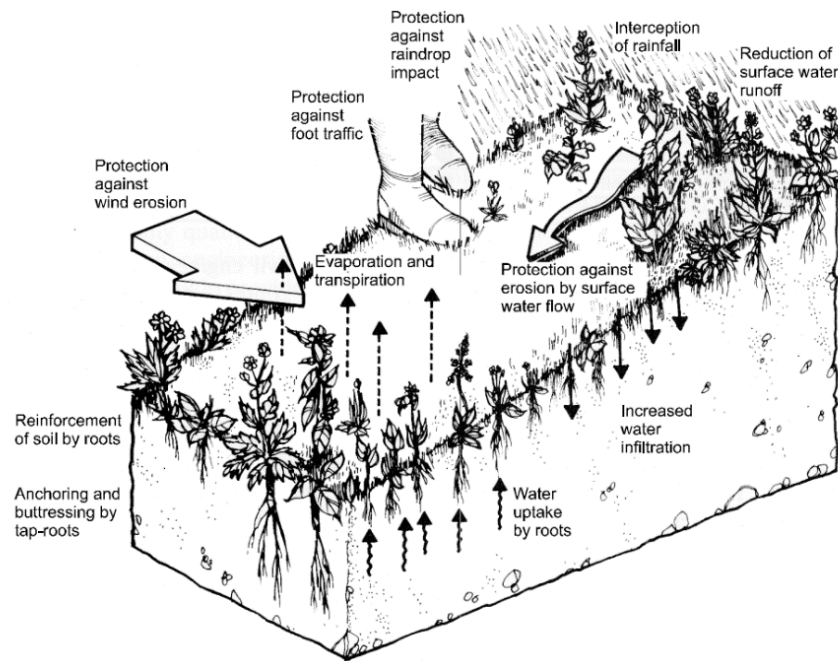


Figure 2.5 Impact of vegetation on soil (Coppin and Richards, 1990)

2.5 Vetiver Grass

Vetiver grass, also known as *Chrysopogon Zizanioides* and *vetiveria Zizanioides*, is an effective landslide mitigation alternative that can survive for approximately sixty years. Sunshine vetiver is the only genotype of vetiver species approved by the USDA (United States Department of Agriculture) for planting in the United States, as it is deemed minimally invasive (invasiveness score of -8) because no volunteer seedlings have been observed from plantings in the Pacific Islands over the past 15 years (Joy, 2009). According to research undertaken by the US Army Corps of Engineers on the invasive properties of vetiver, the plant may produce seeds, but they do not develop and produce seedlings in actual field conditions.

Vetiver is a non-competitive plant that avoids native plant species and has a dense bushy root system, shown in Figure 2.6, that can grow up to 3 m under ideal conditions within the first year of planting (D’Souza et al., 2019; Hellin and Haigh et al., 2002). It yields superior results in humid climates and rich, fertile soils, and can also grow in sandy soils, where no native grass can survive. Vetiver is not resistant to cold and can’t survive freezing temperatures (Sharif. M., 2000); however, it can withstand adverse environmental circumstances such as droughts and flooding, heat, extreme soil pH, alkalinity, salinity, and the toxicity of Al and Mn (Truong and Claridge., 1996). Typical ranges of environmental stress that vetiver can withstand are a pH 3.3–9.5 and 15 °C to 55 °C (Danh et al., 2009). In addition to its use as a remedy for slope instability, vetiver has many other global applications.



(a)

(b)

Figure 2.6 (a) Long busy network of vetiver roots (Kim et al., 2022), and (b) vetiver roots grown in sandy soil after 110 days (Badhon et al., 2021)

2.6 Different Applications of Vetiver

One of the advantages of vetiver is its diversified applications, e.g., it can be seen in the landfill, as well as at holistic healthcare facilities. It is used for phytoremediation, as it stabilizes, extracts, and filters heavy metal contaminants from landfills and wastewater (Danh et al., 2010), especially Pb and Zn (Antiochia et al., 2007), thus making it a bioengineering solution for landfill rehabilitation and leachate treatment (Truong et al., 2010). (See Table 2.3 [Phusantisampan et al., 2016].) Vetiver is also effectively used to enhance the quality of soil and treat wastewater by removing contaminants (Babalola et al., 2007) such as oil (Brandt et al., 2006) and trinitrotoluene (TNT) from soils pretreated with a urea chaotropic agent (Das et al., 2010). It is effective in treating wastewater by reducing the biochemical oxygen demand (BOD) and enhancing the removal of total nitrogen (TN) and total phosphorus (TP) (Darajeh et al., 2016).

Ash derived from vetiver grass (VGA) contains approximately 7% more silica and potassium oxide (K₂O) than fly ash and is categorized as a Class C pozzolana by the ASTM standards. VGA mortar can be used to construct chemically exposed foundations, maritime projects, sewers, and other buildings (Nimityongskul et al., 2003).

Vetiver roots can improve crop output by enhancing infiltration (Dousset et al., 2016) and improving the soil's capacity to retain water and nutrients (Babalola et al., 2007), and its effectiveness in reducing erosion exceeds that of the ground modification chemical polyhedral oligomeric silsesquioxanes, or POSS (Kidd et al., 2011). It is also utilized in ceramic production as a flux agent at low temperatures (600 °C) to produce a glassy phase due to its high potassium and silica content (Islam et al., 2013; Gnansounou et al., 2017).

Vetiver grass is used for making oil, which has is therapeutic and impacts several critical physiological processes through tissue remodeling and cholesterol metabolism (Han and Parker, 2017). For example, virulent and avirulent strains of tuberculosis are combatted with vetiver oil (Saikia et al., 2012), its unique scent makes it an effective insect repellent for outdoor pests, and it has been successfully used to eliminate subterranean termites (Zhu et al., 2001). Vetiver roots and grass are rich in carbon; consequently, residues from vetiver oil production are suitable for producing activated carbon. Vetiver's use has expanded to natural food additive production, herbal drinks, commercial mushroom cultivation, and vermicomposting (Chomchalow et al., 2015; Akther et al., 2010; Balasubramanyan et al., 1996). In 120 nations across the globe, vetiver is utilized in a myriad of ways, and its use is rising (Truong and Loch, 2004).

Table 2.3 Heavy Metal Absorption Capacity of Vetiver Compared to Vascular Plants (Danh et al. 2010)

| Name of heavy metals | Threshold Levels in Soil (mg/kg) | | Threshold Levels in Plants (mg/kg) | |
|----------------------|----------------------------------|-----------------|------------------------------------|-----------------|
| | Vetiver | Vascular plants | Vetiver | Vascular plants |
| Arsenic | 100–250 | 20 | 21–72 | 1–10 |
| Cadmium | 20–60 | 1.5 | 45–48 | 5–20 |
| Copper | 50–100 | Not available | 13–15 | 15 |
| Chromium | 200–600 | Not available | 5–18 | 0.02–0.20 |
| Lead | >1500 | Not available | >78 | Not available |
| Mercury | >6 | Not available | >0.12 | Not available |
| Nickel | 100 | 7–10 | 347 | 10–30 |
| Selenium | >74 | 2–14 | >11 | Not available |
| Zinc | >750 | Not available | 880 | Not available |

2.7 Mechanical Properties of Vetiver

Vetiver’s long, bushy roots interact with the soil to produce a new composite substance that has roots with excellent tensile strength. The vetiver roots affect the soil by transmitting shear stress in the soil matrix to the tensile strength in the roots. During rainfall events, vetiver's deep roots increase water penetration rates and provide traction to prevent the soil layer from sliding (Dousset et al., 2016). Figure 2.7 illustrates mature vetiver stabilizing a slope following a rain-induced shallow slope failure.



Figure 2.7 Vetiver stabilizing a previously failed highway slope in Mississippi.

Various researchers have shown that vetiver impacts soil’s shear strength, hydraulic permeability, pore pressure, and slope slip surface under severe rainfall conditions and surface runoff. Therefore, it is essential to consider the tensile strength and shear strength of vetiver roots when designing a bioengineering solution that uses vetiver.

2.7.1 Tensile strength and shear strength of vetiver roots

Both roots and soil resist horizontal forces in root-reinforced soil, and the tensile strength produced by the roots contributes to the strength of the soil (Badhon et al., 2021). Vetiver's lengthy, bushy root structure can have a mechanical effect on a slope by reinforcing and removing water for transpiration and evaporation. Similar to other root reinforcements, the contribution of vetiver roots to soil shear strength or root cohesion can be determined by the following equation:

$$S_r = T_R * [A_R/A] * (\sin \theta + \cos \theta \tan \phi') \quad \text{Equation 2.11}$$

Where T_R = mobilized root tensile stress on the root, A_R/A = Root area ratio or ratio between root and total area, ϕ' = the friction angle of soil, θ = is the angle of root deformation (Wu et al., 1979).

To precisely anticipate the soil shear strength produced by vetiver roots, the ultimate tensile strength of the roots must be accurately estimated, as it mobilizes the force on the slope exerted by the roots' movement (Islam et al., 2021). While the root is reinforced, the shear strength value of the soil can be calculated by the following equation:

$$\tau = S_r + c + \sigma \tan \phi' \quad \text{Equation 2.12}$$

Where c is the effective cohesion of soil, σ is the usual stress.

A constant value of 1.2 can be used for the added cohesion value provided by the roots, replacing the latter part of the equation with the condition that the range of θ will be from 48-72 degrees (Wu et al., 1979). In that case, the value of S_r can be obtained by Equation 2.15:

$$S_r = 1.2 * T_R (A_R/A) \quad \text{Equation 2.13}$$

Numerous researchers have precisely predicted the tensile strength of vetiver root systems. The root strength decreases as its diameter grows (Figure 2.8), and the tensile strength of smaller-diameter roots before rupture under tension is greater, while the tensile strength of larger-diameter roots is lower.

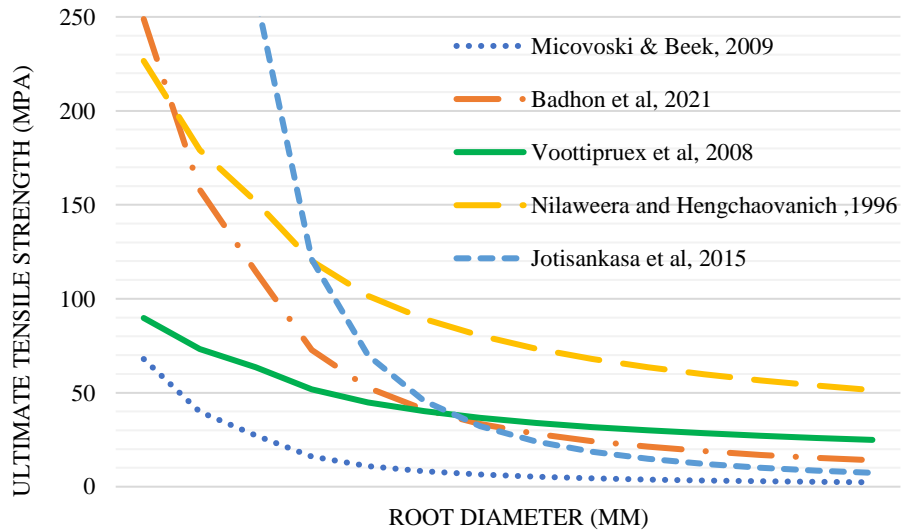


Figure 2.8 Variations of root tensile strength of vetiver roots with increased diameter

2.7.2 Pullout force on vetiver-rooted soil

The root strength of root-soil composite materials mobilizes the force generated by soil's movement, and an extensive root system has a greater mobilization capacity when covering a potential failure surface. The pulling force must be derived as a limiting condition of loading on a slope (Waldron and Dakessian, 1981), and the pull-out strength is the tangential friction between the root and soil that depends more on root bending, root filaments and branches, and root tensile strength at breakages than on slope conditions (Abe and Iwamoto, 1986; Tsukamoto, 1986). The uprooting force increases in vetiver-rooted soil until it reaches its maximum value, then decreases due to root slippage or rupture (Figure 2.9a). The root pullout strength of vetiver is significantly affected by root spreading, as the value of the force increases with the spreading of the roots (Figure 2.9(b)). (Mickovski et al., 2005).

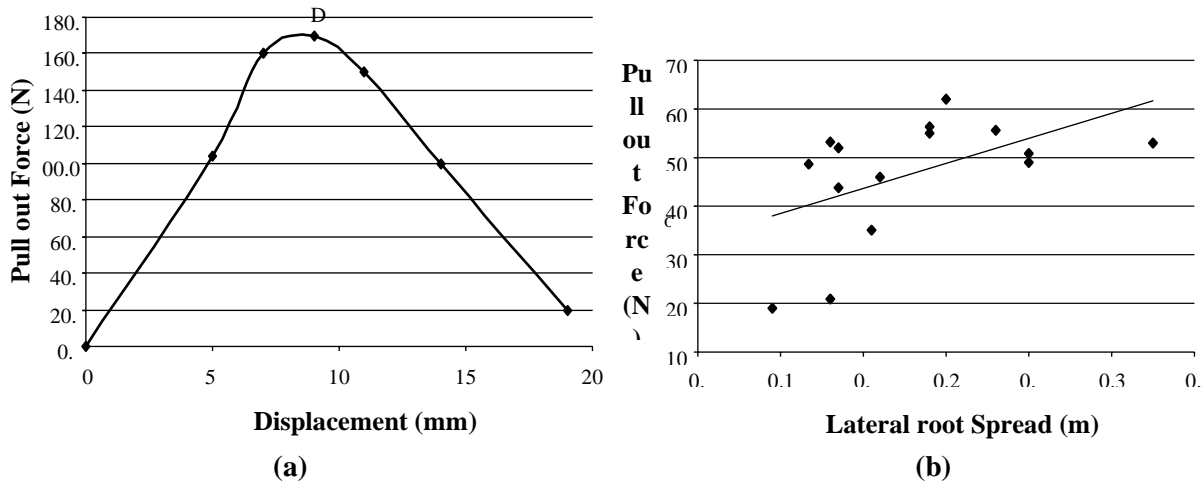


Figure 2.9 Variations of pullout force of vetiver roots: (a) with displacement (Newton vs. mm), (b) lateral root spread (Newton vs. mm) (Figure courtesy of Mickovski et al., 2005)

2.7.3 Impact of vetiver on soil shear strength

The shear strength of soil is the maximum shear stress it can withstand before failure. Cohesion, or the force that holds soil particles together, and the resistance of particles caused by friction or interlocking when particles move over one another provide most of the shear strength (Flerchinger et al., 2005). The shear strength of soil is calculated from the following equation:

Error! Reference source not found..

Where c is the cohesion of soil, σ' is the effective stress, and ϕ' is the friction angle.

Triaxial and direct shear testing are frequently used interchangeably to assess the shear strength of soil, despite the possibility of variations in test results (Castellanos and Brandon, 2013). Researchers employ direct shear testing to determine that the strong tensile strength of vetiver's long, bushy roots influences soil cohesion, friction angle, and shear strength (Rahardjo et al., 2014). Mickovski and Van Beek (2009) examined the influence of vetiver on clay soil in Spain, Islam et al. (2013) explored vetiver-rooted soil in Bangladesh's low-plasticity clay and silty sand, and Ali and Osman (2008) investigated the influence of vetiver on sandy soil in Malaysia, and all found that vetiver increases the soil's cohesiveness and peak shear stress. (See Figure 2.10) D'Souza et al. (2019) found that vetiver-rooted sandy soil exhibits greater peak shear stress values than non-rooted soil, but the values decrease with increasing depth, and 2.11) In addition, root area ratio impacts the soil shear strength which means peak shear stress value increases with

the increase of root area ratio (see Figure 2.12). Vetiver rooted soil show more ductile behaviour compared to the not rooted soil (see Figure 2.13).

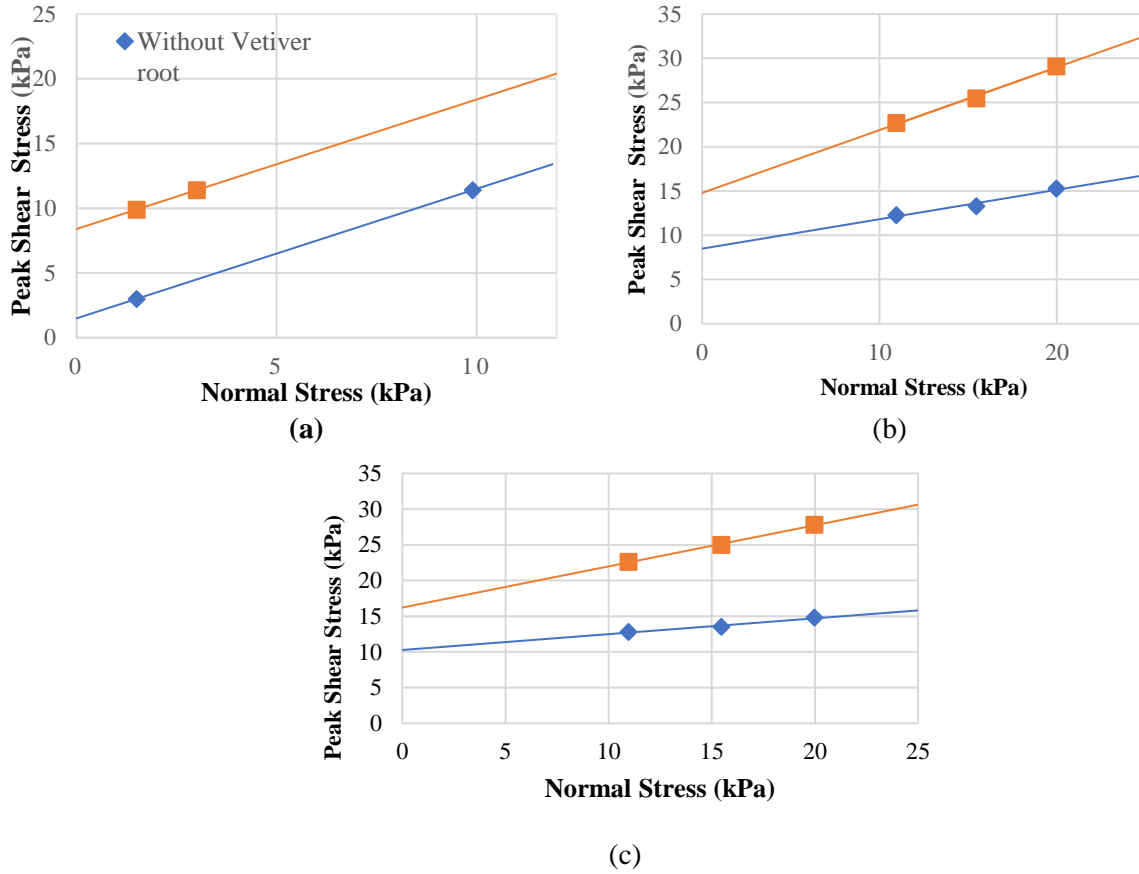


Figure 2.10 Comparison of the undrained shear strength of non-rooted and vetiver-rooted soil under different normal loading: (a) clay soil (values issued from Mickovski and Van Beek, 2009), (b) silty sand (values issued from Islam et al., 2013), (c) low plasticity clay (values issued from Islam et al., 2013)

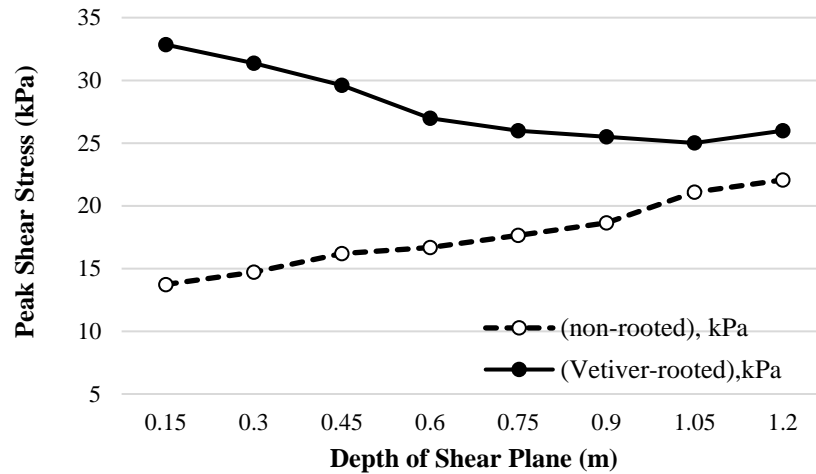


Figure 2.11 Variations of peak shear stress values with depth in vetiver-rooted soil based on a direct shear test (values issued from D’Souza et al., 2019)

The root area ratio (RAR) correlates directly with shear strength, as shown in the following equation:

$$(\tau = Sr + c + \sigma \tan \phi') \quad \text{Equation 2.12}$$

It also indicates that the RAR influences the peak shear stress in soils with vetiver roots. Experiments revealed that the peak shear stress values increase with the root area ratio (RAR), showing that roots with a higher RAR have stronger shear strength (Figure 2.12). Rooted soil may also sustain more significant strain, allowing for larger deformation before failure in vetiver-rooted soil than in unrooted soil (Figure 2.13 (b) and (c)).

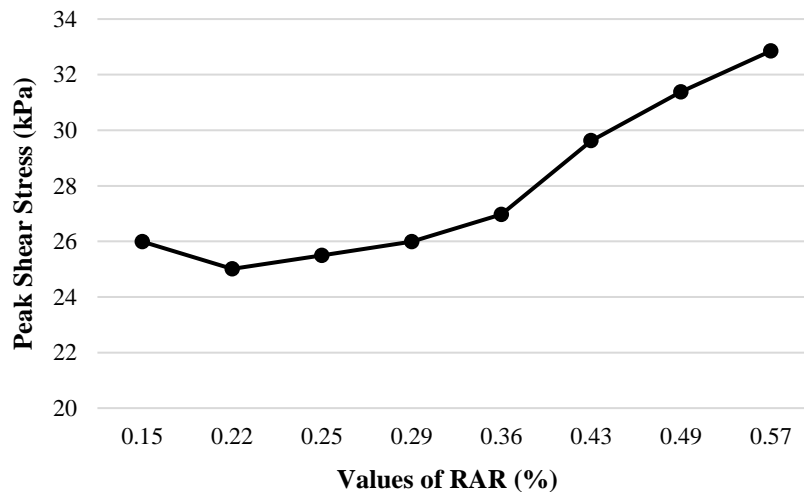


Figure 2.12 Variations of peak shear stress with root area ratio in vetiver- rooted soil based on a direct shear test (Values issued from D’Souza et al., 2019)

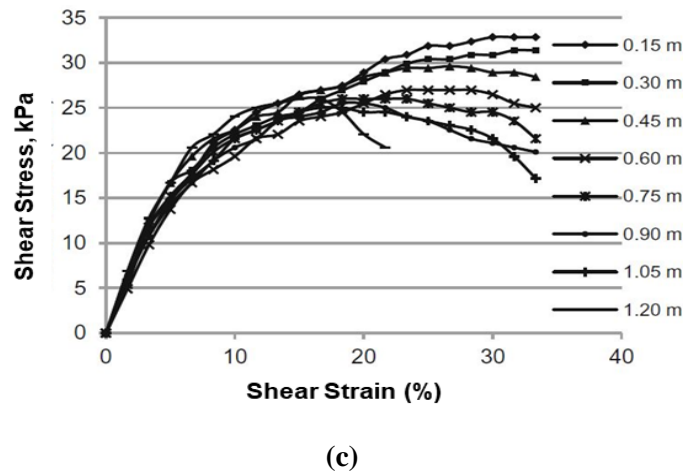
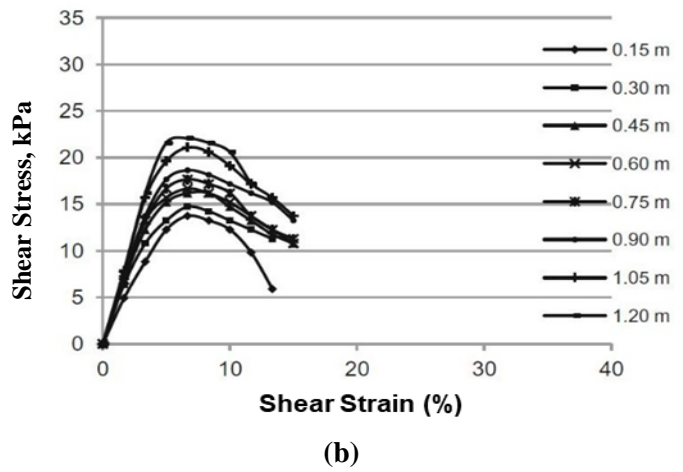
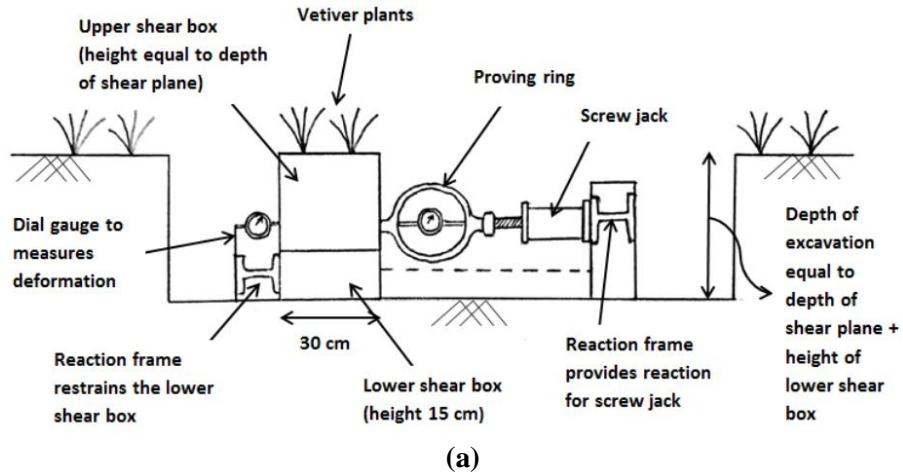


Figure 2.13 Variations of shear stress under different strain conditions and depths: (a) laboratory setup, (b) unrooted soil, c) vetiver-rooted soil (figure courtesy of D'Souza et al., 2019)

Triaxial testing was performed on vetiver grass cultivated on poorly graded sand in the tropical environment of Singapore. Based on the Mohr-Coulomb failure envelope derived from the test findings in saturated soil circumstances, vetiver roots increased the cohesion value from 2 kPa to 10 kPa and the friction angle from 29 degrees to 34 degrees. (See Figure 2.14.) These results exceeded those of orange jasmine,

another native plant and confirmed the results of the direct shear tests by showing that vetiver-rooted soil can endure higher deformation than soil without roots, before reaching its maximum shear stress in an unsaturated state. As the rooted soil demonstrates ductility before collapse, it can also be an early warning system for future landslides.

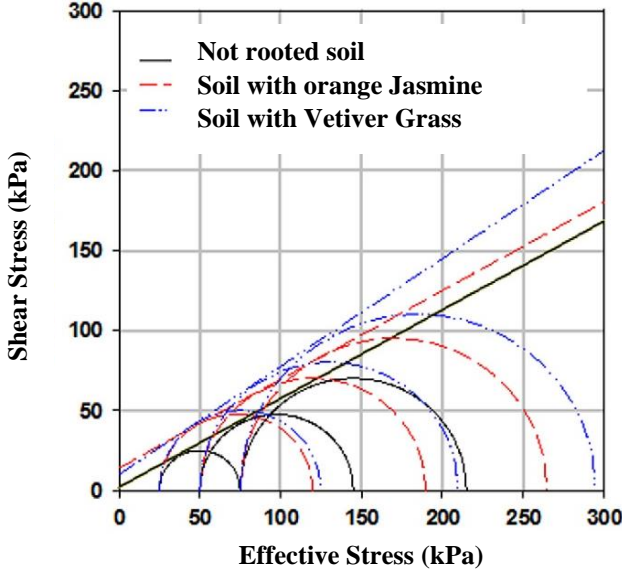


Figure 2.14 Comparison of Mohr-Coulomb failure envelopes at zero matric suction with the original soil, soil with local orange jasmine tree, and vetiver grass roots (figure courtesy of Rahardjo et al., 2014)

Chapter 3: Laboratory Testing

This chapter describes the laboratory tests conducted on the tensile strength of vetiver root. It briefly discusses the testing device, testing method, and test results, using MATLAB regression analysis. The root tensile properties of the vetiver, based on the analysis, are also described, including the variations of stress-strain under axial loading conditions and the variations of the axial load on the vetiver with deformation and strain. Finally, it introduces the secant modulus of elasticity, E_s , based on the stress-strain curve.

3.1 Laboratory Testing Preparation

There are no commercial vetiver farms in Mississippi, so vetiver grass was purchased out of state and shipped to Mississippi for these studies. In July 2021, the roots were transplanted into garden soil in plastic garden beds and bins at Jackson State University and were grown for one year. No fertilizer was used, and it was watered five days a week. The first root sample, shown in Figure 3.1, was extracted in January 2022, as provided in Figure 3.1, after which it was thoroughly rinsed with water to remove soil from the root system.

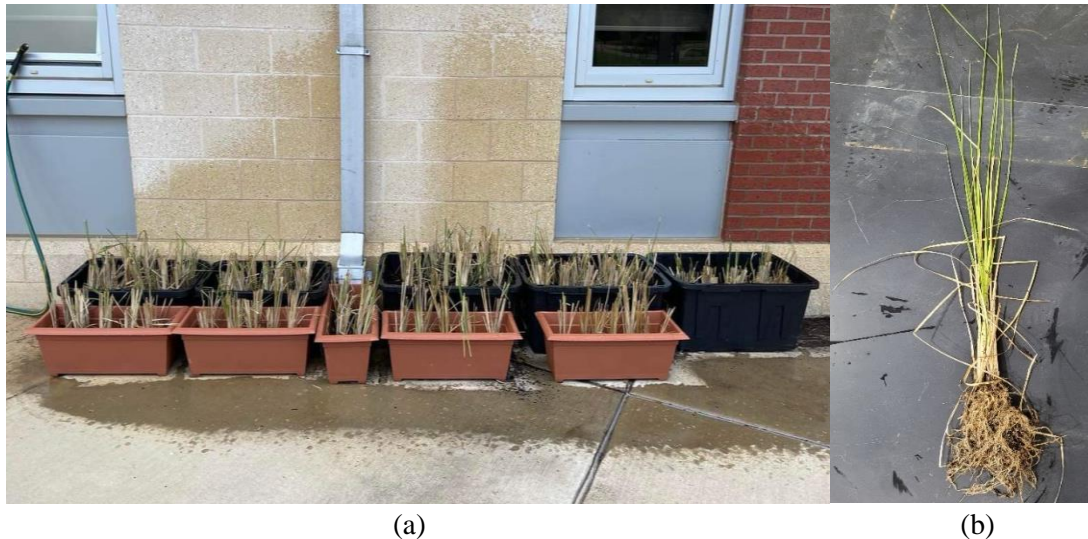


Figure 3.1 (a) Vetiver grown at Jackson State University, (b) vetiver collected for root testing

The roots were tested using the GeoJac digital load actuator, which can be used for automated unconfined compression testing, triaxial testing, and consolidation testing (incremental and constant strain rate). The loading device has a load cell with 8.9 kN of loading capacity and a linear variable displacement transducer (LVDT). The LVDT moves downward with the downward movement of the load cell. The entire device is operated from a computer and includes a user-friendly interface of the settings during testing. The

equipment must be calibrated, and the strain rate and maximum strain limit must be set before use. (See Figure 3.2.)

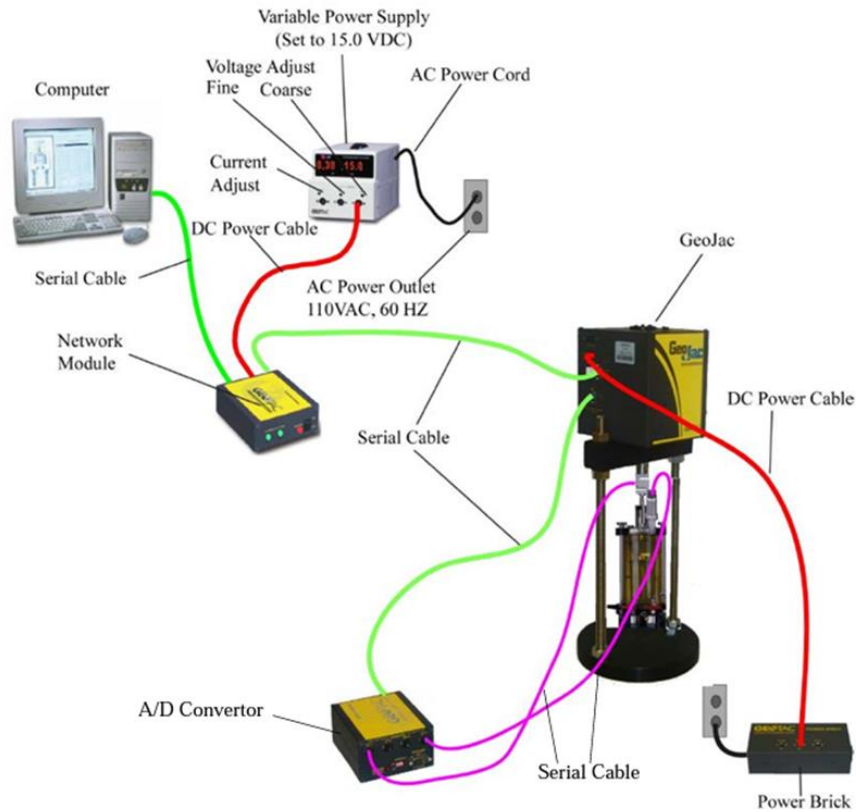


Figure 3.2 GEOJAC testing device (figure courtesy of Liu, 2015)

The device was modified and plates were developed for measuring the tensile strength of the vetiver roots; the plate used in this study is shown in Figure 3.3. The metal circular plate has two rubber pads inside so that the vetiver can be clamped between them. The size of the opening between the pads can be adjusted with a screw to secure the vetiver to the plate. Before each test, roots of approximately 2 mm in length were firmly clamped and precisely aligned vertically so they wouldn't shift while the load was applied. The root samples were reduced to a length of approximately 50 mm for testing, and the clamping was tested to ensure that the roots did not slip and that the roots broke in the tensile load at two-thirds of their length (Mickovski and Van Beek, 2009). The tests were performed immediately after the samples were extracted from the soil, as it was determined that they lose moisture quickly if they are rinsed and allowed to air-dry. Trials were conducted to select the strain rate per minute (1%); the optimal breaking point at the two-thirds distance was not observed at the lower strain value. In lower strains, the testing device reached the largest degree of downward displacement before the root breaking point, which required multi-stage loading for the root. Therefore it was determined that at 1% of strain per minute, the load cell is restricted because it has reached its maximum allowable movement. After much trial and error, a strain-per-minute of 5% was fixed as the test rate for vetiver roots, and the roots were tested at a maximum of 50% strain at a rate of 5% of strain per minute.

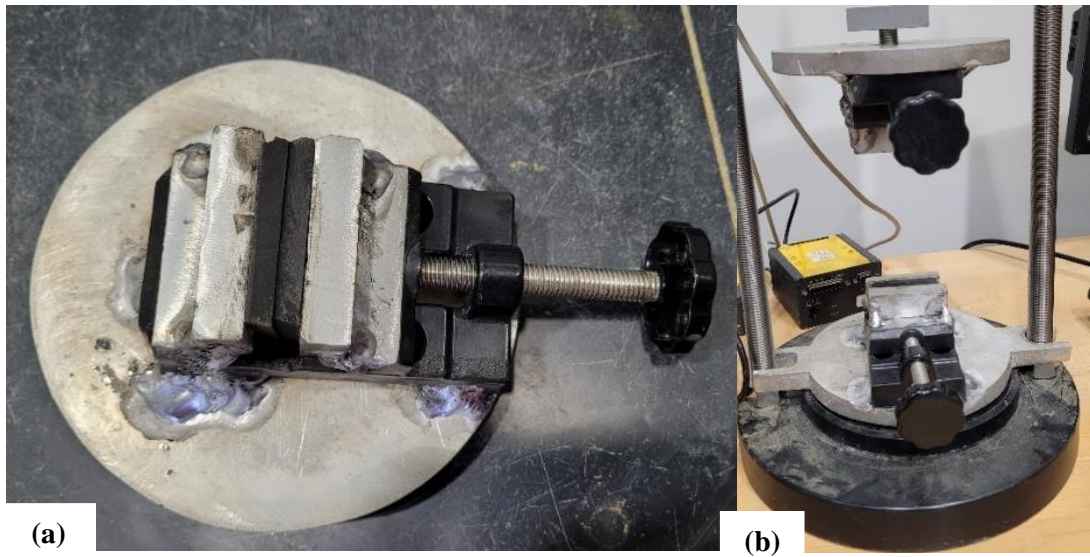


Figure 3.3 (a) Circular plate for vetiver root strength testing, (b) GeoJac with plate before testing

3.2 Vetiver Root Strength Testing

The first set of root sample testing was completed in January 2022; the second set was completed in July 2022. An effective root length of 50 mm was maintained for each test, and a strain rate of 5% per minute was applied on the roots with a maximum strain rate of 50%. The 50 mm root samples were clamped on both sides and kept in tension until they failed.

The roots that failed during loading were selected for further analysis based on the criteria that the root samples with varied diameters were represented and the roots failed at two-thirds of their length. The results did not include other roots that failed at the clamps. Figure 3.4 depicts a root specimen before and after failure. Twenty (20) vetiver root samples were selected from each group to predict the tensile strength.

3.3 Data collection

After performing the tests for tensile strength, the root stress was calculated for the different strain conditions. The load cell was estimated for a 50 mm diameter soil sample or 2026 mm² area, and the root stress values were 2 mm in length and varied in diameter. The root stress was calculated per Equation 3.1:

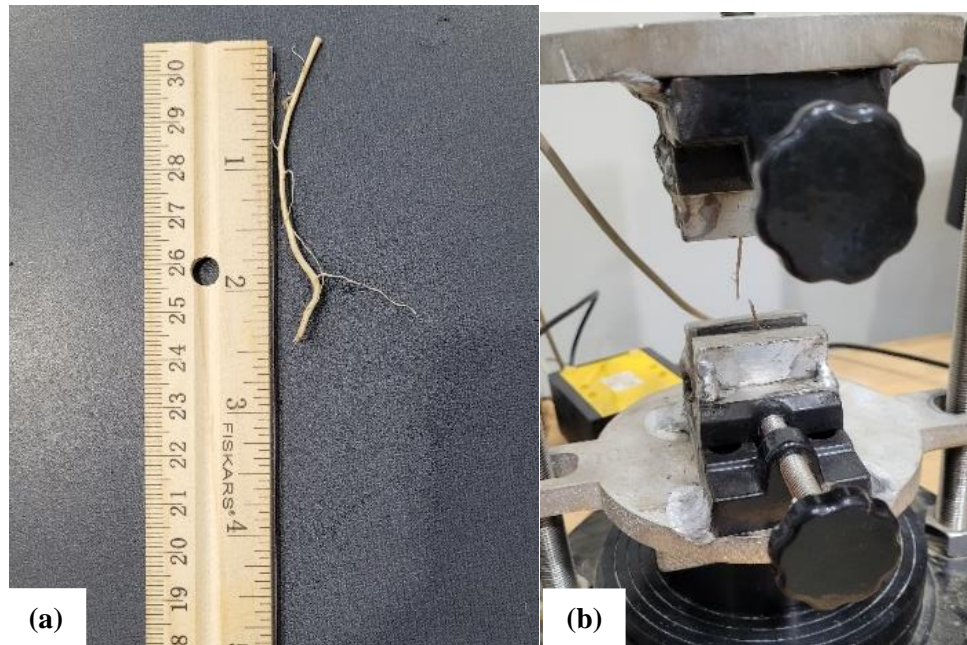


Figure 3.4 (a) Two-inch vetiver root before testing, (b) rupture of vetiver root

3.4 Data analysis

All the test data were computed following the root strength test to determine the root load. Root strain values were gathered, depending on the root's diameter and length of 50 mm. MATLAB regression analysis was performed on the root stress and root strain values to obtain the best-fitting curve for the roots. It is possible to employ a basic linear regression model, but it was observed that the variables in the roots of the vetiver are not linearly connected. Therefore, a nonlinear regression model was utilized until the stress-strain curve fit nicely with the power function ($y = ax^b$). Regression analysis was conducted for load vs. deformation and tensile strength versus root diameter, and the root squared (R^2) values and root mean square error (RMSE) values were examined to see whether the model best fits the actual data points.

3.5 Results

3.5.1 Stress vs. strain

Understanding tensile property requires examining the stress variation with increasing strain. As the loading condition increases, the stress level also increases. In axial stress circumstances, it was observed that roots do not fail abruptly; rather, stress promotes ductility. In addition, the elongation feature lacks correct elasticity, as there is no lasting deformation before the yield point. The stress-strain behavior corresponds more closely with the power function for vetiver roots, indicating that the roots are more elastoplastic than elastic or plastic. Most root stress values exist beneath 40% strain conditions, but some may show failure stress at strain conditions exceeding 50%. An empirical equation for determining the stress value from the strain is provided in the following equation, which was derived from Figure 3.5.

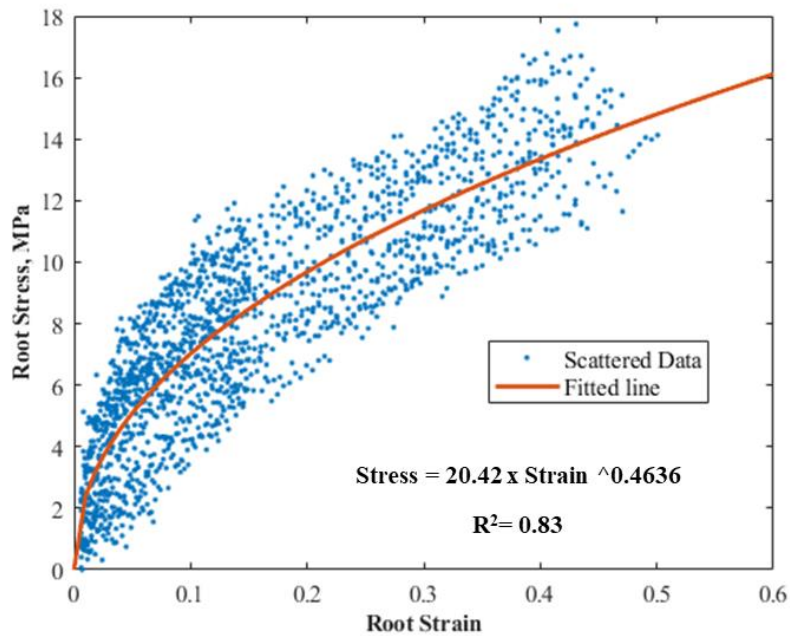


Figure 3.5 Root stress vs. root strain curve for vetiver roots (based on six-month samples) (MPa vs. mm/mm)

The model equation was tested with one-year samples and confirmed that the model could accurately predict the root stress-strain behavior of vetiver roots grown in expansive soil conditions. The best-fit curve drawn on the stress-strain properties of vetiver is shown in Figure 3.6.

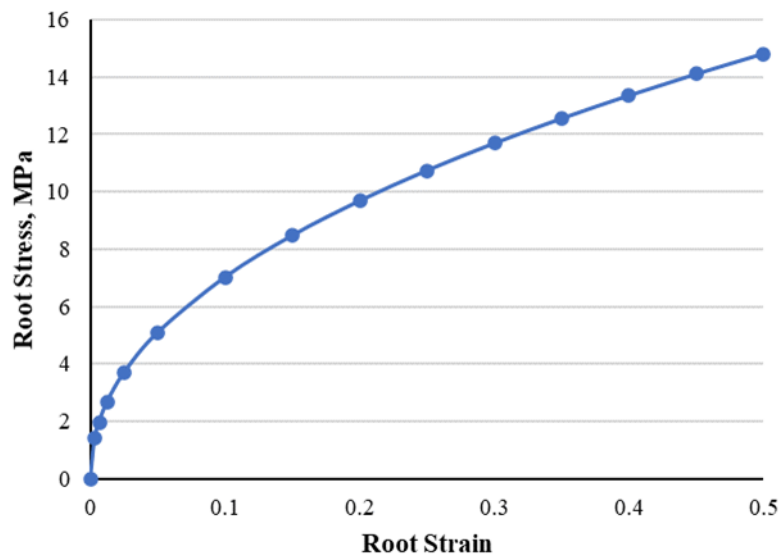


Figure 3.6 Best-fit root stress vs. root strain curve (MPa vs mm/mm)

The stress-strain behavior was tested on four random samples to check the validity of the root stress-strain relation, and the results showed that Equation 3.2 accurately predicts the variations of root stress in increasing strain in axial loading conditions (Figure 3.7).

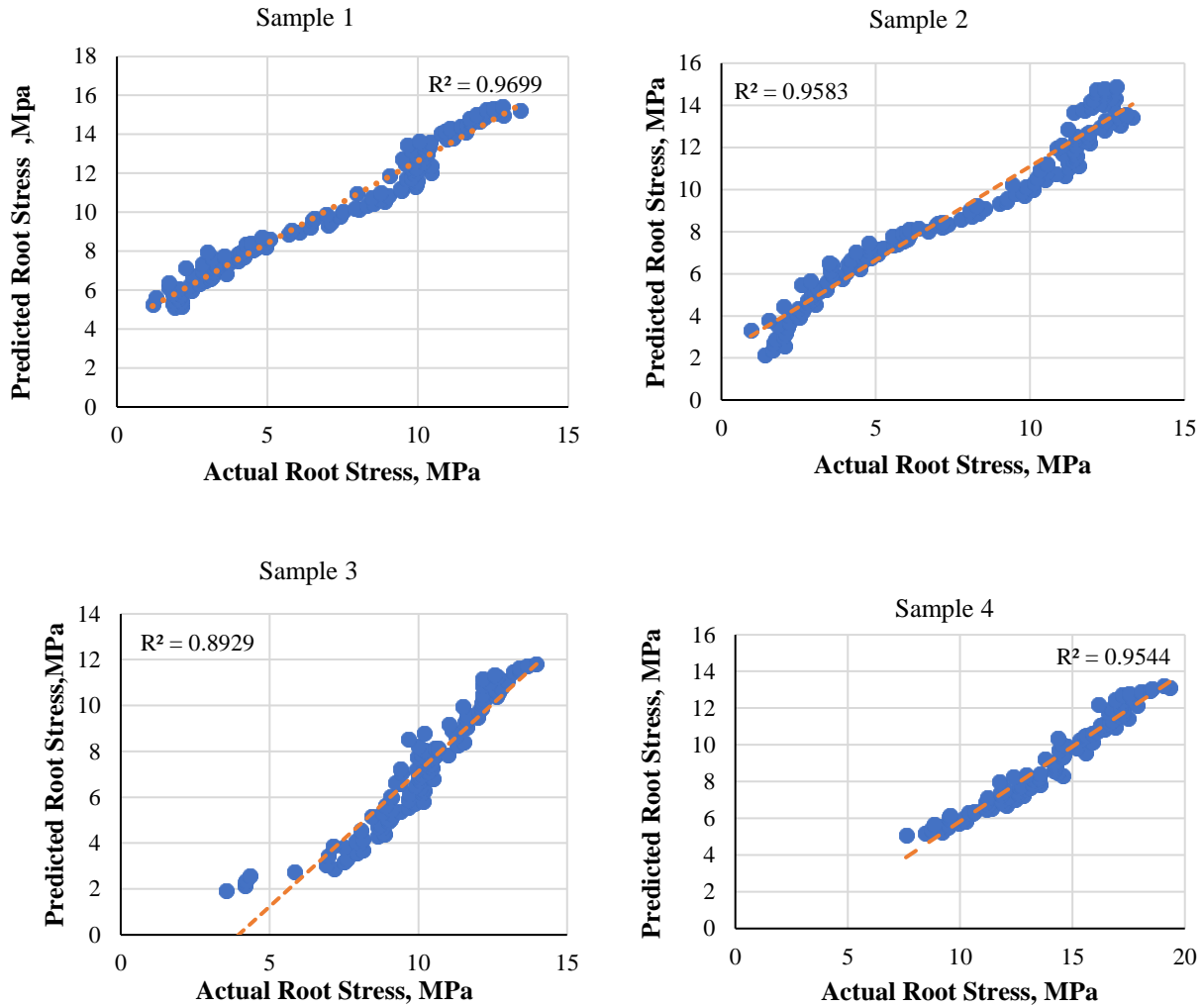


Figure 3.7 Actual vs predicted stress on stress-strain curve equation (MPa Vs. MPa)

It was observed that a single root of vetiver grass can experience up to 13.35 MPa of tensile stress under axial loading conditions (Figure 3.8), and an average of 50 vetiver roots grown in a laboratory can sustain up to 667.5 MPa. Given that a vetiver plant develops multiple roots and that 60-grade rebar has a minimum tensile strength of 520 MPa, the value is highly promising.

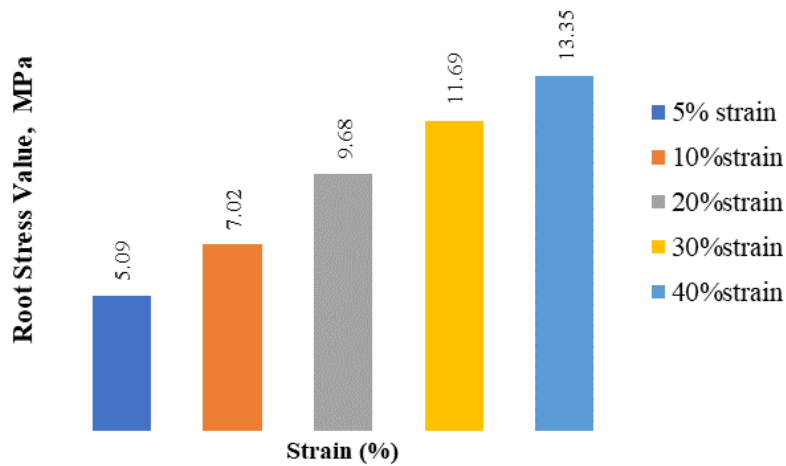


Figure 3.8 Vetiver root strength at different root strains (MPa Vs. mm/mm %)

3.5.2 Load vs. deformation

As shown in Figure 3.9, when the roots are longer, there is a linear increase in load. Up to 13 N of force root can exhibit a 40% strain condition, which is considered a failure strain. Experiments have shown that soil moisture significantly affects root growth and development and roots. As moisture content decreases in roots, root tensile strength drops significantly.

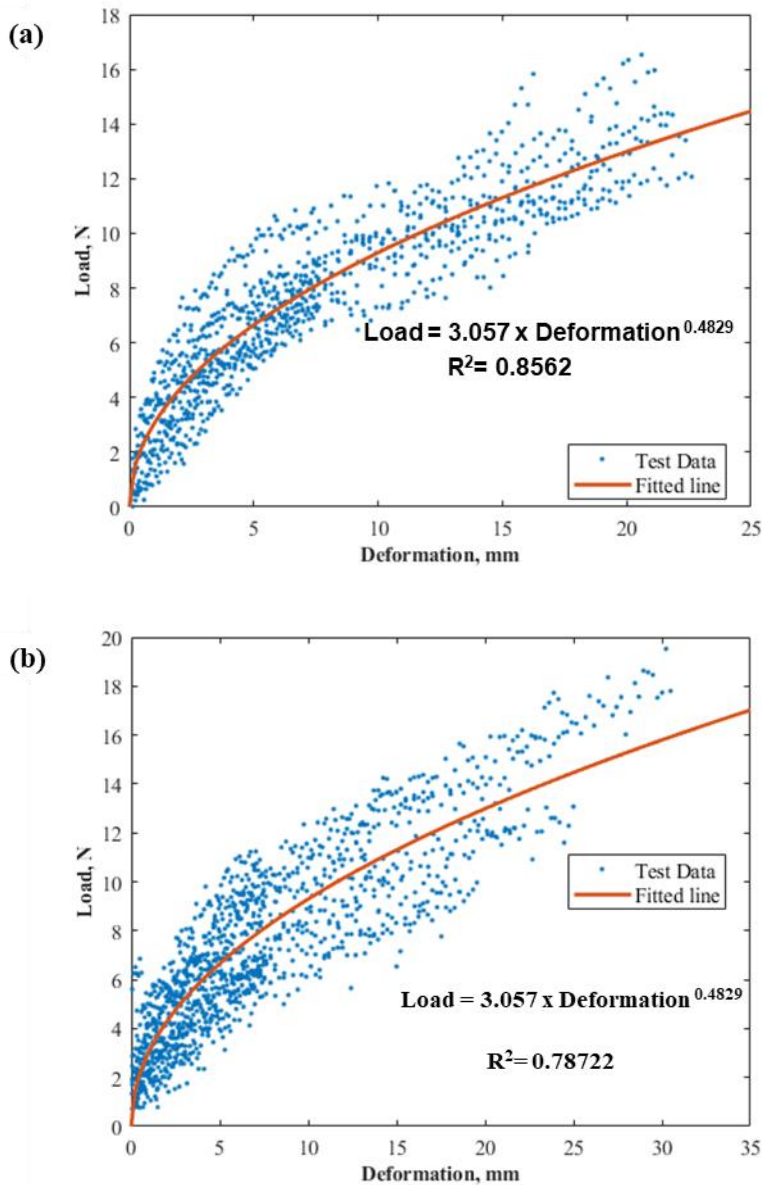


Figure 3.9 Load vs. deformation curve for vetiver roots at: (a) six months and (b) one year (N vs. mm)

3.5.3 Ultimate tensile strength vs. root diameter

Figure 3.10 shows that root strength is determined by the root's biological components: smaller diameter roots contain more cellulose and are therefore stronger than those with a larger diameter (Genet et al., 2005). The ultimate tensile strength of vetiver roots exhibits a similar trend of fluctuation with diameter. The root

ultimate strength data variations were plotted in the one-year sample data analysis and show that roots with a smaller diameter have greater strength; however, the strength declines as the diameter increases.

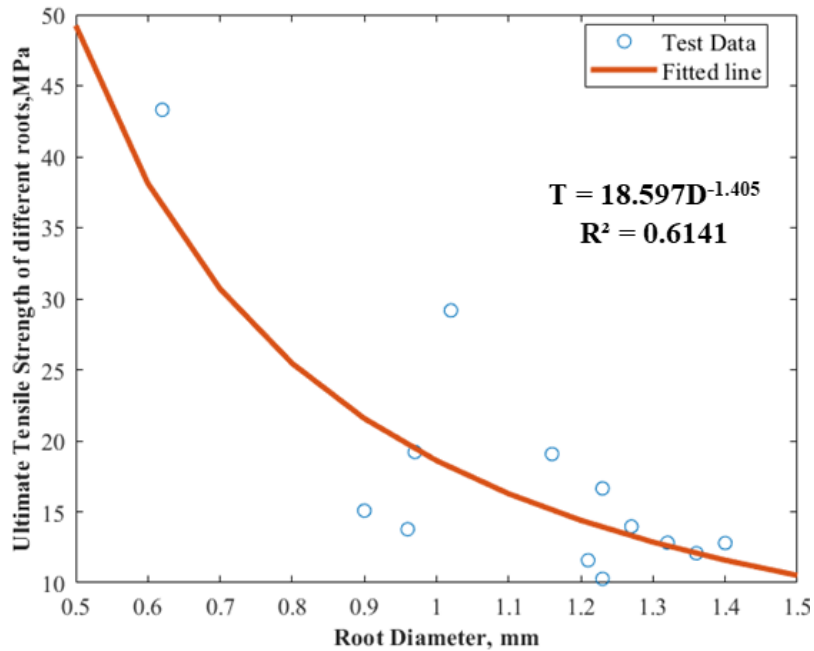


Figure 3.10 Variations of root ultimate tensile strength with root diameter (MPa vs. mm)

Although Nilaweera and Hengchaovanich (1996) measured higher value of vetiver root strength than in other circumstances, the subsequent results on root tensile strength are more reliable due to significant improvement of load testing device. The present study on the tensile strength of vetiver root is in close agreement with that of Jotisankasa et al. (2015), who also examined the root strength of vetiver grown in a controlled laboratory environment (Figure 2.8). Figure 2.8 was modified to include data from this study in Figure 3.11

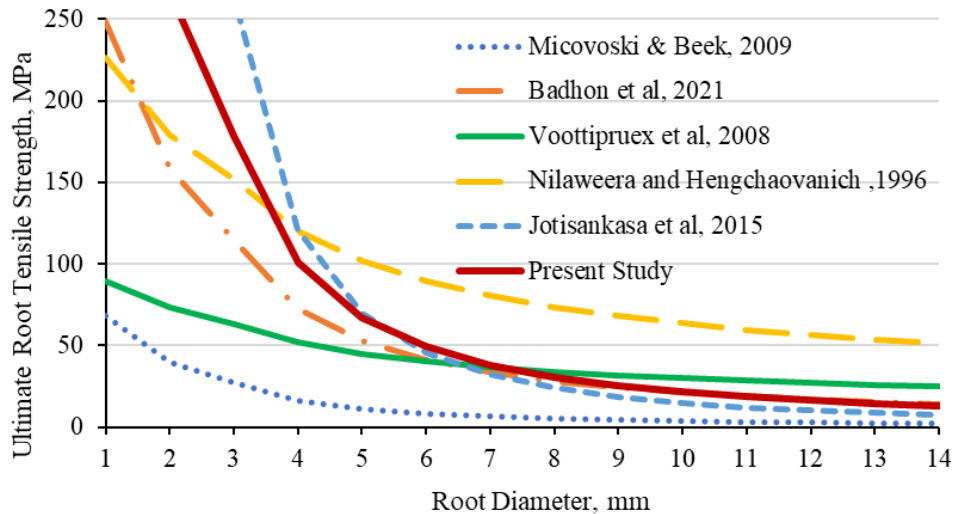


Figure 3.11 Comparison of results of this study’s ultimate tensile strength tests with those of other researchers

This study, as well as the results of Mickovsky and Beek's tests in 2009, determined that the ultimate tensile strength of vetiver roots is 17.7 MPa; Nilaweera and Hanchaovanich (1996) determined that it is 75. From the best-fit stress-strain curve, the value was determined to be 13.35 MPa. The variations in test results from different studies indicate that soil and climate influence vetiver growth and eventually impact root tensile strength. (See Figure 3.12.)

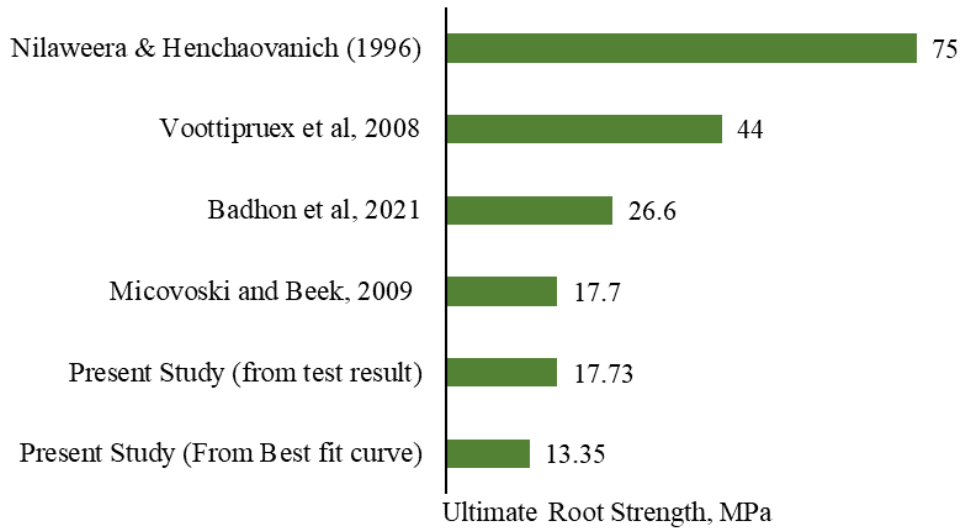


Figure 3.12 Comparison of ultimate tensile strength (in MPa) determined by various studies

Chapter 4: Field Investigation of Slopes Improved with Vetiver Grass

4.1 Site Selection

The primary objective of this field investigation was to evaluate the performance of slopes planted with vetiver grass roots and understand the failure mechanisms of Yazoo clay slopes. The use of vetiver as a bioengineering solution to stabilize slopes constructed with expansive soil is minimal in the US due to a limited study of the field performance in US soil types and hydrological conditions. For example, some of those who introduce vetiver to US industries are scientists and biologists, and they often do not consider its impact on infrastructure. Consequently, it is imperative that the vitality of vetiver in expansive clay and its response to changes in the US climate be explored. In the present study, 'Sunshine' vetiver grass was planted on the two slopes, as presented in Table 4.1. Slope 1 consists of a levee section at the U.S. Army Engineer Research and Development Center (ERDC) in Vicksburg, MS, and Slope 2 is a highway embankment along the I20E exit towards Terry Rd in Jackson, MS. Slope 2 has a record of previous failure and repair.

Table 4.1 Selected Site Locations

| Site No | Site Location | Site Coordinate | Aerial view |
|---------|---------------|-------------------------------------|--|
| Slope 1 | ERDC | 32° 18' 8.15"N, 90° 51' 20.34"W |  |
| Slope 2 | Terry Road | 32° 16' 48.92"N, 90° 12' 44.03"W | |

4.2 Slope 1: ERDC Test Levee Section

Slope 1 is the downstream land side of the downstream catch basin levee that is located at the Rapid Levee Repair Test Facility constructed in 2010 at the ERDC. It is a three-horizontal-to-one-vertical (3H:1V) slope with a crest height of 3.7 m above the bottom of the catch basin and the downstream land side toe. Per the construction drawings, the top of the riser pipe in the catch basin is at an elevation of 45.4 m MSL, and the levee crest is at EL 46.3 m MSL, providing a freeboard of 0.9 m. The levee is comprised of loess (low plasticity silt) that was left in place on the site, overlain by on-site loess fill that was compacted in a 22.9 cm maximum lift thickness to 95% of its maximum dry density and $\pm 2\%$ of its optimum moisture content. A 61 cm thick high plasticity clay barrier capping the levee is overlain by 10.2 cm of topsoil for vegetative cover. The planting seasons of the hulled and un-hulled Bermuda grass used onsite were from April 1st to August 31st and September 1st to February 28th, respectively. Ryegrass may have also been used at the time of construction, based on the specifications. The vegetative cover of the levee was fully grown and regularly maintained at the time of this study. The soil pH is between 6.0 and 7.0. Figure 4.1 shows aerial and west-side views of the slope. The levee was stable, with no visual seepage on the slope or toe of the downstream levee at the time of the study. The field demonstration of vetiver was performed in two phases to investigate its growth during the summer and the winter.



Figure 4.1 Location of Slope 1: (a) aerial view, and (b) looking east

4.2.1 Phase 1: Summer growth monitoring

Vetiver was first planted in May 2020 since early summer is the optimal time to plant perennial grass in Mississippi. Using traditional gardening methods, 200 young vetiver plants (also called tillers) with root lengths less than 10.2 cm were planted at 0.3 m center-to-center staggered spacing in a test section 6.1 m long and 3 m wide. Photos of the section and a vetiver tiller are presented in Figure 4.2. After planting, root growth was visually monitored on alternate days, when watering occurred. During the first week, no significant growth was noticed; however, new roots were noticed at the end of the week



Figure 4.2 Planting vetiver on test levee at ERDC: (a) looking east, (b) vetiver tiller before planting, (c) planted vetiver, and (d) looking north after planting

Two weeks after being planted, the vetiver was watered and monitored bi-weekly, and it was observed that approximately more than 90% of the roots were firmly anchored in the soil. After one month, the grass could not be pulled out by hand, indicating that it was growing well and that the roots were probably about 20.3 to 25.4 cm. Since the test levee section could not be excavated, soil properties, root length, and other vetiver properties were not measured; however, since the grass was growing, it was assumed that its roots were penetrating deeper into the soil. Photos of the vetiver section were taken during monitoring after one week, one month, and two months, and are presented in Figure 4.3.



Figure 4.3 2020 Summer growth observed during monitoring of vetiver at one week, one month, and two months

Phase 1: Winter Growth

In late October 2020, more vetiver was planted on the test levee slope. Traditional gardening methods were also used in Phase 2 to plant 1,000 vetiver tillers from the crest to the toe of the levee downstream slope, a 12.2 m long section. Each tiller was planted in a staggered grid at 0.3 m center-to-center spacing, enlarging the study area to 12.2 m in length and 9.1 m in width. Again, the vitality of the vetiver was determined using qualitative visual inspection. The grass was not watered, as it received adequate rainfall. Although

vetiver is a perennial grass, it goes dormant in the winter, begins growing again in the spring, and continues to thrive through summer and fall. Accordingly, no growth was observed until the end of March 2021, when substantial growth was noticed. By the end of summer 2021, more than 95% of the planted grass had survived and was anchored solidly in the levee slope. The vetiver growth between October 2020 and September 2021 is presented in Figure 4.4.



Figure 4.4 2020 winter through 2021; summer growth at 2 weeks, 1 month, 2 months, 5 months, 6 months, and 11 months

The grass was mowed regularly, and those monitoring the field noticed the vetiver’s vitality during the summer months. The appearance and growth of the shoots were an indirect indication of the growth of the roots, which grow both vertically and horizontally, as the growth rates are usually similar. The tallest shoot height observed in one visit was 1.4 m in August 2022, as shown in Figure 4.5. It is not known whether this growth was typical, as fewer visits were made to the site in 2022 and the height of the grass would have had to be measured immediately following mowing and just prior to the next mowing. Based on vetiver’s vitality, the observations made in this study, and its perennial nature, it can be concluded that it can be effectively used at this site to stabilize the slope.



Figure 4.5 Tallest vetiver grass height observed and measured (1.4 m) in August 2022

4.2.2 Field instrumentation

The field was instrumented in one day with sensor and gauges installed in the middle of Slope 1 at depths of 15.2 cm and 45.7 cm to monitor the moisture content, matric suction, soil temperature, air temperature, and rainfall. Industrial grade sensors from METER consisted of a TEROS 10 moisture sensor, TEROS 21 soil water potential sensor, ATMOS 14 vapor pressure, relative humidity (RH), temperature and barometric pressure sensor, ECRN-100 double-spoon tipping bucket rain gauge, and a ZL6 data logger. The data logger was installed to download data via the ZENTRA utility app on a field laptop during field visits. The field instrumentation profile and equipment are shown in Figure 4.6; an aerial of the assembly is shown in Figure 4.7. In the first month of data collection, a complimentary subscription to the ZENTRA CLOUD enabled data to be uploaded continuously to the cloud and accessed remotely.

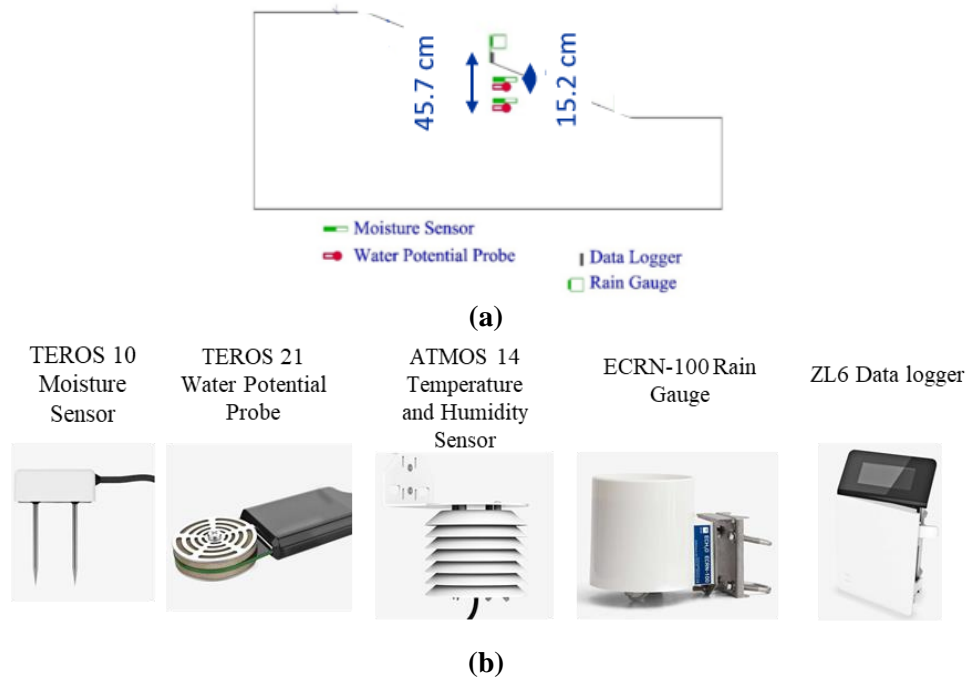


Figure 4.6 (a) Instrumentation profile at ERDC, and (b) individual sensors at ERDC



Figure 4.7 Instrumentation setup at ERDC

4.2.3 Field monitoring results

The data loggers were programmed to automatically collect data from all the sensors at 15-minute intervals, and the JSU team visited the slope routinely to transfer data from the logger to the field laptop. Field monitoring was performed to collect in situ soil properties that were influenced by weather changes, with particular emphasis on rain events. The field monitoring results of the moisture content, matric suction, soil temperature, and air temperature are presented in Figure 4.8. Precipitation measurements recorded at the nearby weather station were significantly greater than those indicated by the rain gauges at the site and were accepted as being accurate. (See Figure 4.8.)

The variations in the moisture content at the center of the test section are presented in Figure 4.8(a). The moisture content at 15.2 cm and 45.7 cm depths were approximately equal, with an average moisture content of 32% and 31%, respectively; the maximum moisture content was 36% and 35% at 15.2 cm and 45.7 cm depths, respectively. These measurements corroborate the average moisture content of 38% for Yazoo clay in Mississippi espoused by Lee (2012). Standard deviations were 4% and 3% for the 15.2 cm and 45.7 cm depths, respectively. Significant variations (0-13%) in moisture content were observed for the summer and fall seasons, whereas winter and spring experienced more moderate variations (0-3%). This reflects the variations in rainfall and the reduced daily rainfall observed in winter and spring. During the 2.5 year monitoring period, one rainfall event, which occurred on June 8, 2020 and exceeded 76 mm, was considered extreme. The sensors were not operable from late October 2021 to late January 2022; consequently, no data is available for that timeframe.

A matric suction of -208 kPa was measured at 15.2 cm depth during late summer and early fall of 2020, as shown in Figure 4.8(b). Negative suction measurements indicate that the soil was unsaturated, which is typical for soil above the groundwater table. Increased suction has been directly related to an increase in the shear strength of the soil (Nobahar et al., 2019). The maximum suction at a depth of 45.7 cm was -124 kPa; the average matric suction was -29 kPa and -33 kPa for 15.2 cm and 45.7 cm depths, respectively. Standard deviations were 26 kPa and 28 kPa for 15.2 cm and 45.7 cm depths, respectively. Significant variations in the matric suction were observed for the summer and fall seasons; moderate

variations and low suction values were observed for the winter and spring. This reflects the dormant phase of vetiver, when transpiration in the roots is significantly less than during the growing season.

Soil temperature was measured by the moisture and suction sensors, and the air temperature was measured by a barometer, as shown in Figure 4.8(c). The average temperature for the 15.2 cm and 45.7 cm depths was 22 °C, and the maximum soil temperature was 32 °C for 15.2 cm depth and 31 °C for 45.7 cm depth. The average air temperature was 21 °C, the maximum air temperature was 49 °C, and the minimum air temperature was -10 °C. The temperature of the soil was relatively stable, with a standard deviation of 7 °C and 6 °C for 15.2 cm and 45.7 cm depths, respectively, despite significant variations in the air temperature (standard deviation of 11 °C) that occurred between reading intervals. The significant soil and air temperature changes occurred with the change in seasons, reflecting the seasonal weather changes.

While the first three months of monitoring are often considered an adjustment period, the data captured within this period corroborates the data collected afterward. Slope 1 appeared to be maintaining normal moisture levels, indicating that it's unlikely that there are perched water zones within the levee. The slope never reached saturation, where a matric suction of zero would occur, suggesting that the seepage line is below 45.7 cm deep and beyond the scope of our measurements. Lastly, the soil and air temperature did not show abnormal trends during the study period; therefore, it is impossible to determine whether desiccation cracks exist in the soil from wetting and drying between summer and winter. The lack of excess moisture, however, indicates the absence of increased infiltration that would otherwise travel through desiccation cracks. Slope 1 is in a stable condition, and it can be concluded that the vetiver grass improved the pre-treatment condition of the slope in 2020.

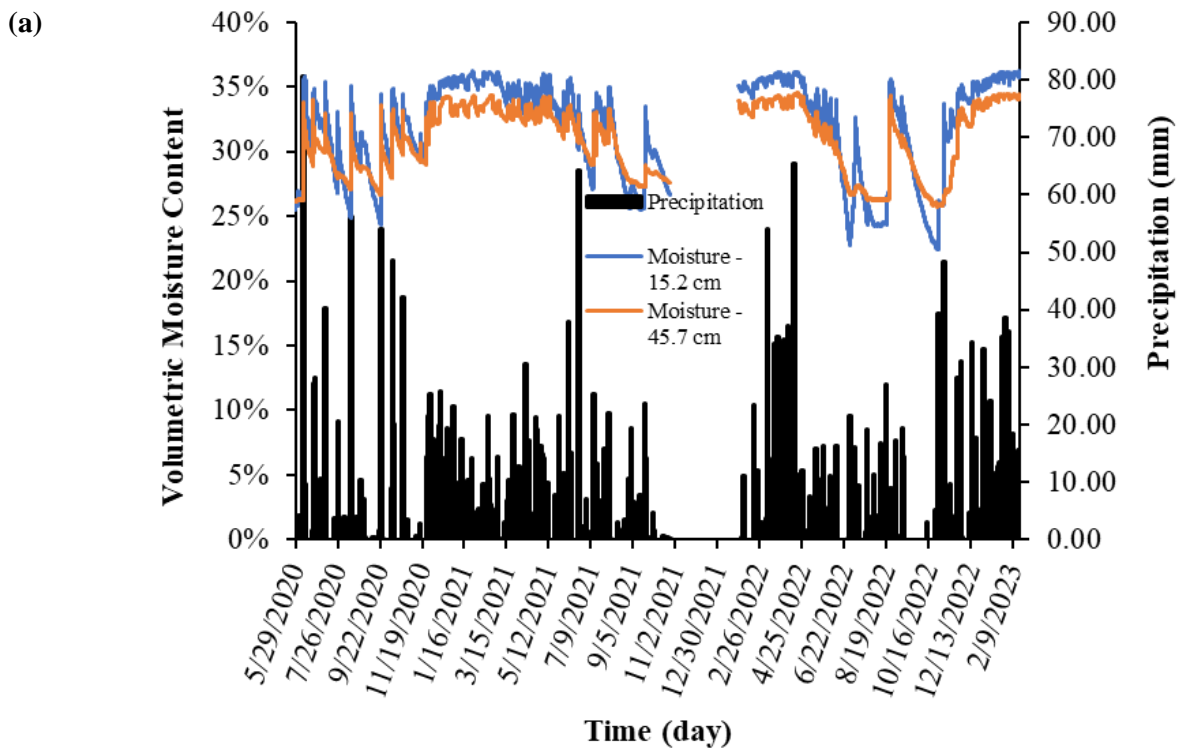


Figure 4.8 (Continued)

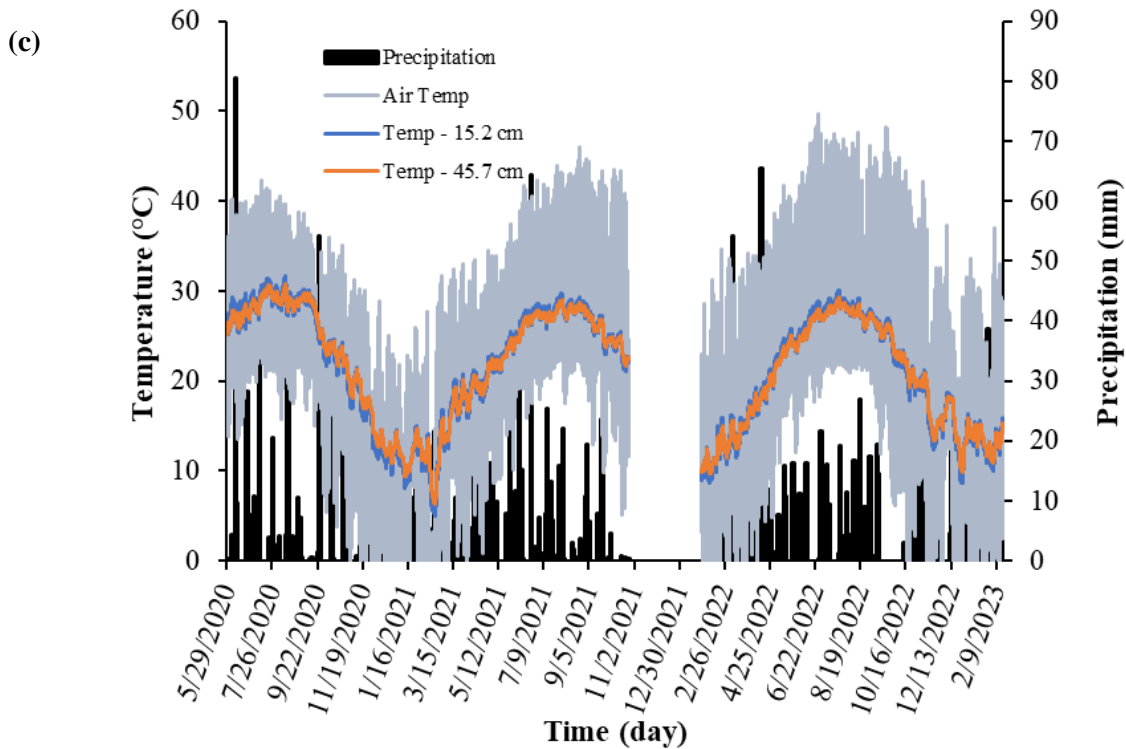
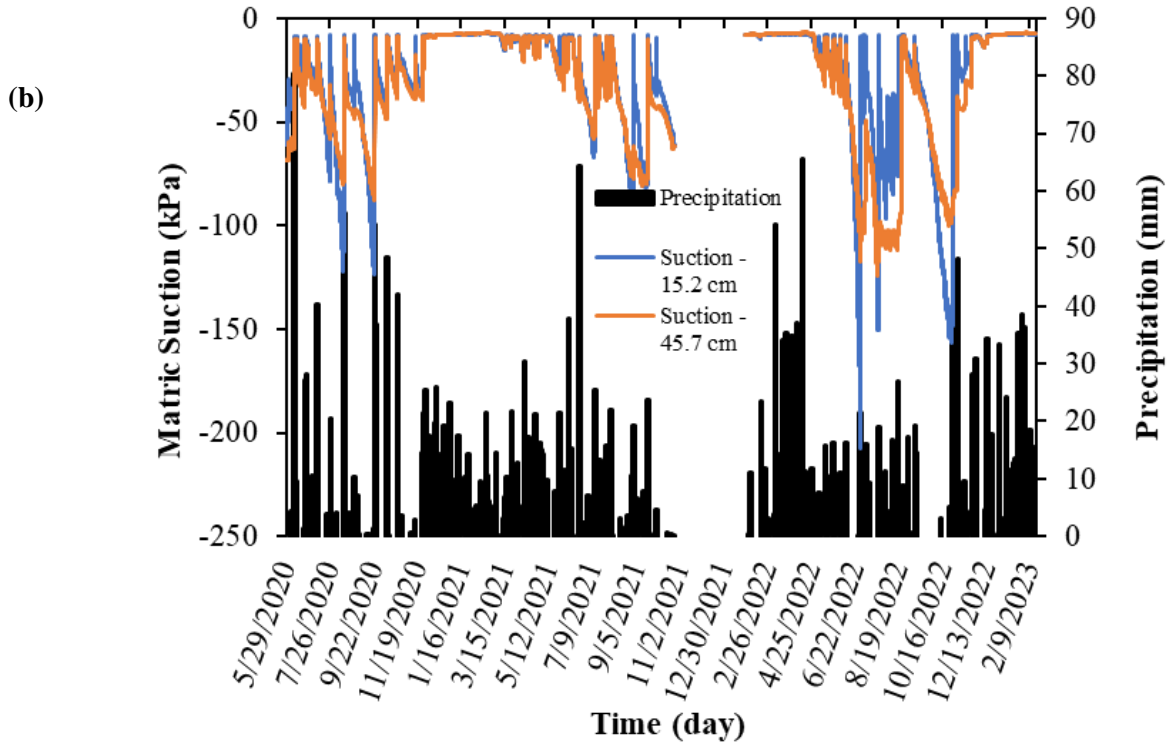


Figure 4.8 Field measurements of Slope 1: (a) moisture (mm-day), (b) suction (kPa-day), and (c) temperature (degree celsius- day)

4.3 Slope 2: Terry Rd Highway Embankment Section

Slope 2 is a 3.5 H:1V to 4H:1V slope with a height of 4.6 m from the toe (Terry Rd) to the crest (exit ramp of I20E) that is located along the I20 E exit toward Terry Road. The location and a site photo are presented in Figure 4.9. The slope near the bridge has experienced shallow landslides that were repaired using H-piles. Following the repair, a 6 m² area north of the repaired slope section was selected as the test section for vetiver grass. A brief overview of the forensic investigation has been provided for informational purposes only.

Thompson Engineering performed cone penetration testing (CPT) at Slope 2, using standard 9.7 cm² piezozones, and boreholes were drilled for inclinometers and field instrumentation. The depth, location, and purpose of each of the boreholes and CPT sounding are presented in Table 4.2. Two slope inclinometers with 9.1 m depth were installed at the repaired and as-built slope sections. The as-built section served as the control section that could be compared with the performance of the repaired section. Three 4.6 m deep boreholes were drilled in both sections: one each at the crest, middle, and toe of the slope. The layout of the boreholes and CPTs is presented in Figure 4.10. Vetiver was planted in May 2020, using traditional gardening tools. Figure 4.11 depicts the relative size and location of the vetiver-reinforced section, repaired, section, and control section.



Figure 4.9 Location of Slope 2

Table 4.2 Forensic Investigation at Slope 2

| Borehole/CPT Sounding | Color of the Symbol in Figure 4.10 | Borehole Depth (m) | Slope Area | Purpose |
|-----------------------|------------------------------------|--------------------|----------------|--|
| Inclinometer 1 | Blue | 9.1 | As-built slope | Continuous Shelby Tube Sampling and Install Inclinometer |
| Inclinometer 2 | | 9.1 | Repaired slope | |
| BH-1 | Red | 4.6 | As-built slope | Instrumentation |
| BH-2 | | 4.6 | As-built slope | |
| BH-3 | | 4.6 | Repaired slope | |
| CPT 1 | Green | 9.1 | As-built slope | CPT Test |
| CPT 2 | | 9.1 | Repaired slope | |
| CPT 3 | | 7.6 | As-built slope | |
| CPT 4 | | 7.6 | Repaired slope | |
| CPT 5 | | 6.1 | As-built slope | |
| CPT 6 | | 6.1 | Repaired slope | |



Figure 4.10 CPT and borehole locations at Slope 2

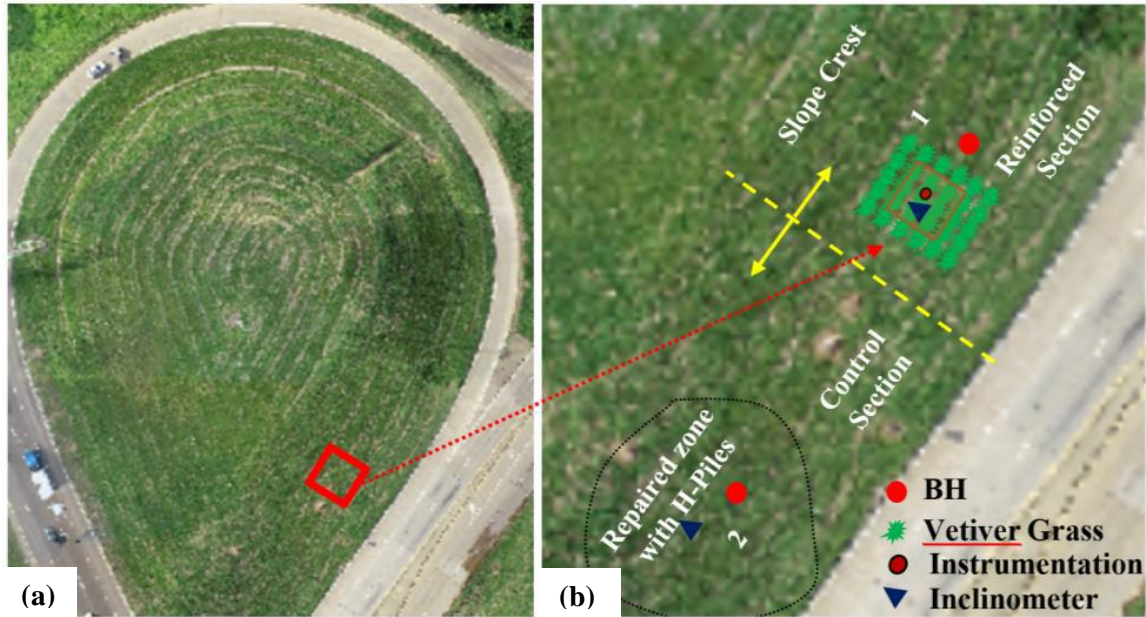


Figure 4.11 (a) Initial state of Terry Rd section, and (b) repaired control and vetiver grass sections

4.3.1 Vetiver planting and growth monitoring

Vetiver grass tillers were transplanted at 0.6-0.9 m spacing along the length and width of the slope. Immediately after planting, it was watered daily, then the frequency gradually decreased - from every other day to weekly; it was not fertilized. Based on rainfall patterns, it was determined that it needs weekly watering. The growth was monitored weekly, and the initial results were encouraging. Figure 4.12 shows the substantial growth that occurred in Yazoo clay within five months (from June 2020 to October 2020). So far, the vetiver has grown at least 2.1 m in Yazoo clay under excessive rainfall.



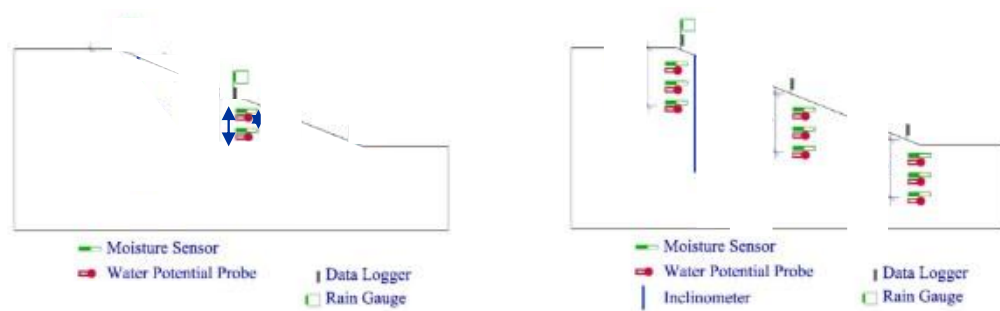
Figure 4.12 Planting vetiver on highway embankment at Terry Rd: (a) looking southwest from reinforced section, (b) looking southwest at reinforced section after vetiver has achieved a few weeks' growth, and (c) looking southwest from reinforced section in October 2020

4.3.2 Field instrumentation

Slope 2 was instrumented with inclinometers, GS-1 moisture sensors, TEROS 21 soil water potential sensors, an ECT-1 air temperature sensor, an ECRN-50 tipping-bucket rain gauge, and an EM 50 data logger from METER weinstre to collect information pertaining to the moisture content, matric suction, soil temperature, air temperature, and rainfall. In some instances, sensors and data loggers had to be replaced due to malfunctioning, e.g., a TEROS 10 replaced a GS-1 in the vetiver section, an ATMOS 41 replaced the ECT-1 and ECRN-50, and a ZL6 data logger replaced the EM 50. The moisture and water potential sensors were installed at the crest, middle, and toe of the slope at depths of 15.2 cm, 45.7 cm, 1.5 m, 3 m, and 4.6 m. Details of the instrumentation are provided in Table 4.3, and the instrumentation profile and photos and locations of the instrumentation are provided in Figure 4.13 (a) Instrumentation profile for vetiver section on Terry Rd. (left) and across all sections (right), and (b) original sensors

Table 4.3 Field Instrumentation for Data Collection

| Instrumentation | Purpose | Location | Depth (m) | Number of Sensors |
|--|--|----------------------------|-------------------------|--------------------------|
| TEROS 10 or GS1 Moisture Sensor | Collect Volumetric Moisture Content | Crest, middle, toe | 0.15, 0.46, 1.5, 3, 4.6 | 11 |
| TEROS 21 Water Potential Probe | Collect Matric Suction | Crest, middle, toe | 0.15, 0.46, 1.5, 3, 4.6 | 11 |
| ATMOS 14 Temperature and Humidity Sensor | Collect Vapor Pressure, Relative Humidity (RH), Air Temperature, and Barometric Pressure | At the middle of the slope | Atmosphere | 1 |
| ECT-1 Temperature and Humidity Sensor | Collect Vapor Pressure, Relative Humidity (RH), Air Temperature, | At the middle of the slope | Atmosphere | 1 |
| ECRN 100 or ECRN 50 Rain Gauge | Collect Precipitation Data | At the middle of the slope | Atmosphere | 1 |
| ZL6 or EM 50 Data Logger | Data Collection and Storage | At the middle of the slope | Atmosphere | 4 |



(a)



(b)

Figure 4.13 (a) Instrumentation profile for vetiver section on Terry Rd. (left) and across all sections (right), and (b) original sensors

4.3.3 Field monitoring results

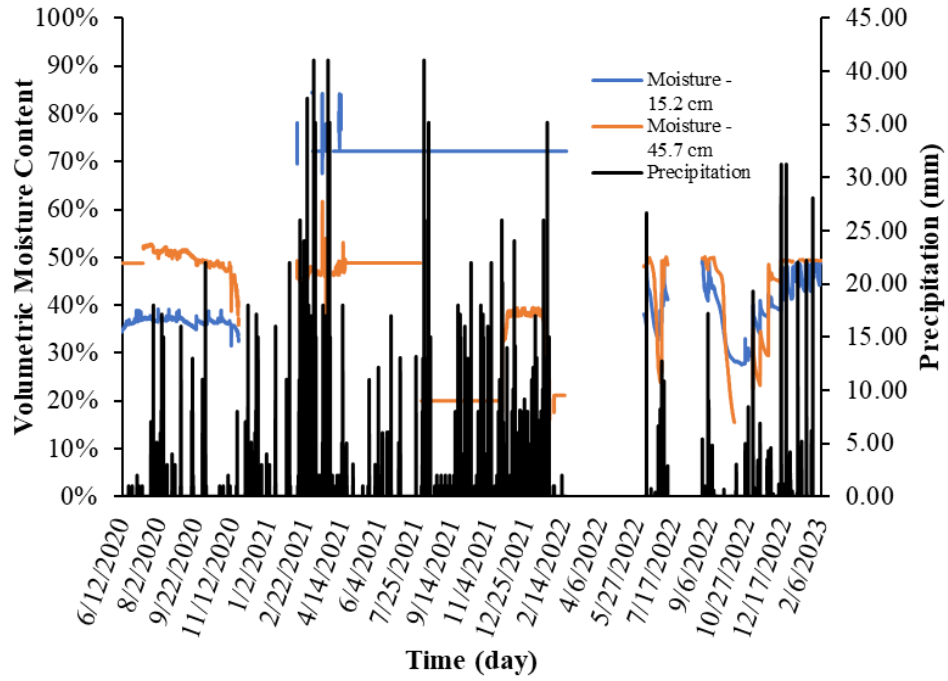
The data from the instrumentation was routinely collected and transferred to the field laptop, and the results, including moisture content, matric suction, soil temperature, and air temperature, are provided in Figure 4.14. The EM 50 data logger was programmed to collect data hourly, but when it was replaced with a ZL6, data was initially collected every 15 minutes, then later reduced to 1.5-hour intervals. Several problems made the data collection challenging. Some of the sensors were tampered with and disconnected from the data logger; and extended rainfall events occasionally caused sensors to disconnect, probably due to the proximity of the data logger to the ground and the higher height of the slope, which increased the runoff. Malfunctions of the data loggers also caused gaps in the data and led to replacing one EM 50 and two ZL6 data loggers. These complications significantly reduced the amount of valuable data, as seen in the graphs.

The variations of moisture content at the center of the test section are presented in Figure 4.14(a). The moisture content at 15.2 cm and 45.7 cm depths shows three different trends, with an average moisture content of 64% and 37%, respectively. In 2020, the moisture at 45.7 cm exceeded that at 15.2 cm, then in 2021, this trend reversed. Finally, in 2022 and 2023, the original trend returned. The maximum moisture content was 85% and 62% at 15.2 cm and 45.7 cm depths, respectively. The moisture content at 45.7 cm is comparable to the average moisture content of 38% for Yazoo clay in Mississippi and similar to Slope 1. Standard deviations were 15% and 12% for the depths of 15.2 cm and 45.7 cm, respectively. Significant variations (15 - 40%) in moisture content were observed between the three major trends and within each trend period. Seasonal changes were less apparent than those observed in Slope 1. On August 24, 2022, precipitation exceeded 76 mm at Slope 2 and another time reached 85 mm, which exceeds the maximum rainfall event at Slope 1; however, no data was recorded at this site during the 2.5-year monitoring period due to malfunctioning equipment.

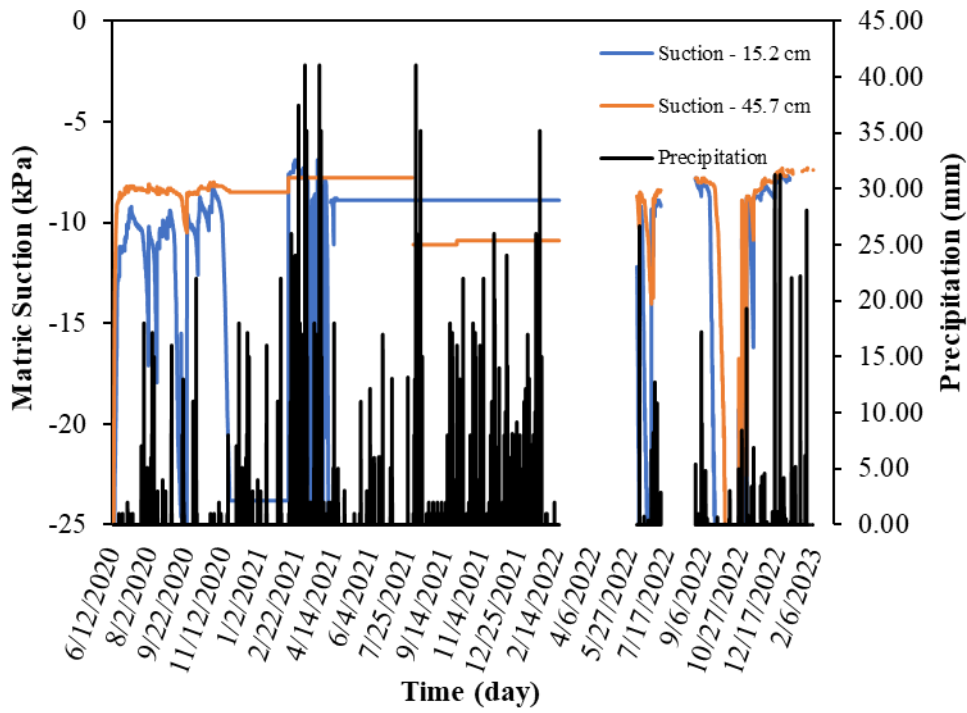
The matric suction is presented in Figure 4.14(b). During June 2020 and from September through October 2022, the suction was 24 kPa at 15.2 cm depth; the maximum suction at a depth of 45.7 cm was -48 kPa. The average matric suction for 15.2 cm and 45.7 cm depths was approximately equal at -10 kPa and -9 kPa, respectively, and the standard deviations were 4 kPa and 3 kPa for 15.2 cm and 45.7 cm depths, respectively. No significant trends were observed for the summer and fall seasons and minimal fluctuations were observed in 2021, except for an increase in suction at a depth of 45.7 cm, which corroborates the stable moisture content during this period. Overall, the suction was significantly lower than that observed for Slope 1, but the soil and air temperature did not show similar trends.

The average soil temperature at 15.2 cm and 45.7 cm depths, per measurements derived from the moisture and suction sensors, was 17 °C and 24 °C, respectively; the maximum soil temperature was 34 °C and 24 °C, respectively. The temperature of the soil was relatively unstable for the 15.2 cm depth (a standard deviation of 8 °C for 15.2 cm depth and 5 °C for 45.7 cm depth.) The average air temperature, measured by the ECT-1 and ATMOS 14 and presented in Figure 4.14 (c), was 21 °C; the maximum air temperature was 38 °C, and the minimum was -11 °C. More significant soil and air temperature changes occurred with changes in the seasonal weather patterns. These moisture, suction, and temperature trends provide insight into the slope's soil characteristics, potential infiltration of rainfall, and available air voids for initiating suction in the vetiver section.

Slope 2 appeared to maintain heightened moisture levels in 2021, indicating that there could have been perched water zones within the highway embankment. Like Slope 1, the soil never reached saturation, where a matric suction of zero would occur, suggesting that if a perched water zone exists, it may be below a depth of 45.7 cm and therefore beyond the scope of our measurements. There were anomalous trends in the soil temperature during the study, which consisted of constant rather than fluctuating soil temperatures, but it could not be discerned whether they were due to the malfunctioning sensors or some other cause, so the data was removed. Therefore, it cannot be determined whether the desiccation cracks in the soil are from wetting and drying between summer and winter. The excess moisture, however, indicates the presence of increased infiltration that would otherwise travel through desiccation cracks, which contrasts with Slope 1. Although the slope is shallower, Slope 2 appears less stable than Slope 1. The inclinometer data will assist in determining whether the vetiver is able to improve the pre-investigation condition of the slope in 2020.



(a)



(b)

Figure 4.14 (Continued)

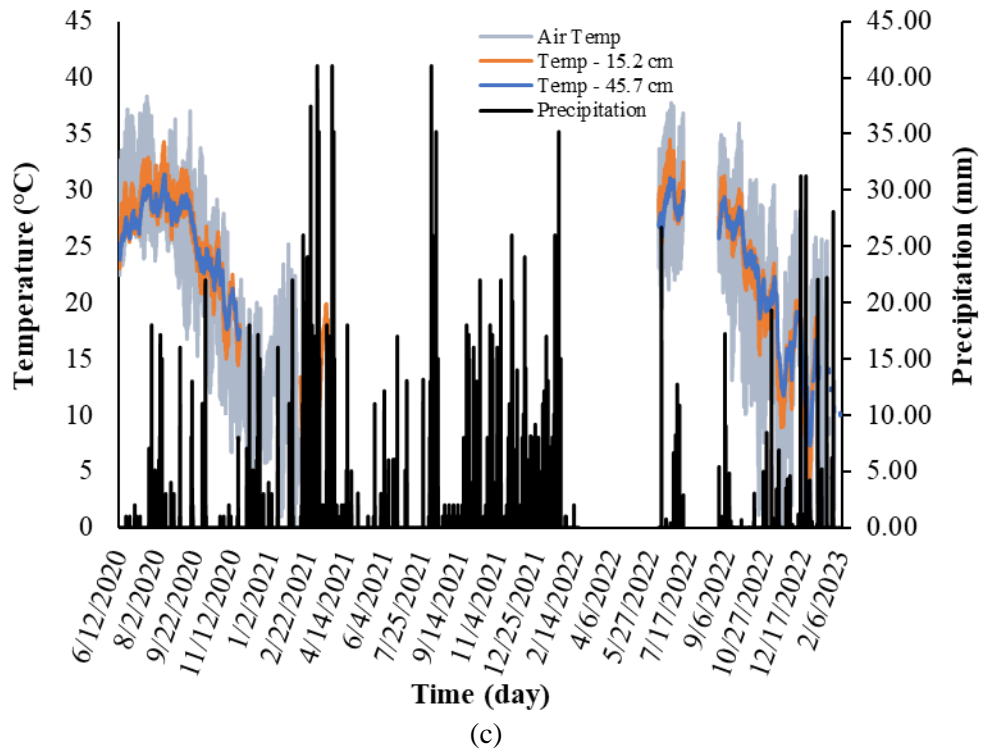


Figure 4.14 Field measurements of Slope 2: (a) moisture(cm-day), (b) suction(kPa-day), and (c) temperature (degree Celsius per day)

4.3.3.1 Inclinometer Results

Figure 4.15 depicts the instrumentation layout for the 9.1 m long inclinometer casing pipe installed in the H-pile-repaired section and in the vetiver reinforced (as-built) section that was set up to monitor the slope movement for Slope 2. The two boreholes are designated as Inclinometer 1 and Inclinometer 2.



Figure 4.15 Instrumentation layout at Slope 2 in 2018

Horizontal movement from the slope was collected using slope inclinometer measurements collected at 0.6 m intervals along the inclinometer pipe, then was downloaded and analyzed to determine the slope movement. The movement data from Inclinometer 1 at the vetiver-reinforced section and Inclinometer 2 at the section repaired with H-piles are presented in Figure 4.16 (a) and (b), respectively. The dashed lines in Figure 4.16(a) represent readings that were taken following the planting of the vetiver grass. As observed from the inclinometer data, the movement in the as-built section of Slope 2 was consistent across all readings. The movement was more restricted at depths of 1.5 m or lower, and the maximum movement occurred at 0.3 m, the point from which the readings began. All other readings were removed to account for the casing stickup and movement due to the lack of soil compaction around the casing. In addition, the depth of the slope movement that exceeded 10 mm was around 2.5 m, which is shallow. Movement in the repaired section of Slope 2, at Inclinometer 2 was low, due to the deep H piles mitigating the deep-seated slope slip surfaces. However, displacement was observed, and the trend was increasing.

Since May 2020, the section reinforced with vetiver grass had displacement up to 118 mm (4/12/2023), which is 93 mm more than when the first reading was taken after planting it on May 31, 2020. From the inclinometer installation on October 18, 2018 to the last reading before vetiver reinforcement on May 3, 202, the slope had displacement up to 53 mm at a depth of 0.3 m. The slope moved at a rate of roughly 34 mm per year before the vetiver grass was planted; since then, the rate has reduced to 32 mm per year. Vetiver roots typically reach a depth of 3-3.9 m in the first year and aren't easily dislodged under high-velocity flows (Hengchaovanich, 1999; Hengchaovanich and Nilaweera, 1998; Truong, 2000). The results of the extended monitoring of the field performance and the lab testing results will be taken into account in future research investigations, and the effects of the vetiver root system will be further studied in the numerical investigations of the slope.

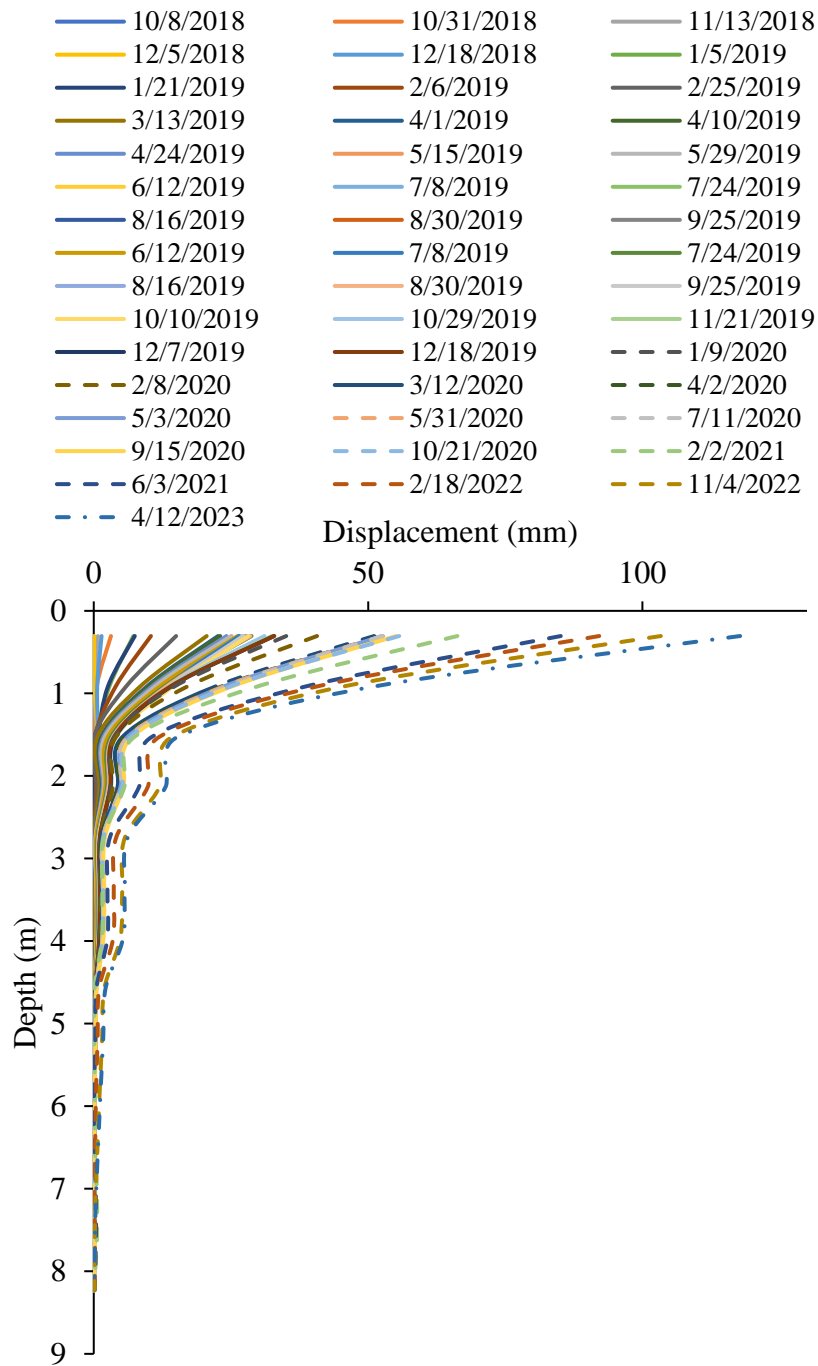


Figure 4.16 Horizontal displacements of the monitoring area (Inclinometer 1)

Vetiver grass was planted, using traditional gardening methods, in expansive Yazoo clay on Slopes 1 and 2, and thrived without the aid of fertilizer. The substantial growth that both sites experienced within five months of planting is attributed to the subtropical climate of Mississippi and the grass's ability to penetrate clayey soil, which cannot be said of all grasses. Additionally, the time between the removal of each tiller from the mother plant, shipment from the vetiver farm, and transplantation at the site was minimized to increase the survival rate. While the initial planting was done in the spring for both sites, the winter planting

at Slope 1 demonstrated that vetiver can grow when it is planted during the dormant season since it is perennial. Field monitoring results provided further insight into the variations in weather, soil temperature, moisture, and suction at discrete points within the slopes to characterize the soil conditions and determine broader stability implications.

Slopes 1 and 2 are approximately 44 miles apart and located in Vicksburg, MS and Jackson, MS, respectively. Both locations are within 10 miles of a river: Slope 1 is east of the Mississippi River, while Slope 2 is west of the Pearl River. While the air temperatures deviated more widely from the average at Slope 1 than at Slope 2, the soil temperatures deviated approximately the same. The maximum air temperature was higher at Slope 1; the minimum air temperature was lower at Slope 2. The average soil temperature at Slope 1 was closer to the average air temperature, whereas the average soil temperature at Slope 2 was higher. The average air temperature was the same at both sites.

The average rainfall was greater at Slope 1 than at Slope 2, but the maximum rainfall observed during the study was more significant at Slope 2. While weather comparisons suggest soil behaviors at both sites, the type of infrastructure each slope consists of is the strongest indicator of these trends; namely, Slope 1 is a levee section and as such is subject to a constant reservoir level; Slope 2 is a highway embankment and is subject to perched water conditions. The results that most strongly correlate to these differences are the those of moisture and suction. The average moisture content at Slopes 1 and 2 is close to the average of Yazoo clay, except for the shallowest depth at Slope 2, which is nearly double the average moisture content of Yazoo clay. In addition, the maximum moisture content of Slope 1 is less than the average moisture content of Yazoo clay, while it is more than double that of the average of Yazoo clay at Slope 2 for the shallowest depth. These are indications of more significant infiltration and storage that could lead to perched water conditions. Perched water conditions led to a previous failure at Slope 2 and necessitated H-pile installation for slope repair. While vetiver was planted in a section that did not fail (the as-built section), inclinometer results and visual observations of the slope have shown that this reinforced area of the slope is stable despite excessive moisture. Slope 1 did not show any instability before or after planting the vetiver. Suction results further indicate the stability of Slope 1, with average matric suctions exceeding those of Slope 2 by more than three times. Since suctions at both slopes were negative, it can be confirmed that instrumentation was placed in the vadose zone at both depths for each site. These results provide the foundation for conducting numerical analyses that can further assess the effectiveness of vetiver grassroots on Yazoo clay.

Chapter 5: Numerical Analyses of Slopes Improved with Vetiver

5.1 Numerical Modeling Background

While the field investigation of the slopes provided insight into the vitality of vetiver grass growing in Jackson and Vicksburg, Mississippi, as well as the benefits of planting it on slopes constructed of high plasticity clay, numerical analyses allowed a more time-efficient and controlled setting in which to examine the effects of various parameters this study investigates; i.e., the significance of suction, saturation, and rainfall in determining changes in a levee's slope or highway embankment's flow, deformation, and stability. Slide 2 and PLAXIS 2D can simulate how these parameters may change by converting plane strain geometric models into finite elements (finite element analysis, FEA). Using soil properties, phreatic surfaces, and precipitation data, analyses can couple flow and deformation through material models, soil data sets, flow functions, boundary conditions, and phases representing concurrent or antecedent rainfall. Other considerations include mesh size, number of nodes for the triangular element, and model calibration.

5.2 Scenario 1: Slope 1 Levee Improved with Vetiver Modeled as a Root-Soil Composite in Slide

The marginal condition of Slope 1 was simulated with rainfall and floodwater to reach a factor of safety (FOS) equal to or below unity following an extreme weather event as a transient condition. In this model, the weathered Yazoo clay extended from the ground surface to a depth of 0.9 m, 0.3 m below the compacted clay cap at ERDC, so roughly half of the failure surface would be through the Yazoo clay. The weathered Yazoo clay was underlain by in situ loess that extended to a depth of 15.2 m below the bottom of the catch basin. The catch basin height was 0.9 m below the crest of the levee.

The analysis was performed in two stages. In Stage 1, the steady-state seepage analysis was conducted, using the FEA package in Slide 2 to determine the phreatic surface at the downstream slope. Once the phreatic surface for the steady-state seepage condition was determined, the stability analysis was conducted by employing the limit equilibrium technique, using both Spencer and Morgenstern-Price methods to determine the initial FOS. In Stage 2, the catch basin water level was raised 38.1 cm above the steady state level of 2.7 m during a four-day storm to simulate the river flooding in Central MS in August 2022 (Mississippi Emergency Management Agency, 2022) following extreme rainfall. While the rain intensity could not be as high as the partial duration series-based intensity-duration-frequency curves for a four-day storm between a return period of 100 and 500 years, a rain intensity/infiltration rate of 0.5 mm/hr was also used to represent the transient condition. Table 5.1 provides the soil parameters for the numerical analysis. Shear strength parameters were taken from the stability analysis of the levee site, where soil properties were based on a previous geotechnical field investigation and design parameters (GEA, LLC, 2010). While the natural loess (undisturbed CL) properties and weathered Yazoo clay (compacted CH liner) index properties were used directly, the shear strength of the weathered Yazoo clay (compacted CH liner) was reduced by the same percentage reduction (77%) obtained after Yazoo clay is subjected to seven wet-dry cycles (Khan et al., 2019) to represent a further weathered state of the clay after construction. The shear strength parameters increased in the test section where vetiver was planted and is assumed to have grown to 3 m depth after one year. The model and stability analysis results are presented in Figure 5.1. The FOS was approximately 1.4 for Stage 1 and 0.6 for Stage 2.

Table 5.1 Soil Parameters for Scenario 1

| Soil Type | Cohesion (c) | Friction Angle (Φ) | Unit Weight (γ) | Permeability (K) | Anisotropy (K_v/K_h) |
|--|--------------|---------------------------|--------------------------|------------------|--------------------------|
| - | kPa | degrees | kg/m ³ | cm/sec | - |
| Natural Loess (Undisturbed CL) | 4.8 | 12 | 6.7 | 1.00E-05 | 2 |
| Natural Loess with Vetiver (Undisturbed CL) | 9.9 | 18 | 6.7 | 1.00E-05 | 2 |
| Weathered Yazoo Clay (Compacted CH Liner) | 2.3 | 15 | 6.6 | 1.00E-07 | 3 |
| Weathered Yazoo Clay with Vetiver (Compacted CH Liner) | 4.6 | 16 | 6.6 | 1.00E-07 | 3 |

The Mohr-Coulomb model assumes that the soil behaves as a linear elastic, perfectly plastic model, and drained in account to consider the consolidated soil condition since significant time was passed after the construction of the levee. Desiccation cracks are often present that allow the vertical permeability to be greater than the horizontal, which is the opposite of the usual condition. This is represented by the anisotropy of each layer, with weathered layers having more significant anisotropy.

Triaxial and direct shear tests of vetiver grass planted in soil and grown over time have proven that the roots increase the shear strength of the soil. Eab et al. (2015) planted vetiver roots in fine Edosaki sand, let it grow for four months, sheared it at 0.9 m depth, and tested it at everyday stresses less than 100.5 kPa, using a direct shear testing device per ASTM D3080 (1998). The shear strength of the soil increased by 7 kPa in cohesion and 7° in internal friction. The tests were repeated after six months under the same testing conditions except that a sizeable direct shear box was used, and the results showed a shear strength increase of 6 kPa in cohesion and 7 degrees in internal friction. These test results led to the conclusion that vetiver grass can grow up to approximately 1.8 m in six months, at an average rate of 30.5 cm per month, which is consistent with consolidated-drained (CD) triaxial tests conducted by Rahardjo et al. (2014), in which the soil was sheared within 0.9 m depth at a net confining pressure of 49.8 kPa and matric suctions less than 100.5 kPa during a one-year maturation period. A shear strength increase of 8 kPa in cohesion and 5 degrees in internal friction was observed for Old Alluvium, a silty, clayey sand where vetiver was planted at field scale. Wang et al., 2020, studied vetiver planted in weak expansive clay and determined the shear strength properties of the soil after 90 and 180 days by performing direct shear tests, Four specimens were sheared at depths between the ground surface and 0.3 m in direct shear tests, following the Trade Standard of P. R China (SL237-021 1999). After 180 days, with everyday stresses between 95.8 kPa and 407 kPa, the test results indicated a minimum 97% increment in cohesion and 15.4% growth in friction angle, which suggests that the shear strength gain in weak expansive soil may not be as significant as that obtained in sands. These studies illustrate that vetiver roots can improve shear strength. The increase in cohesion and friction angle used in this analysis on weathered Yazoo clay is conservative, considering it has grown for two years.

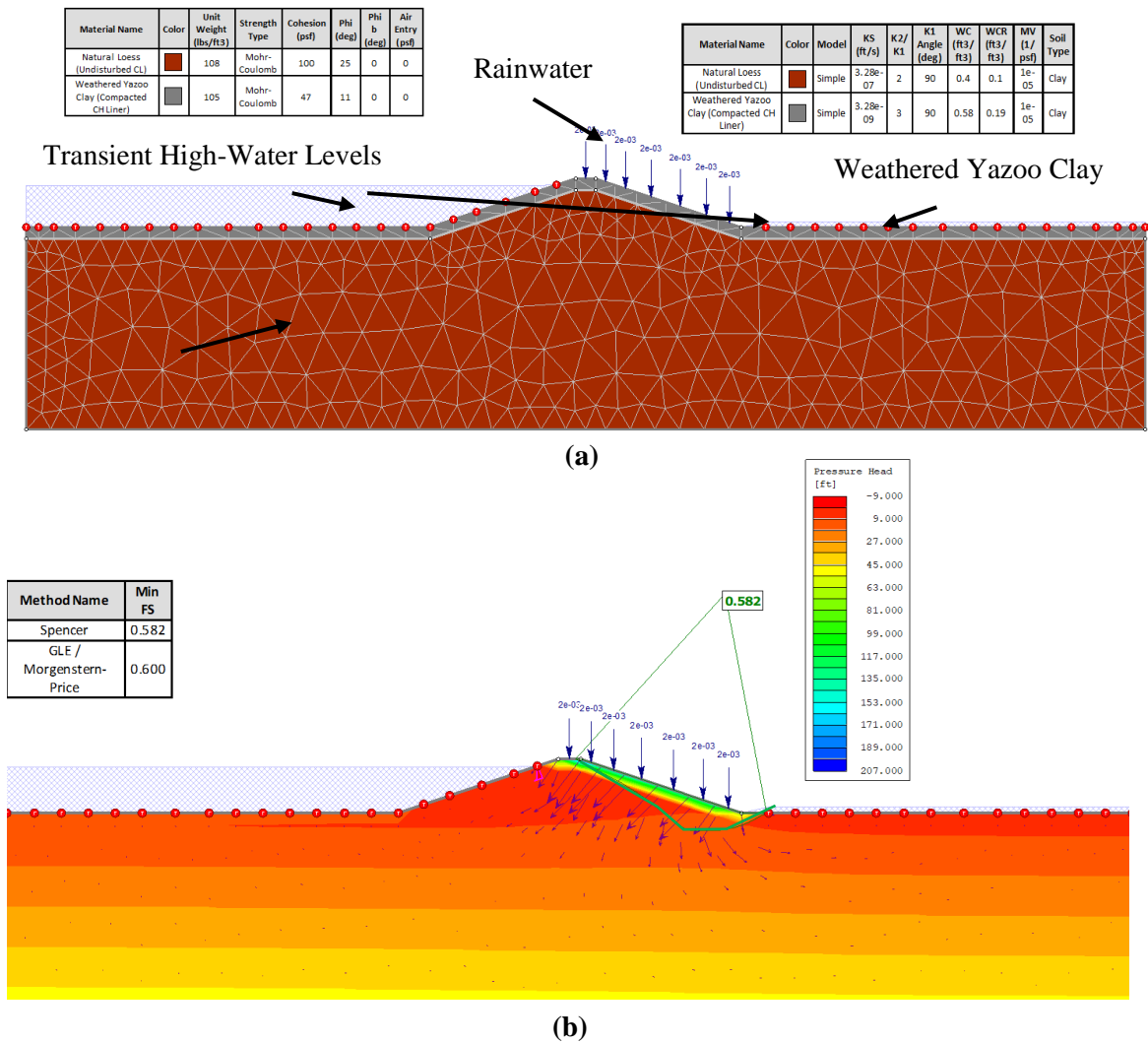
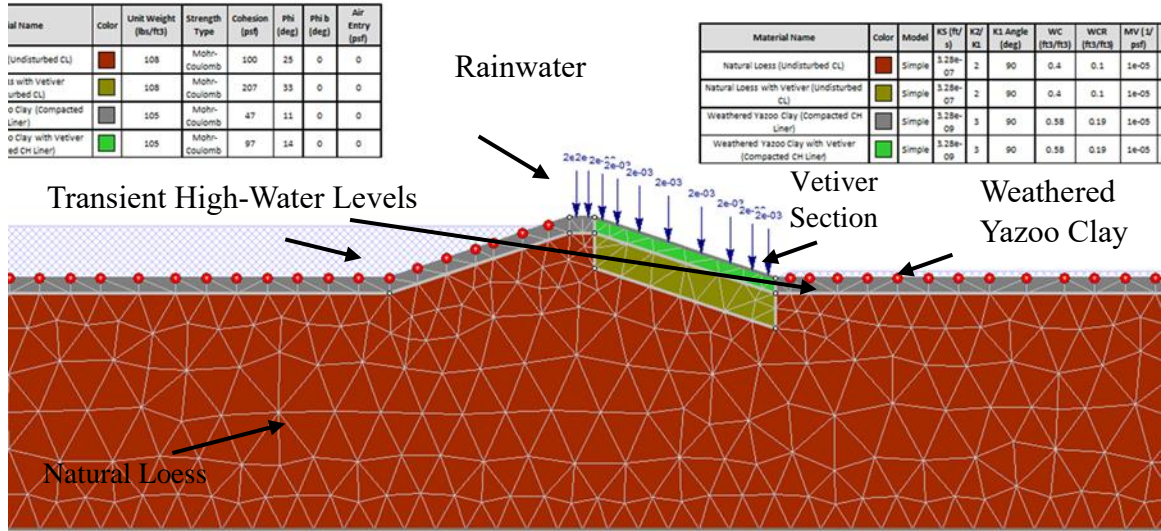


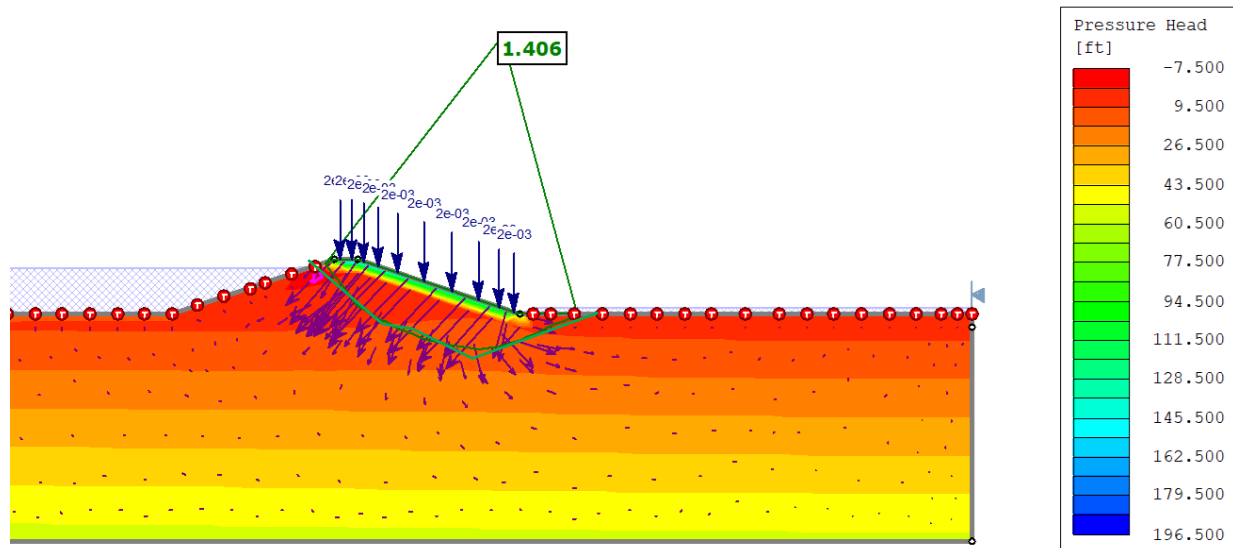
Figure 5.1 Four-day storm transient condition for Slope 1 without vetiver (Stage 2): (a) profile, (b) results

The shear strength of the weathered Yazoo clay was increased at full depth by the vetiver grass; the loess silty clay was increased within 3 m depth. The increment in shear strength for the weathered Yazoo clay was 2.3 kPa for cohesion, and the friction angle increment was 1°. The cohesion and friction angle for the loess silty clay increased by 5.1 kPa and 4°, respectively. It should be noted that the increments in both studies were based on four-to-six-month scenarios, while the vetiver at ERDC had been planted for more than 18 months. Therefore, the strength gained is expected to be higher than that described in the literature.

The results of the soil model and stability analysis are presented in Figure 5.2 and show that the with the planting of vetiver, the safety factor of the levee downstream slope decreased from approximately 1.6 to 1.4, rendering the slope safe from the marginal condition.



(a)



(b)

Figure 5.2 Four-day storm for Slope 1 with vetiver (Stage 2): (a) profile, (b) results

5.3 Scenario 2: Levee Improved with Vetiver Modeled as a Root-Soil Composite in Slide

Another marginal condition of the slope was simulated with a back analysis to reach the safety factor close to unity. In this model, the weathered Yazoo clay extended from the ground surface to a depth of 3 m, which is considered the active zone for central Mississippi. The weathered Yazoo clay was underlain by unweathered Yazoo clay that extended to a depth of 6.1 m below the bottom of the reservoir. A low-plasticity clay was overlain by the weathered Yazoo clay, extending to a depth of 4.6 m below the bottom of the reservoir. The reservoir height was 1.5 m below the crest of the levee. The analysis was performed in two stages. In Stage 1, the steady-state seepage analysis was conducted in the FEA package in Slide 2 to determine the phreatic surface at the downstream slope. Once the water table for the steady-state seepage condition was determined, the stability analysis was conducted using the Spencer and Morgenstern-Price limit equilibrium methods. To reach a safety factor close to unity, various back analysis iterations were

conducted. The shear strength parameters for the marginal condition (factor of safety ~ 1.0) of the slope are presented in Table 5.2. The results of the model and stability analysis are presented in Figure 5.3.

Table 5.2 Soil Parameters for Scenario 2

| Soil Type | Cohesion (c) | Friction Angle (Φ) | Unit Weight (γ) | Permeability (K) | Anisotropy (Kv/Kh) |
|---------------------------------|-------------------------|---|--|-----------------------------|-------------------------------|
| - | kPa | degrees | kg/m ³ | cm/sec | - |
| Weathered Highly Plastic Clay | 3.4 | 12 | 7.5 | 1.00E-07 | 1 |
| Unweathered Highly Plastic Clay | 5.3 | 18 | 7.5 | 1.00E-07 | 1 |
| Low Plasticity Clay | 14.4 | 15 | 7.5 | 1.00E-05 | 1 |
| Vetiver Reinforced Soil | 6.9 | 16 | 7.5 | 1.00E-07 | 1 |

The Mohr-Coulomb model was again used to simulate the soil behaving as a linear elastic perfectly plastic model and assuming that it has been drained to account for consolidation since construction. In addition, desiccation cracks were not considered in this scenario, representing the isotropy of each layer.

The shear strength of the weathered Yazoo clay increased within the 3 m depth of the vetiver root. Considering the trends described in the literature provided in the previous Scenario, the increment in shear strength for cohesion is conservatively considered as 3.6 kPa and the friction angle increment 4°. It should be noted that the increment in the studies considered was based on the 4-to-6-month scenario, while the vetiver was planted at the ERDC for more than 28 months. Therefore, the strength gain is conservative and is expected to be higher than is represented by the literature. The results of the soil model and stability analysis are presented in Figure 5.4. The factor of safety of the levee downstream slope increased from approximately 1.0 to 1.5, which renders the slope safe from marginal conditions.

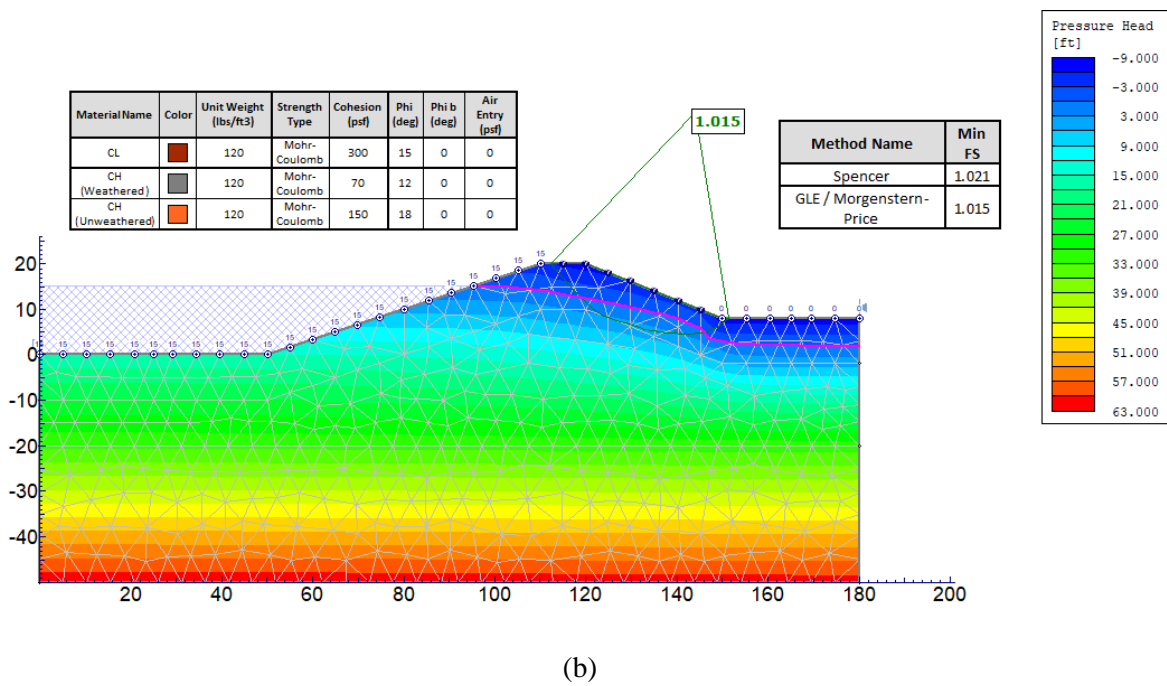
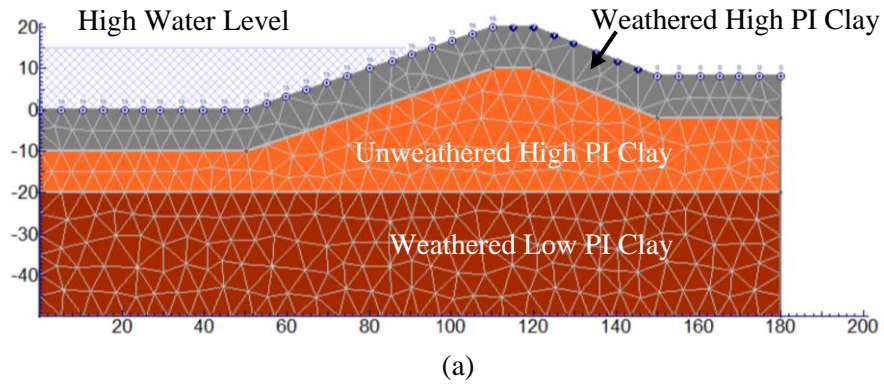
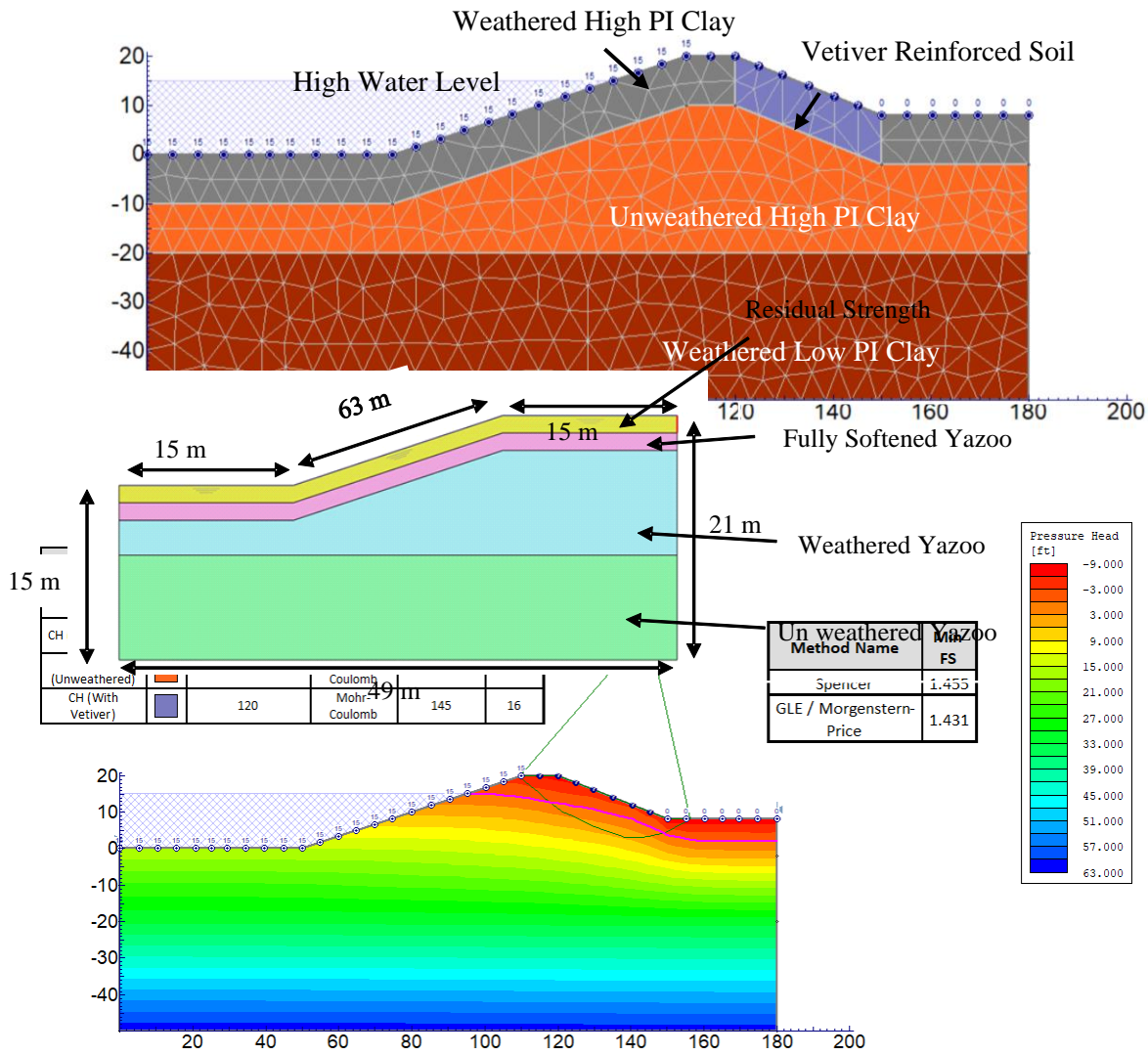


Figure 5.3 Back analysis of the failure condition of the levee: (a) initial levee profile, and (b) results



(b)

Figure 5.4 Slope failure following maturation of vetiver section: (a) levee with vetiver, and (b) results

5.4 Scenario 3: Slope 2 Highway Embankment Improved with Vetiver as a Bio-Anchor

Vetiver was modeled as a bio-anchor on Slope 2. The numerical study used the finite element analysis program PLAXIS 2D with a 15-noded mesh, and the variations in the safety values and failure depth were investigated. The modeled incline of the slope was 49 m long, with a soil thickness of 21 m at the crest and 15 m at the toe; the topsoil possessed residual shear strength. Nobahar et al. (2020) tested the residual strength of Yazoo clay and determined a cohesion value of 5.45 kPa and a friction angle of 12.8°. The remaining three layers were fully softened, weathered, and unweathered Yazoo clay. The geometry and soil properties of the slope are provided in Figure 5.5, and a perched water condition was modeled at 1.5 m depth, as provided in Figure 5.6.

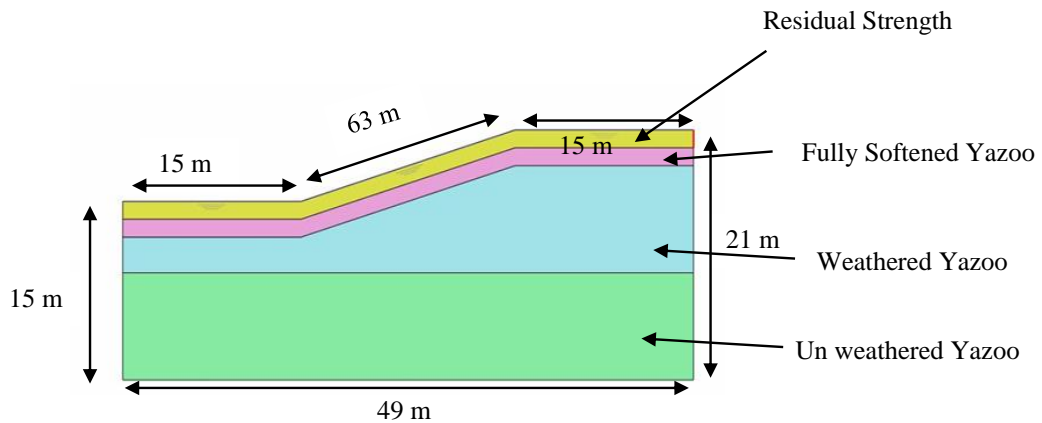


Figure 5.5 Geometry and soil stratigraphy of Slope 2

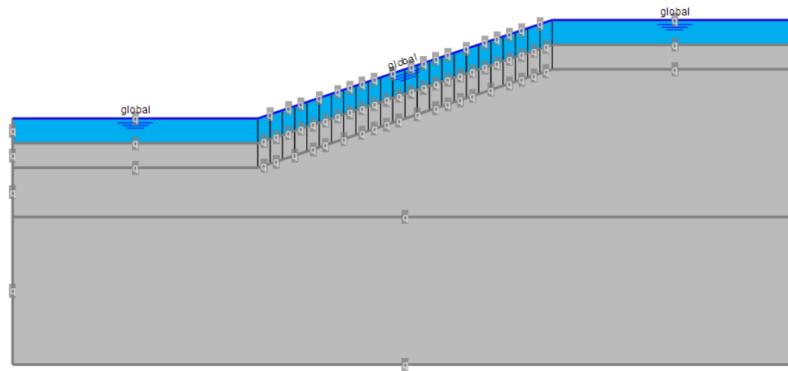


Figure 5.6 Perched water condition to 1.5 m depth

Using back calculation, the failure condition was made to approximate the Terry Rd historical slope failure discussed in Chapter 4. Field observations suggested a displacement of 12.7 mm at an approximate depth of 1.5 m, and the back-analysis model was constructed to reflect the same failure pattern. Adjustments were made to make the model's parameters agree with Khan et al.'s (2020) numerical analysis until the failure pattern matched at 1.5 m depth. Table 5.3 outlines the final values for inputs. Figure 5.7 illustrates the failure condition.

Table 5.3 Soil Parameters for Scenario 3

| Parameter | | Residual Strength | Fully Softened Yazoo | Weathered Yazoo | Unweathered Yazoo |
|---|-------------------|--------------------------|-----------------------------|------------------------|--------------------------|
| Bulk unit weight (γ_{unsat}) | kN/m ³ | 19.79 | 19.79 | 19.77 | 20 |
| Saturated unit weight (γ_{sat}) | kN/m ³ | 21.2 | 21.2 | 21.2 | 20 |
| Horizontal permeability ($k_z=k_x$) | cm/sec | 1.23E-5 | 1.23E-5 | 1.98e-10 | 1.98e-10 |
| Vertical permeability (k_y) | cm/sec | 1.23E-5 | 1.23E-5 | 1.98e-10 | 1.98e-10 |
| Cohesion (c) | kN/m ² | 5.45 | 10.8 | 11.9 | 18.3 |
| Friction angle (Φ) | degrees | 12.8 | 18 | 19 | 20 |

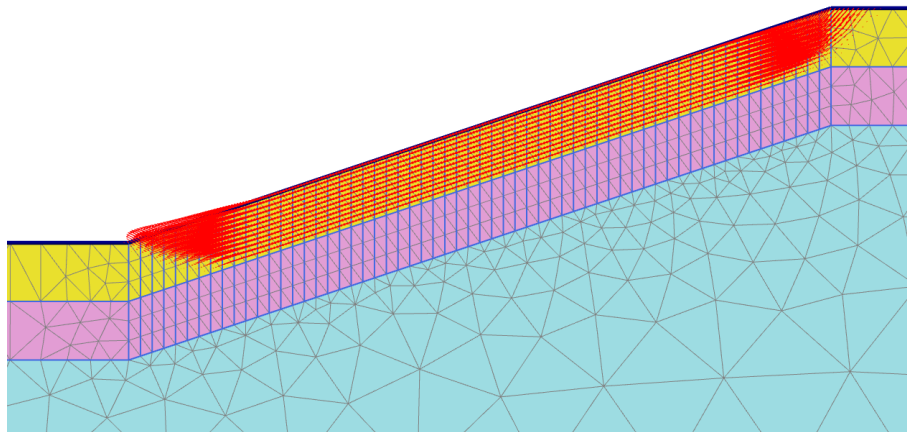


Figure 5.7 Failure of Slope 2 at 1.5 m depth in back calculated model

A ground anchor is an embedded structural component that transfers tensile force into the earth. Figure 5.8 shows that vetiver was incorporated into the model as a bio-anchor to show the effect of vetiver grass on the stability of the slope, as its roots' strong tensile strength allows it to anchor the soil when the slope shifts. Roots reside as embedded beam elements within the soil as slender elements (Yang et al., 2014). The length of the beam was 3 m, which is the optimal length for the growth of the vetiver, and the distance between the plants was 150 mm. A reduction factor was considered for the evaluation of the root

strength. The literature often uses a strength reduction factor in analyses (Tsige et al., 2019); in the present study, a strength reduction factor of 2 in root tensile strength was considered in the analysis

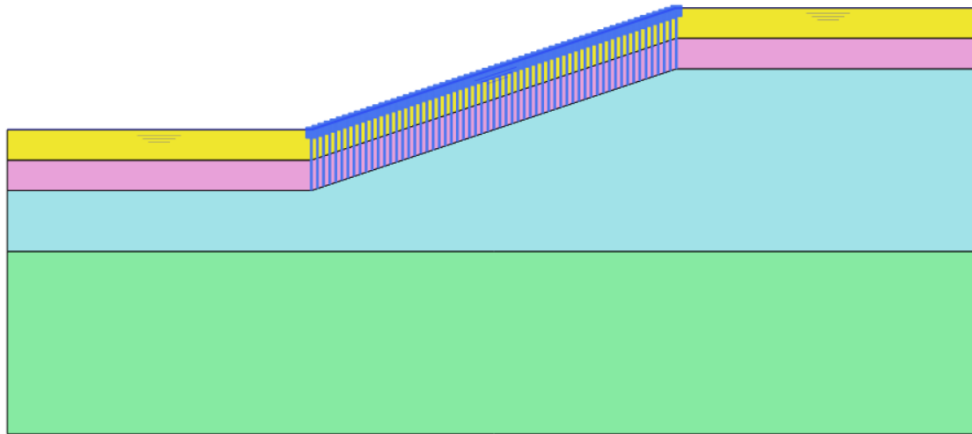


Figure 5.8 Vetiver roots modeled as embedded beams

The vetiver roots improved the FOS values. Before vetiver was planted, the failure depth was 1.5 m, and the FOS value was approximately 1.1. After it was planted, the FOS value increased from approximately 1.1 to 1.9 and the failure depth increased from 1.5 m to 3 m (Figure 5.9).

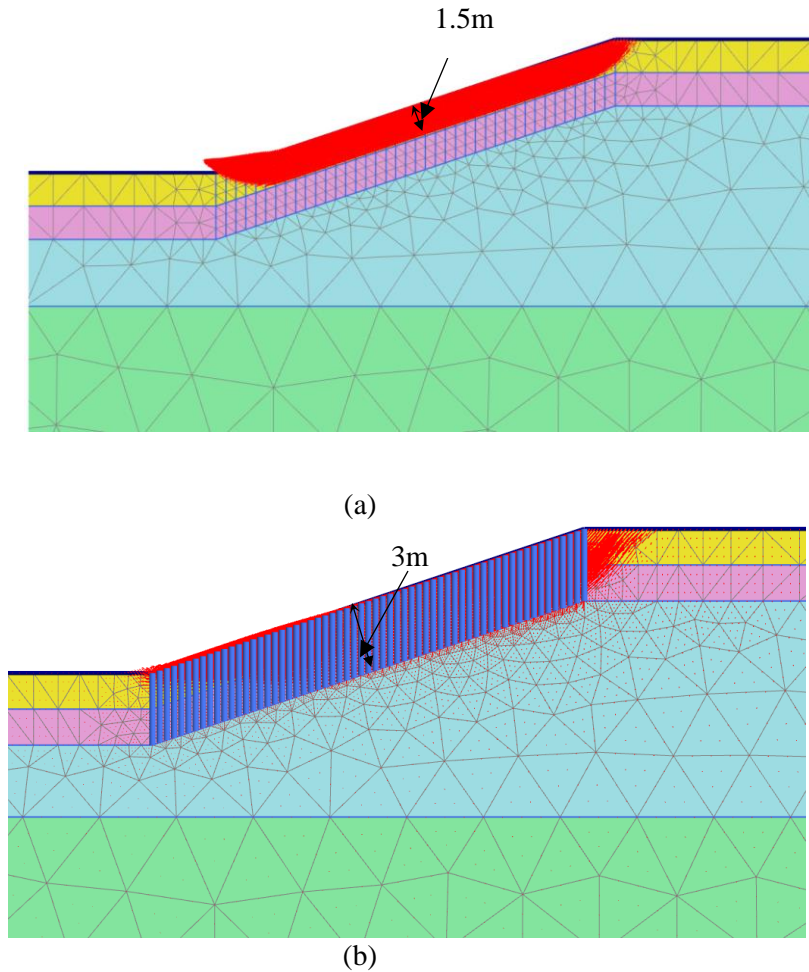


Figure 5.9 Comparison of slope failure mitigation (in meters) of slopes planted with vetiver with those not planted with vetiver

5.5 Comparison of Scenarios 1 through 3, Results, and Discussion

Scenarios 1 through 3 present the impact of planting vetiver grass roots as a root-soil composite or a bio-anchor. Slide 2 utilizes finite element analysis to determine seepage and limit-equilibrium when determining the slope stability; Plaxis 2D utilizes finite element analysis throughout seepage and slope stability analyses. The root-soil composite and bio-anchor models were not run on both Slide 2 and Plaxis 2D; however, the results of the two programs are often similar when the input parameters are comparable. Both Scenario 1 and 3 predicted the stability of the field-scale reinforcement of the slopes at ERDC (Slope 1) and Terry Rd. (Slope 2), where the slope geometry was identical to the site. Scenario 2 presented a more critical case of a levee that was asymmetrical and marginally stable, and required the reinforcement of vetiver.

The slopes of Scenarios 1 and 2 were steeper than that of Scenario 3, and while the thickness of the layers varied, the stratigraphy of each scenario was weathered Yazoo clay overlying unweathered Yazoo clay. Scenario 3 includes the residual strength of weathered Yazoo clay overlying a fully softened strength to represent repeated wetting and drying to the extent that desiccation cracks increase infiltration, creating excess moisture. Therefore, this scenario is more critical to creating an existing marginal stability condition

that requires planting vetiver than the soil conditions at the test section of Slope 2. The effects of climate, beyond utilizing weathered Yazoo soil parameters were also introduced through rainfall, transient reservoir high-water levels, and perched water conditions. Scenarios 1 and 2 consisted of high-water reservoir levels and Scenario 1 also included rainfall with a transient water level, while Scenario 3 had a perched water condition. The numerical analyses provided further insight into the performance of slopes improved with vetiver and the failure characteristics of slopes in Yazoo clay.

The scenarios presented resulted in shallow slope failures that are rotational or translational. Shallow failures have fewer consequences than global failures, but they are more damaging than surface sloughing and require more than just maintenance repairs for mitigation. Non-circular (optimized) toe failures occurred in Scenarios 1 and 2, while a translational toe failure occurred in Scenario 3. In Scenarios 1 and 3, vetiver reinforcement significantly altered the shape of the failure, thereby increasing the safety factor. The failure surface was pushed deeper into the slope, requiring a greater effort to mobilize the landmass. The Scenario 2 failure surface entered at the crest of the upstream slope and exited beyond the toe when the vetiver was planted, extending the failure's entry and exit points and requiring more effort to mobilize the failure. While the use of bio-anchors in mitigating translational failure of a residual strength surficial layer provides a more significant gain in factor of safety from the original condition in comparison to the soil-root composite scenarios, the spacing of the vetiver modeled as bio-anchors is half the spacing of the vetiver modeled as a soil-root composite. Therefore, these cases do not represent similar mitigative designs, but the bio-anchor model can be considered a more reinforced design due to more vetiver tillers being planted per area.

It is essential to note that the vetiver reinforcement in all the scenarios increased the factor of safety to acceptable levels—more significant than 1.4 on the downstream side for a maximum surcharge pool for levees and more significant than 1.3 following construction for a highway embankment. The shapes of the failure surfaces in Scenarios 1 and 2 were less predictable outside of numerical methods than in Scenario 3 because the differences in shear strength and pore pressures between the layers were not as stark. All the scenarios, however, represent Mississippi's maritime and multimodal transportation infrastructure conditions.

Chapter 6: Conclusion

Earthen infrastructures, such as levees, constructed with high-plasticity clay are becoming less stable because of increasing temperatures and precipitation caused by climate change. Vetiver grass is widely used in Asia to mitigate this problem, as its roots extend to depths greater than 3 m and increase the shear strength of the soil to combat shallow slope failures that typically occur between 1.8 - 2.4 m depths. This study determined that vetiver planted on a levee and highway embankment constructed of high-plasticity clay in Mississippi can effectively reinforce the soil, thereby reducing shallow slope failures.

Numerical analyses were conducted using models of a levee and a highway embankment planted with vetiver that incorporated the effects of extreme precipitation, high reservoir water levels, and perched water conditions. Slide 2 and Plaxis 2D slope stability programs were used, and the results showed that the safety values were higher for slopes with planted with vetiver due to the increased shear strength of the weathered Yazoo clay.

A spacing of 150 mm is a conservative recommendation for planting vetiver in maritime and multimodal transportation infrastructures to address marginal conditions or prepare soil for construction. This spacing yielded the highest improvement in FOS; however, it was not representative of the field conditions at Slope 1 and 2, which performed well under extreme precipitation events that occurred during the study period. Therefore, a spacing of 0.3 - 0.9 m can also be considered, based on small-scale testing prior to implementation and numerical modeling with representative input parameters. The greater the uncertainty in parameters such as moisture, matric suction, seepage, and perched water conditions, the closer the spacing should be however, the plantings should also be staggered across rows (cross-slope) and columns (along the slope). Since excavation is not encouraged, as it could compromise the structure, experimental planting vetiver in an environment as close as possible to the field conditions and at the same time of the field plantation would allow vetiver to be excavated to quantitatively determine the properties of the vetiver grassroots, including the growth rate, tensile strength, and shear strength of the soil-root composite. This could be an aspect of future study.

Future studies at these sites would be beneficial for determining vetiver's effectiveness in stabilizing slopes. They could include excavating a small section the size of the maximum diameter of a vetiver plant, a section roughly equidistant from four vetiver plants (approximately 150 mm for 0.3 m center-to-center spacing), and a section located downslope of the vetiver test section to determine the grassroot length, soil-root composite structure, soil-root composite properties (e.g. unit weight, shear strength, moisture, specific gravity, etc.), soil properties with the roots removed, and root properties with the soil removed. The soil test results could be compared with adjacent areas that are not within the test section and do not have vetiver roots. These studies would allow for a better approximation of in situ soil properties to refine numerical analyses and create less conservative designs. They would also allow comparisons of the soil matrix on sites with and without seepage.

Other future studies could compare the growth of vetiver in different types of soils and varying climatic conditions. If excavation is not permitted, measuring the height of the grass shoot immediately before and after routine maintenance (lawn mowing) could assist with determining the root depth, but its growth both vertically and horizontally needs to be considered. The length of the root before it is transplanted and throughout the duration should be measured at preset intervals. A field plan illustrating the location of each tiller of interest from the boundaries of the test section would help keep track of the locations and improve the precision and accuracy of the measurements. The length of shoots planted in various location in the test section may also indicate areas where local changes in soil properties or hydrological conditions affect the vitality of the plants.

References

- Acharya, K. P., Bhandary, N. P., Dahal, R. K., and Yatabe, R. (2016). Seepage and slope stability modeling of rainfall-induced slope failures in topographic hollows. *Geomatics, Natural Hazards, and Risk*, 7(2), 721-746.
- Ali, F. H., and Osman, N. (2008). Shear strength of soil containing vegetation roots. *Soils and Foundations*, 48(4), 587-596.
- Antiochia, R., Campanella, L., Ghezzi, P., and Movassaghi, K. (2007). The use of Vetiver for remediation of heavy metal soil contamination. *Analytical and Bioanalytical Chemistry*, 388, 947-956.
- Babalola, O., Oshunsanya, S. O., and Are, K. (2007). Effects of Vetiver grass (*Vetiveria nigriflora*) strips, Vetiver grass mulch, and an organometal fertilizer on soil, water, nutrient losses, and maize (*Zea mays*, L) yields. *Soil and Tillage Research*, 96(1-2), 6-18.
- Badhon, F. F., Islam, M. S., Islam, M. A., and Arif, M. Z. U. (2021). A simple approach for estimating the contribution of Vetiver roots in the shear strength of a soil-root system. *Innovative Infrastructure Solutions*, 6(2), 96.
- Battisti, D. S., and Naylor, R. L. (2009). Historical warnings of future food insecurity with unprecedented seasonal heat. *Science*, 323(5911), 240-244.
- Brandt, R., Merkl, N., Schultze-Kraft, R., Infante, C., and Broll, G., (2006). The potential of vetiver (*Vetiveria zizanioides* (L.) Nash) for phytoremediation of petroleum hydrocarbon-contaminated soils in Venezuela. *Int J Phytoremediation*. 8(4):273–284. doi:10.1080/15226510 600992808.
- Bishop, D. M., and Stevens, M. E. (1964). Landslides on logged areas in southeast Alaska. US Forest Service research paper NOR;-1.
- BS 5930. (1981). Code of practice for site investigations. British Standard Institution, London
- Cai, F., and Ugai, K. (2004). Numerical analysis of rainfall effects on slope stability. *International Journal of Geomechanics*, 4(2), 69-78.
- Cardinali, M., Galli, M., Guzzetti, F., Ardizzone, F., Reichenbach, P., and Bartoccini, P. (2006). Rainfall induced landslides in December 2004 in south-western Umbria, central Italy: types, extent, damage, and risk assessment. *Natural Hazards and Earth System Sciences*, 6(2), 237-260.
- Carter, M., and Bentley, S., P. (1991). Correlations of soil properties, Pentech
- Castellanos, B. A., and Brandon, T. L. (2013, September). A comparison between the shear strength measured with direct shear and triaxial devices on undisturbed and remolded soils. In *Proceedings of the 18th International Conference on Soil Mechanics and Geotechnical Engineering, Paris (Vol. 2013, pp. 317-320)*.
- Charles, L. (2008). Geotechnical aspects of buildings on expansive soils in Kibaha, Tanzania. Doctoral Thesis, Division of Soil and Rock Mechanics, Department of Civil and Architectural Engineering, Royal Institute of Technology Stockholm, Sweden.
- Cho, S. E. (2014). Probabilistic stability analysis of rainfall-induced landslides considering spatial variability of permeability. *Engineering Geology*, 171, 11-20.
- Coppin, N.J., Richards, I.J. (1990). Use of vegetation in civil engineering. London: CIRIA, Butterworths.
- Cruden, D. (Ed.). (2018). *Landslide Risk Assessment*. Routledge.
- D'Souza, D. N., Choudhary, A. K., Basak, P., and Shukla, S. K. (2019). Assessment of vetiver grass root reinforcement in strengthening the soil. In *Ground Improvement Techniques and Geosynthetics: IGC 2016 Volume 2 (pp. 135-142)*. Springer Singapore.

- Dai, F. C., Lee, C. F., and Ngai, Y. Y. (2002). Landslide risk assessment and management: an overview. *Engineering Geology*, 64(1), 65-87.
- Danh, L. T., Truong, P., Mammucari, R., and Foster, N. (2010). The economic incentive for applying Vetiver grass to remediate lead, copper, and zinc-contaminated soils. *International Journal of Phytoremediation*, 13(1), 47-60.
- Danh, L. T., Truong, P., Mammucari, R., Tran, T., and Foster, N. (2009). Vetiver grass, *Vetiveria zizanioides*: a choice plant for phytoremediation of heavy metals and organic wastes. *International Journal of Phytoremediation*, 11(8), 664-691.
- Darajeh, N., Idris, A., Masoumi, H. R. F., Nourani, A., Truong, P., and Sairi, N. A. (2016). Modeling BOD and COD removal from palm oil mill secondary effluent in floating wetland by *Chrysopogon zizanioides* (L.) using response surface methodology. *Journal of Environmental Management*, 181, 343-352.
- Das, P., Datta, R., Makris, K. C., and Sarkar, D. (2010). Vetiver grass is capable of removing TNT from soil in the presence of urea. *Environmental Pollution*, 158(5), 1980-1983.
- DeGraff, J. V. (1979). Initiation of shallow mass movement by vegetative-type conversion. *Geology*, 7(9), 426-429.
- Douglas, S. C., and Dunlap, G. T. (2000). Light commercial construction on Yazoo clay. Proc., 2nd Forensic Congress, ASCE, Reston, Va., 607-616
- Dousset, S., Abaga, N. O. Z., and Billet, D. (2016). Vetiver grass and micropollutant leaching through structured soil columns under outdoor conditions. *Pedosphere*, 26(4), 522-532.
- Eab, K.H., Likitlersuang, S. Takahashi, A. (2015). Laboratory and modelling investigation of a root-reinforced system for slope stabilization. *Soils and Foundations*, Volume 55, Issue 5, Pages 1270-1281, ISSN 0038-0806. <https://doi.org/10.1016/j.sandf.2015.09.025>
- Endo, T., and Tsuruta, T. (1969). Effects of tree roots upon the shearing strengths of soils. 18th Annual Report of the Hokkaido Branch, Government Forest Experimental Station, Tokyo, 167-179.
- Flerchinger, G. N., Lehrsch, G. A., and McCool, D. K. (2005). Freezing and thawing processes.
- Gnansounou, E., Alves, C. M., and Raman, J. K. (2017). Multiple applications of Vetiver grass—a review. *International Journal of Education and Learning Systems*, 2.
- Gray, D. H. (1981). Forest vegetation removal and slope stability in the Idaho Batholith (Vol. 271). US Department of Agriculture, Forest Service, Intermountain Forest, and Range Experiment Station.
- Gray, D. H., and Sotir, R. B. (1996). Biotechnical and soil bioengineering slope stabilization: a practical guide for erosion control. John Wiley and Sons.
- Groisman, P. Y., and Easterling, D. R. (1994). Variability and trends of total precipitation and snowfall over the United States and Canada. *Journal of Climate*, 7(1), 184-205.
- Han, X., and Parker, T. L. (2017). Anti-inflammatory activity of clove (*Eugenia caryophyllata*) essential oil in human dermal fibroblasts. *Pharmaceutical Biology*, 55(1), 1619-1622.
- Hellin, J., and Haigh, M. J. (2002). Better land husbandry in Honduras: towards the new conserving soil, water, and productivity paradigm. *Land Degradation and Development*, 13(3), 233-250.
- Hengchaovanich, D. (2003, October). Vetiver system for slope stabilization. In Proceedings of 3rd International Vetiver Conference, Guangzhou, China (pp. 301-309).
- Henkel, D. J.; Skempton A. W. (1954). A landslide at Jackfield, Shropshire, in a heavily overconsolidated clay. *Geotechnique*, 131-137.
- Holtz, W. G. and Gibbs, H. J. (1956). Engineering properties of expansive clays. *Transactions, American Society of Civil Engineers*, vol. 121, pp. 641-677.

- Holtz, R. D., and Kovacs, W. D. (1981). *An Introduction to Geotechnical Engineering*, Prentice-Hall, Englewood Cliffs, NJ, 733 pp
- Islam, M. A., Islam, M. S., Chowdhury, M. E., and Badhon, F. F. (2021). Influence of Vetiver grass (*Chrysopogon zizanioides*) on infiltration and erosion control of hill slopes under simulated extreme rainfall conditions in Bangladesh. *Arabian Journal of Geosciences*, 14(2), 119.
- Islam, M. S., Arifuzzaman, Md. Shahin, H., and Nasrin, S. (2013). Effectiveness of Vetiver root in embankment slope protection: Bangladesh perspective. *International Journal of Geotechnical Engineering*, 7(2), 136-148.
- Johnson, K. A., and Sitar, N. (1990). Hydrologic conditions leading to debris-flow initiation. *Canadian Geotechnical Journal*, 27(6), 789-801.
- Jotisankasa, A., and Sirirattanachat, T. (2017). Effects of grassroots on soil-water retention curve and permeability function. *Canadian Geotechnical Journal*, 54(11), 1612-1622.
- Joy, J. R. (2009). Plant Guide “SUNSHINE” VETIVER GRASS *Chrysopogon zizanioides* (L.) Roberty Plant Symbol = CHZI Contributed by: USDA NRCS Pacific Islands Area Plant Materials Program. Retrieved from https://plants.usda.gov/DocumentLibrary/plantguide/pdf/pg_chzi.pdf
- Kalia, A. C. (2018). Classification of landslide activity on a regional scale using persistent scatterer interferometry at the Moselle valley (Germany). *Remote Sensing*, 10(12), 1880.
- Karl, T. R., and Knight, R. W. (1998). Secular trends of precipitation amount, frequency, and intensity in the United States. *Bulletin of the American Meteorological Society*, 79(2), 231-241.
- Khan, M. S., Amini, F., and Nobahar, M. (2020). Performance evaluation of highway slopes on Yazoo clay (No. FHWA/MDOT-RD-20-286). Mississippi. Dept. of Transportation.
- Kidd, J. T., Song, C. R., Al-Ostaz, A., Cheng, A. H. D., and Jang, W. (2011). Erosion control using modified soils. *International Journal of Erosion Control Engineering*, 4(1), 1-9.
- Kim, K., Riley, S., Fischer, E., and Khan, S. (2022). Greening Roadway Infrastructure with Vetiver Grass to Support Transportation Resilience. *Civil Eng* 3, no. 1: 147-164. <https://doi.org/10.3390/civileng3010010>
- Krogstad, F. (1995). A physiology and ecology-based model of lateral root reinforcement of unstable hillslopes (Master's thesis, University of Washington)
- Krzeminska, D., Kerkhof, T., Skaalsveen, K., and Stolte, J. (2019). Effect of riparian vegetation on stream bank stability in small agricultural catchments. *Catena*, 172, 87-96.
- Kunkel, K. E., Andsager, K., and Easterling, D. R. (1999). Long-term trends in extreme precipitation events over the conterminous United States and Canada. *Journal of Climate*, 12(8), 2515-2527.
- Kurupparachchi, T., and Wyrwoll, K. H. (1992). The role of vegetation clearing in the mass failure of hillslopes: Moresby Ranges, Western Australia. *Catena*, 19(2), 193-208.
- Lee, L. T., Jr. (2012). “State Study 151 and 236: Yazoo Clay Investigation.” MDOT State Study 236, US Army Corps of Engineers.
- Leknoi, U., and Likitlersuang, S. (2020). Good practice and lesson learned in promoting Vetiver as the solution for Thailand's slope stabilization and erosion control. *Land Use Policy*, 99, 105008.
- Liu, C. (2015). Stress-strain behavior by image analysis, mix density, and pre-strain effects of EPS geofabric (Doctoral dissertation, Syracuse University).
- Lucian, C. (2008). Geotechnical aspects of buildings on expansive soils in Kibaha, Tanzania. Ph.D. Thesis, Division of Soil and Rock Mechanics Department of Civil and Architectural Engineering Royal Institute of Technology Stockholm, Sweden, 196 pp

- Lukas, J., Mahoney, K., Perry, M., Thompson, C. (July 12, 2022). Extreme precipitation and dam safety in a changing climate [Webinar]. Association of State Dam Safety Officials (ASDSO). https://www.damsafety.org/training-center/webinar/extreme-precipitation-and-dam-safety-changing-climate?utm_source=Emailandutm_medium=ASDSO%2FInformzandutm_campaign=Informzand_zs=LiHrk1and_zl=geHR8
- Maffei, M. (Ed.). (2002). *Vetiveria: the genus Vetiveria*. CRC Press.
- Mickovski, S. B., and Van Beek, L. P. H. (2009). Root morphology and effects on soil reinforcement and slope stability of young Vetiver (*Vetiveria zizanioides*) plants grown in a semi-arid climate. *Plant and soil*, 324(1-2), 43-56.
- Mickovski, S. B., Van Beek, L. P. H., and Salin, F. (2005). The uprooting of Vetiver uprooting resistance of Vetiver grass (*Vetiveria zizanioides*). *Plant and Soil*, 278, 33-41.
- Mohamed, W. W., Osman, N., and Abdullah, R. (2022). A review of bioengineering techniques for slope stability in Malaysia. *International Journal of Environmental Science and Technology*, 1-16.
- National Oceanic and Atmospheric Administration (NOAA). (2014). NOAA's National Weather Service Hydrometeorological Design Studies Center Precipitation Frequency Data Server (PFDS). <https://hdsc.nws.noaa.gov/hdsc/pfds/>
- Nobahar, M., Khan, M., Ivoke, J., and Amini, F. (2019). Impact of rainfall variation on slope made of expansive Yazoo clay soil in Mississippi." *Transportation Infrastructure Geotechnology* 6, 318–336. <https://doi.org/10.1007/s40515-019-00083-w>
- Nguyen, T. S., Likitlersuang, S., and Jotisankasa, A. (2019). Influence of the spatial variability of the root cohesion on a slope-scale stability model: a case study of a residual soil slope in Thailand. *Bulletin of Engineering Geology and the Environment*, 78, 3337-3351.
- Nimityongskul, P., Panichnava, S., and Hengsadadekul, T. (2003). Use of Vetiver grass ash as cement replacement materials. ICV-3 held in Guangzhou, China, 6-9.
- Nix, K. E., Henderson, G., Zhu, B. C., and Laine, R. A. (2006). Evaluation of Vetiver grass root growth, oil distribution, and repellency against formosan subterranean termites. *HortScience*, 41(1), 167-171.
- Nobahar, M., Khan, M. S., and Ivoke, J. (2020). Combined effect of rainfall and shear strength on the stability of highway embankments made of Yazoo clay in Mississippi. *Journal of Geotechnical and Geological Engineering*, Springer US, Online ISSN 0960-3182, Jan 9th.
- Phusantisampan, T., Meeinkuirt, W., Saengwilai, P., Pichtel, J., and Chaiyarat, R. (2016). The phytostabilization potential of two ecotypes of *Vetiveria zizanioides* in cadmium-contaminated soils: greenhouse and field experiments. *Environmental Science and Pollution Research*, 23, 20027-20038.
- Punetha, P., Samanta, M., and Sarkar, S. (2019). Bioengineering as an effective and eco-friendly soil slope stabilization method: A review. *Landslides: Theory, Practice and Modeling*, 201-224.
- Rahardjo, H., Lim, T. T., Chang, M. F., and Fredlund, D. G. (1995). Shear-strength characteristics of residual soil. *Canadian Geotechnical Journal*, 32(1), 60-77.
- Rahardjo, H., Satyanaga, A., Leong, E. C., Santoso, V. A., and Ng, Y. S. (2014). Performance of an instrumented slope covered with shrubs and deep-rooted grass. *Soils and Foundations*, 54(3), 417-425.
- Reneau, S. L., and Dietrich, W. E. (1987). Size and location of colluvial landslides in a steeply forested landscape. IAHS-AISH publication, (165), 39-48.

- Riestenberg, M. M. (1994). Anchoring of thin colluvium by sugar maple roots and white ash on hillslopes in Cincinnati (Vol. 2059). US Government Printing Office.
- Riestenberg, M. M., and Sovonick-Dunford, S. (1983). The role of woody vegetation in stabilizing slopes in the Cincinnati area, Ohio. *Geological Society of America Bulletin*, 94(4), 506-518.
- Runkle, J., Kunkel, K.E., Champion, S.M., Frankson, R., Stewart, B.C., and Nielsen-Gammon, J. (2022). Mississippi state climate summary 2022. NOAA Technical Report NESDIS 150-MS. NOAA/NESDIS, Silver Spring, MD, 5 pp
- Saikia, D., Parveen, S., Gupta, V. K., and Luqman, S. (2012). Anti-tuberculosis activity of Indian grass KHUS (*Vetiveria zizanioides* L. Nash). *Complementary Therapies in Medicine*, 20(6), 434-436.
- Schiechl, H. M., and Stern, R. (1996). Ground bioengineering techniques for slope protection and erosion control.
- Seed, H. B., Mitchell, J. K. and Chan, C. K., (1960). The strength of compacted cohesive soils. *Journal of the Soil Mechanics and Foundations Division, ASCE, Soil Mechanics, and Foundation division*, vol. 88, No. SM-3, pp. 53-87.
- Seed, H. B., Woodward, R. J., Jr. and Lundgren, R. (1962). Prediction of swelling potential for compacted clays. *Proceedings, ASCE Research Conference on Cohesive Soils, Boulder, American Society of Civil Engineers, New York*, pp. 877-964.
- Sharif, M. (2000). US Army experience: Cold tolerance and seed viability characteristics of Vetiver. In *Proc. Second Intern. Vetiver Conf.*
- Sidle, R. C. (1992). A theoretical model of the effects of timber harvesting on slope stability. *Water Resources Research*, 28(7), 1897-1910.
- Skempton, A. W. (1970). First-time slides in over-consolidated clays. *Geotechnique*, 20(3), 320-324.
- Stark, T. D., and Duncan, J. M. (1991). Mechanisms of strength loss in stiff clays. *Journal of Geotechnical Engineering*, 117(1), 139-154.
- Stokes, A., Douglas, G. B., Fourcaud, T., Giadrossich, F., Gillies, C., Hubble, T., ... and Walker, L. R. (2014). Ecological mitigation of hillslope instability: ten key issues facing researchers and practitioners. *Plant and Soil*, 377, 1-23.
- Swanston, D. N., Lienkaemper, G. W., Mersereau, R. C., and Levno, A. B. (1988). Timber harvest and progressive deformation of slopes in southwestern Oregon. *Bulletin of the Association of Engineering Geologists*, 25(3), 371-381.
- Taylor, A. C. (2005). Mineralogy and engineering properties of the Yazoo clay formation. Jackson Group, Master's Thesis, Mississippi State University.
- Tourtlot, H., A. (1973). Regional geochemical investigations. *Front Range Urban Corridor, Colorado, Geological Society of America*, v. 5, no. 6, p. 520-521.
- Truong, P. (1999). *Vetiver grass technology for mine rehabilitation (Vol. 19)*. Bangkok: Office of the Royal Development Projects Board.
- Truong, P. N., and Claridge, J. (1996). Effects of heavy metals toxicities on Vetiver growth. *Vetiver Newsletter*, 15, 32-36.
- Truong, P. N., Foong, Y. K., Guthrie, M., and Hung, Y. T. (2010). Phytoremediation of heavy metal-contaminated soils and water using Vetiver grass. *Environmental Bioengineering: Volume 11*, 233-275.
- Truong, P., and Loch, R. (2004). Vetiver System for erosion and sediment control. In *Proceeding of 13th International Soil conservation Organization Conference* (pp. 1-6).

- Tsige, D., Senadheera, S., and Talema, A. (2019). Stability analysis of plant-root-reinforced shallow slopes along mountainous road corridors based on numerical modeling. *Geosciences*, 10(1), 19.
- United States Geological Survey (2018). Overview of rainfall-induced landslides. *Landslide Hazards*. <https://www.usgs.gov/programs/landslide-hazards/science/overview-rainfall-induced-landslides>
- Waldron, L. J. (1977). The shear resistance of root-permeated homogeneous and stratified soil. *Soil Science Society of America Journal*, 41(5), 843-849.
- Waldron L.J., Dakessian S. (1981) Soil reinforcement by roots: calculation of increased soil shear resistance from root properties. *Soil Science* 132: 427-435.
- Wang, G. Y., Huang, Y. G., Li, R. F., Chang, J. M., and Fu, J. L. (2020). Influence of vetiver root on the strength of the expansive soil-experimental study. *PLoS One*, 15(12), e0244818.
- Weaver, C., C. (1989). *Clays, muds, and shales. Development in Sedimentology* 44, Elsevier Science
- WLOX. 2022 Prepare South Mississippi Hurricane Special - Part 2 [Video file]. (2022, May 26). Retrieved from <https://www.wlox.com/video/2022/05/26/prepare-south-mississippi-hurricane-special-part-6/>
- Wu, T. H., McKinnell III, W. P., and Swanston, D. N. (1979). Strength of tree roots and landslides on Prince of Wales Island, Alaska. *Canadian Geotechnical Journal*, 16(1), 19-33.
- Yang, M., Défossez, P., Danjon, F., and Fourcaud, T. (2014). Tree stability under wind: simulating uprooting with root breakage using a finite element method. *Annals of Botany*, 114(4), 695-70
- Zhan, L. T., Chen, P., and Ng, C. W. W. (2007). Effect of suction change on water content and total volume of expansive clay. *Journal of Zhejiang University-SCIENCE A*, 8(5), 699-706.
- Zhu, B. C., Henderson, G., Chen, F., Fei, H., and Laine, R. A. (2001). Evaluation of Vetiver oil and seven insect-active essential oils against the Formosan subterranean termite. *Journal of Chemical Ecology*, 27, 1617-1625.
- Ziemer, R. R., and Swanston, D. N. (1977). Root strength changes after logging in southeast Alaska (Vol. 306). Department of Agriculture, Forest Service, Pacific Northwest Forest and Range Experiment Station.